IDENTIFICATION AND FUNCTIONAL CHARACTERIZATION OF NECROTROPHIC EFFECTORS IN *PARASTAGONOSPORA NODORUM*

A Dissertation
Submitted to the Graduate Faculty
of the
North Dakota State University
of Agriculture and Applied Science

By

Yuanyuan Gao

In Partial Fulfillment of the Requirements
for the Degree of
DOCTOR OF PHILOSOPHY

Major Department:
Plant Pathology

November 2015

Fargo, North Dakota

North Dakota State University
Graduate School

Title

Identification and Functional Characterization of Necrotrophic Effectors in *Parastagonospora nodorum*

By

Yuanyuan Gao

The Supervisory Committee certifies that this ***disquisition*** complies with North Dakota State University's regulations and meets the accepted standards for the degree of

DOCTOR OF PHILOSOPHY

SUPERVISORY COMMITTEE:

Zhaohui Liu
Chair

Timothy L. Friesen

Justin D. Faris

Robert Brueggeman

Xiwen Cai

Approved:

11-6-2015
Date

Jack Rasmussen
Department Chair

ABSTRACT

The necrotrophic fungus *Parastagonospora nodorum* (teleomorph; *Phaeosphaeria nodorum*), is the causal agent of Septoria nodorum blotch (SNB) on common wheat (*Triticum aestivum* L.) and durum wheat (*Triticum turgidum* L.). SNB is a serious foliar and glume disease which causes significant yield losses in major wheat growing areas and has serious impact on grain quality. *P. nodorum* produces necrotrophic effectors (NEs) that are recognized by and interact with dominant host sensitivity genes in an inverse gene-for-gene manner. The NE-host interaction is critical to induce necrotrophic effector-triggered susceptibility (NETS), resulting in SNB disease. To date, nine NE-host sensitivity gene interactions, following a NETS model, have been identified in the *P. nodorum*-wheat pathosystem. One of the NE-host sensitivity gene interactions, SnTox6-*Snn6* interaction was characterized in this study. The SnTox6-*Snn6* interaction was shown to be light dependent and *Snn6* was located to a major disease susceptibility QTL on wheat chromosome 6A. SnTox1, another NE first identified in our lab, interacts with the corresponding wheat sensitivity gene *Snn1*. SnTox1 was further characterized in this study. The SnTox1 protein harbors C-terminal domains with a high degree of structural homology to plant chitin binding proteins and was subsequently shown to bind chitin, a main component of the fungal cell wall. Therefore, SnTox1 was hypothesized to compete with wheat chitinases to bind chitin, preventing fungal cell wall degradation. To investigate this hypothesis, the SnTox1 binding affinity with chitin was tested, as well as its potential function in the protection against chitinases during fungal mycelial growth. To identify additional NE regions, genome wide association study (GWAS) technology was used. A global collection of 191 *P. nodorum* isolates were genotyped using a restriction-site associated DNA genotyping by sequencing (RAD-GBS) protocol to identify SNP markers. Phenotypic data including fungal

inoculations and culture filtrate infiltrations were collected using 191 *P. nodorum* isolates across several wheat lines. GWAS analyses were performed by regressing the phenotypic data and genotypic data by running multiple GWAS models.

ACKNOWLEDGMENTS

Foremost, my deep gratitude goes to my research advisor Dr. Timothy L. Friesen who gave me guidance on how to view the big picture of my research, to think about my projects as a scientist, and to make my own point of view and not to simply agree with others. His patience, understanding and support helped me to overcome all the difficult situations during my PhD study. With his guidance, I gained a lot of knowledge in the area of my project and improved in my ability to think, do research, and write professionally.

Besides my research advisor, I am also grateful to my academic advisor, Dr. Zhaohui Liu for encouraging me to apply for the PhD position in Dr. Friesen's lab. I am also particularly thankful to him for our numerous discussions and the detailed technical support he provided.

My sincere thanks also goes to my committee members Dr. Justin D. Faris, Dr. Robert Brueggeman, and Dr. Xiwen Cai for the time they put into reviewing my thesis proposal and dissertation, as well as their valuable suggestions for my research project.

I would like to acknowledge the current and former lab members in Dr. Friesen and Dr. Faris' lab. These people include Danielle Holmes and Dr. Zengcui Zhang who taught me the critical lab and greenhouse techniques, Dr. YonMin Kim who offered protein techniques and Dr. Gongjun Shi, Vaidehi Koladia, Jason Axtman, Jacob Jennings, Nathan Wyatt, Steven Carlsen and other grad students who provided various forms of help.

I am also thankful to Dr. Xuehui Li for providing expertise and encouragement in performing genome wide association analysis, and Jonathan Richards for help in creating the SNP pipeline used in the GWAS analysis.

A special acknowledgment is extended to my parents, Zhengxin Gao and Meizhen Fang who gave huge support throughout my life. I thank them with all my heart for their encouragement and the time they put into taking care of my kids.

Finally, I saved the last word of acknowledgment for my dear husband Dr. Chengxiang Qiu and my two sons Jerry Qiu and Daniel R. Qiu. My husband Chengxiang has been with me eight years and made these years the best time of my life. I thank him for the tremendous understanding when I worked long hours in the lab. I also thank him for the effort he made in educating our sons and the happiness he created for the whole family. Particularly, I thank my sons Jerry and Daniel for bringing me plenty fun and happiness.

TABLE OF CONTENTS

LIST OF TABLES

LIST OF FIGURES

GENERAL INTRODUCTION

Plant pathogens are often classified into two groups, the biotrophic pathogens and the necrotrophic pathogens. Necrotrophic pathogens derive food from dead and dying cells (Agrios, 1997) and they kill the host cell quickly after infection and feed on the remains (Glazebrook, 2005). In this process, the necrotrophic effectors (NE, formerly called host-selective toxins or HSTs) are critical for disease development. NEs determine the virulence and pathogenicity of the pathogens that produce them (Wolpert et al., 2002). NEs are toxic only to the plants that serve as hosts for the pathogens and have little or no toxicity against non-susceptible plants (Prell and Day, 2001). Currently, many NEs have been identified and their modes of action have been described (Wolpert et al., 2002). Recently, at least nine NEs have been identified in the necrotrophic fungus *Parastagonospora nodorum* (teleomorph; *Phaeosphaeria nodorum*), the causal agent of Septoria nodorum blotch (SNB) on common wheat (*Triticum aestivum* L.) and durum wheat (*Triticum turgidum* L.). NEs have been shown to play an important role in disease development (Friesen et al., 2008b). SNB is a serious foliar and glume disease which causes significant yield losses in major wheat growing areas and has serious impact on grain quality (King et al., 1983; Fried and Meister, 1987; Wicki et al., 1999). *P. nodorum* - produced NEs are recognized by and interact with dominant host sensitivity genes in an inverse gene-for-gene manner (Liu et al., 2004a; Liu et al., 2004b; Friesen et al., 2006; Liu et al., 2006; Friesen et al., 2007; Friesen et al., 2008b; Abeysekara et al., 2009b). The NE-host interaction is critical to inducing necrotrophic effector-triggered susceptibility (NETS). To date, nine NE-host sensitivity gene interactions, following a NETS model, have been identified in the *P. nodorum*-wheat pathosystem including SnTox1-*Snn1* (Liu et al., 2004a), SnToxA-*Tsn1* (Friesen et al., 2006; Faris et al., 2010), SnTox2-*Snn2* (Friesen et al., 2007), SnTox3-*Snn3-B1* (Friesen et al., 2007;

Liu et al., 2009), SnTox3-*Snn3-D1* (Zhang et al., 2011), SnTox4-*Snn4* (Abeysekara et al., 2009a), SnTox5-*Snn5* (Friesen et al., 2012), SnTox6-*Snn6* (Gao et al., 2015, this study) and SnTox7-*Snn7* (Shi et al., 2015).

The first objective in this study was to use a wheat mapping population that segregated for sensitivity to NEs produced by the local *P. nodorum* isolate Sn6 to identify and characterize a new interaction involving the NE designated SnTox6 and the host sensitivity gene designated *Snn6*. SnTox6 is a small secreted protein that induces necrosis on wheat lines harboring *Snn6*. The SnTox6-*Snn6* interaction was light dependent and was shown to underlie a major disease susceptibility QTL on wheat chromosome 6A. This work expands the knowledge of the wheat-*P. nodorum* interaction and further establishes the SNB system as a model pathosystems for necrotrophic specialist interactions.

The second objective was to functionally characterize SnTox1 to define its role in pathogenesis. The interaction of SnTox1-*Snn1* was first identified in our lab. SnTox1 was shown to correspond with the wheat dominant sensitivity gene *Snn1* and induced an oxidative burst, DNA laddering, and up regulation of pathogen related (PR) genes such as PR-1 and chitinase genes (Liu et al., 2012). These responses result in susceptibility rather than resistance of wheat cultivars which carry the *Snn1* gene. Interestingly, the SnTox1 protein harbors C-terminal domains with a high degree of structural homology to plant chitin binding proteins (Liu et al., 2012) and was subsequently shown to bind chitin, a main component of the fungal cell wall. Therefore SnTox1 was hypothesized to compete with wheat chitinases to bind chitin and prevent fungal cell wall degradation. To investigate this hypothesis, first the SnTox1 binding affinity for different forms of chitin and chitosan was tested. Secondly, the protection function of SnTox1 was tested for mycelial growth against chitinase. In this study, two wheat chitinases were cloned

and expressed and were used to treat several fungal species including *P. nodorum*, *Neurospora crassa*, *Pyrenophora teres* f. *teres* and *Cercospora beticola*. This study supported evidence that SnTox1 has two functions in pathogenesis (i.e. induction of cell death and protection from chitinases).

The third objective was to identify additional NE regions using genome wide association study (GWAS) technology. As mentioned above, the NEs produced by *P. nodorum* are recognized directly or indirectly by wheat dominant sensitivity genes that confer susceptibility. Until now, three NE genes have been cloned including SnToxA, SnTox1 and SnTox3. To identify more NE gene regions, I used GWAS using a global collection of 191 isolates (13 US states, Australia, Denmark, Finland, Latvia, Lithuania, Norway, Sweden, Brazil, Switzerland, China, South Africa, and Iran). All 191 isolates were genotyped by RAD-GBS and the virulence of the 191 isolates were phenotype onto four wheat differential lines including BG223 (SnTox2 sensitive), ITMI37 (SnTox6 sensitive), ITMI44 (SnTox5 sensitive), and LP29 (SnTox5 sensitive) to identify *SnTox2*, *SnTox6*, and *SnTox5* genes. Marker trait association were performed using different models including naive, population structure (Q model), kinship (IBS model), and population structure + kinship (Q+IBS). GWAS analysis was shown to be useful to identify the genomic regions associated with NE sensitivity and pathogen susceptibility.

References

Abeysekara, N.S., Friesen, T.L., Keller, B., and Faris, J.D. 2009a. Identification and characterization of a novel host-toxin interaction in the wheat-*Stagonospora nodorum* pathosystem. Theoretical and Applied Genetics 120:117-126.

Abeysekara, N.S., Friesen, T.L., Keller, B., and Faris, J.D. 2009b. Identification and characterization of a novel host-toxin interaction in the wheat-*Stagonospora nodorum* pathosystem. Theoretical and Applied Genetics 120:117-126.

Agrios, G. 1997. Plant pathology. 4th Edition. Academic Press, New York.

Faris, J.D., Zhang, Z., Lu, H., Lu, S., Reddy, L., Cloutier, S., Fellers, J.P., Meinhardt, S.W., Rasmussen, J.B., and Xu, S.S. 2010. A unique wheat disease resistance-like gene governs effector-triggered susceptibility to necrotrophic pathogens. Proceedings of the National Academy of Sciences 107:13544-13549.

Fried, P., and Meister, E. 1987. Inheritance of leaf and head resistance of winter wheat to *Septoria nodorum* in a diallel cross. Phytopathology 77:1371-1375.

Friesen, T.L., Meinhardt, S.W., and Faris, J.D. 2007. The *Stagonospora nodorum*-wheat pathosystem involves multiple proteinaceous host-selective toxins and corresponding host sensitivity genes that interact in an inverse gene-for-gene manner. The Plant Journal 51:681-692.

Friesen, T.L., Chu, C.G., Xu, S.S., and Faris, J.D. 2012. SnTox5-*Snn5*: a novel *Stagonospora nodorum* effector-wheat gene interaction and its relationship with the SnToxA-*Tsn1* and SnTox3-*Snn3-B1* interactions. Molecular Plant Pathology 13:1101-1109.

Friesen, T.L., Zhang, Z., Solomon, P.S., Oliver, R.P., and Faris, J.D. 2008. Characterization of the interaction of a novel *Stagonospora nodorum* host-selective toxin with a wheat susceptibility gene. Plant physiology 146:682-693.

Friesen, T.L., Stukenbrock, E.H., Liu, Z., Meinhardt, S., Ling, H., Faris, J.D., Rasmussen, J.B., Solomon, P.S., McDonald, B.A., and Oliver, R.P. 2006. Emergence of a new disease as a result of interspecific virulence gene transfer. Nature Genetics 38:953-956.

Gao, Y., Faris, J.D., Liu, Z., Kim, Y.M., Syme, R.A., Oliver, R.P., Xu, S.S., and Friesen, T.L. 2015. Identification and Characterization of the SnTox6-*Snn6* Interaction in the *Parastagonospora nodorum*-Wheat Pathosystem. Molecular Plant-Microbe Interactions. 28:615-625.

Glazebrook, J. 2005. Contrasting mechanisms of defense against biotrophic and necrotrophic pathogens. Annual Review of Phytopathol. 43:205-227.

King, J., Cook, R., and Melville, S. 1983. A review of Septoria diseases of wheat and barley. Annals of Applied Biology 103:345-373.

Liu, Z., Friesen, T., Rasmussen, J., Ali, S., Meinhardt, S., and Faris, J. 2004a. Quantitative trait loci analysis and mapping of seedling resistance to Stagonospora nodorum leaf blotch in wheat. Phytopathology 94:1061-1067.

Liu, Z., Faris, J., Meinhardt, S., Ali, S., Rasmussen, J., and Friesen, T. 2004b. Genetic and physical mapping of a gene conditioning sensitivity in wheat to a partially purified host-selective toxin produced by *Stagonospora nodorum*. Phytopathology 94:1056-1060.

Liu, Z., Faris, J.D., Oliver, R.P., Tan, K.C., Solomon, P.S., McDonald, M.C., McDonald, B.A., Nunez, A., Lu, S., and Rasmussen, J.B. 2009. SnTox3 acts in effector triggered

susceptibility to induce disease on wheat carrying the *Snn3* gene. PLoS Pathogens 5:e1000581.

Liu, Z.H., Friesen, T.L., Ling, H., Meinhardt, S.W., Oliver, R.P., Rasmussen, J.B., and Faris, J.D. 2006. The Tsn1-ToxA interaction in the wheat-*Stagonospora nodorum* pathosystem parallels that of the wheat-tan spot system. Genome 49:1265-1273.

Prell, H.H., and Day, P.R. 2001. Plant-fungal pathogen interaction: a classical and molecular view. Springer Verlag.

Wicki, W., Winzeler, M., Schmid, J., Stamp, P., and Messmer, M. 1999. Inheritance of resistance to leaf and glume blotch caused by *Septoria nodorum* Berk. in winter wheat. Theoretical and Applied Genetics 99:1265-1272.

Wolpert, T.J., Dunkle, L.D., and Ciuffetti, L.M. 2002. Host-Selective Toxins and Avirulence Determinants: What's in a Name? Annual Review of Phytopathology 40:251-285.

Zhang, Z., Friesen, T.L., Xu, S.S., Shi, G., Liu, Z., Rasmussen, J.B., and Faris, J.D. 2011. Two putatively homoeologous wheat genes mediate recognition of SnTox3 to confer effector-triggered susceptibility to *Stagonospora nodorum*. The Plant Journal 65:27-38.

CHAPTER 1. LITERATURE REVIEW

Wheat

The evolution of wheat

Wheat is an important cereal grain crop cultivated worldwide. It is a member of the grass family (*Poaceae*) which includes other crop plants such as sorghum, maize, rice, and barley. Under the *Poaceae* family, wheat (*Triticum*), barley (*Hordeum*), oat (*Avena*), and brome (*Brachypodium*) have been grouped in the sub-family of *Pooidea*. The other two sub-families are *Panicoideae* (Represented by sorghum and maize) and *Ehrharloideae* (represented by rice). All the grass species are believed to have evolved from a common ancestor 50-70 million years ago through genome duplication and chromosome fusion (Bolot et al., 2009). The phylogenetic analysis based on RFLP genome mapping of the species revealed that wheat has the closest relationship with barley. Brome is relatively more related to wheat compared to oats and rice. Sorghum and maize have a distant relationship to wheat (Kellogg, 2001; Gaut, 2002). All wheat species belong to the genus *Triticum*. This genus contains six species: *Triticum monococcum* L. (AA genome), *T. urartu* Tumanian ex Gandilyan (AA genome), *T. turgidum* L. (AABB genome), *T. timopheevii* (Zhuk.) Zhuk. (AAGG genome), *T. aestivum* L. (AABBDD genome), and *T. zhukovskyi* Menabde & Ericz (AAAAGG genome). All the species can be grouped into 3 sections: *Monococcon* (einkorn wheat), containing diploid species; *Dicoccoidea* (emmer wheat), containing tetraploid species; and *Triticum* (common wheat), containing hexaploid species. In these six species, *T. urartu* Tumanian ex Gandilyan was found only in wild, and the two hexaploid species, *T. aestivum* L. and *T. Zhukovskyi* Menabde & Ericz were found only in cultivated form. The other three species can be found in both wild and domesticated forms (reviewed in Matsuoka, 2011). The evolution of wheat is postulated to be the result of the

allopolyploidization through hybridization with species in the genus of *Aegilops* (Tsunewaki, 2009). The species in the section *Monococcun* is thought to have diverged about 1 million years ago (Huang et al., 2002). The evolution of wild tetraploid *T. turgidum* ssp. *dicoccoides* (Körn Ex Asch. & Graebn Thell) (AABB genome) and *T. timopheevii* ssp. *armeniacum* (Jakubz) van slageren (AAGG genome) happened about 0.5 million years ago and after the divergence of *T. monococcum* and *T. urartu* (Faris et al., 2002). *T. turgidum* and *T. timopheevii* were evolved by the hybridization between *T. urartu* Tumanian ex Gandilyan (2n=2x=14, AA) and two plasmon types of diploid *Ae. speltoides* Tausch (SS genome). During this evolution, two independent hybridizations happened and were believed to be associated with the origin of *T. turgidum* and *T. timopheevii* (reviewed in Matsuoka, 2011). The diversification within the AABB and AAGG genome species likely happened through allopolyploid hundreds of thousands of years later. In the period of agricultural development in the Fertile Crescent (about 10,000 years ago), *T. turgidum*, *T. timopheevii* and *T. monococcum* were domesticated (Feldman, 2000; Salamini et al., 2002). The natural hybridization that occurred between the tetraploid cultivars and the diploid *Aegilops* and *Triticum* species resulted in the evolution of hexaploid *Triticum*. The species *T. aestivum* was believed to have arisen through spontaneous hybridization between *T. turgidum* and *A. tauschii Coss* (DD genome donor) 8,000 years ago (Kihara, 1944; McFadden and Sears, 1944), while *T. zhukovskyi* was produced through hybridization between *T. timopheevii* and *T. monococcum* (Kihara, 1966; Dvorak et al., 1993).

Based on the events of common wheat evolution, it is believed that the diploid goatgrass species *Ae. tauschii* Coss is the donor of the DD genome, and *T. urartu* is the donor of the AA genome. *Ae. speltoides* was designated the donor of the BB genome. However some studies showed that the BB genome is highly diverse among the species in the genus *Aegilops*, and at

first it was designated as the SS genome rather than BB. In addition, the BB genome of *Ae. speltoides* is also shared by *Ae. bicornis* (S^b), *Ae. longissima* (S^l), *Ae. searssii* (S^s), and *Ae. sharonesis* (S^{sh}). So the origin of the BB genome is still under debate (Slageren and Areas, 1994). The most popular hypothesis is that *Ae. speltoides*, whose S genome is close to the B genome of bread wheat is the B genome donor of bread and durum wheat, based on supporting evidences including karyotype data, C-banding of chromosomes, cytology, electrophoretic mobilities of proteins, the geographical distributions of wild wheat, low-copy and repetitive DNA sequence analysis by restriction fragment length polymorphism (RFLP) technique and plasmon analysis (Faris et al., 2002). It has been concluded that the D genome originated from *Ae. tauschii*, the A genome from *T. urartu* and the B genome from *Ae. speltoides*. In polyploid wheat, the B genome is shown to be higher in diversification than the A genome (Faris et al., 2002; Petersen et al., 2006).

Domestication of wheat

It is generally agreed that wheat cultivation started about 10,000 years ago (Shewry, 2009) during the Neolithic period when hunters and gatherers started practicing agriculture. Einkorn wheat (*T. monococcum*) which arose from its wild progenitor, *T. boeticum* was the first species of wheat to be domesticated and eventually cultivated (Heun et al., 1997). This diploid species of wheat was a useful crop before the Bronze Age. It's cultivation however, ceased in the Bronze Age in favor of polyploid wheats that were better suited to various climates and had better harvesting properties (Salamini et al., 2002). The second species of wheat to be domesticated was emmer, *T. dicoccum* which is tetraploid and was domesticated from its wild progenitor *T. dicoccoides*. The difference in polyploid wheat gives emmer superior cultivation advantage over einkorn. Domesticated emmer is easy to handle during harvest due to its tough

rachis that keeps spikelets intact (Salamini et al., 2002). The final and probably the most important stage of wheat domestication was the discovery of free-threshing wheat of greater polyploid status. This event included domestication of durum wheat and bread wheat. Durum wheat is tetraploid and known to have been domesticated from its ancestor *T. dicoccum*. Like most hexaploid wheat, durum wheat is free-threshing and cultivated worldwide for making pasta (Peng et al., 2011). The modern species of wheat, mostly cultivated hexaploid bread wheat, *T. aestivum* which has no known ancestor resulted from a cross between two different species; diploid wild grass *T. tauschii* and tetraploid emmer wheat (Dubcovsky and Dvorak, 2007; Shewry, 2009; Charmet, 2011). This hybridization probably happened by accident as the cultivation of emmer wheat expanded.

Major wheat diseases and defense mechanisms

According to a disease survey performed by North Dakota State University, major wheat diseases in the U.S include common bunt caused by *Tilletia caries*, Fusarium head blight caused by *Fusarium spp.*, loose smut caused by *Ustilago tritici*, Septoria nodorum blotch caused by *Parastagonospora nodorum*, leaf rust caused by *Puccinia triticina*, Septoria tritici blotch caused by Zymo*septoria tritici*, stem rust caused by *Puccinia graminis*, stripe rust caused by *Puccinia striiformis*, tan spot caused by *Pyrenophora tritici-repentis*, Cephalosporium stripe caused by *Cephalosporium gramineum*, common root rot caused by *Cochliobolus sativus*, bacterial streak caused by *Xanthomonas campestris*, and virus diseases including barley yellow dwarf, wheat soil borne mosaic and wheat spindle streak mosaic. Most disease losses are caused by fungal pathogens. The complex of SNB and STB were regarded as the most common diseases, since Septoria nodorum blotch (SNB) was found together with Septoria tritici blotch (STB) in many wheat growing regions (McMullen et al., 2002).

To invade plants, fungal pathogens can develop feeding structures, or directly enter host epidermal cells. After successful entry into the host cell by pathogens, plants develop a series of immune events including an oxidative burst, defense gene induction and deposition of callose-rich papillae, and biosynthesis of salicylic acid or jasmonic acid to regulate local or systemic defense mechanisms (Eulgem et al., 1999; Flors et al., 2005; Torres et al., 2006; Heil and Ton, 2008).

The evolution of the plant immune system can be described as a zigzag model (Jones and Dangl, 2006). In phase 1, plants sense the invasion of a pathogen by recognition of pathogen-associated molecular patterns (PAMP), also referred to as microbe-associated molecular patterns (MAMP), which include flagellin, chitin, glycoproteins or lipopolysaccharides (Ahmad et al., 2010). PAMPs and MAMPs are thought to be recognized by pattern-recognition receptors (PRR) resulting in PAMP-trigger immunity (PTI). In phase 2, virulent pathogens produce effectors to suppress PTI and overcome the basal defense of their host. This event is referred to as effector triggered susceptibility (ETS). In phase 3, selected plant varieties develop NB-LRR resistant proteins (R proteins) to recognize specific effectors, giving rise to a hypersensitive response (HR) to limit the growth of pathogens at certain stages of invasion. This event is referred to as effector-trigger immunity (ETI). In phase 4, under the pressure of ETI, selected pathogen isolates modify or eliminate the original effectors and evolve new effectors, while the host concurrently develops new R proteins to recognize the new effectors that trigger ETI (Jones and Dangl, 2006).

Septoria nodorum blotch (SNB) of wheat

Distribution and importance of SNB

SNB is a serious foliar and glume disease which has caused significant yield losses in the major wheat growing areas and has had serious impact on grain quality (King et al., 1983; Fried

and Meister, 1987; Wicki et al., 1999). SNB was first reported in 1845 by Berkeley in England as glume blotch on wheat. According to a 1919 disease survey report , SNB caused 0.25% and 0.5% yield loss in Delaware and Maryland, respectively (Weber 1992). By 1922, SNB had been reported in many countries including Italy, Sweden, Switzerland, Germany, France, Australia and the U.S. (Weber, 1992). Since 1945, SNB has been reported as leaf and glume blotch in additional countries or regions including Canada (Machacek, 1945), Argentina, Brazil, India, Western Europe (Scharen, 1964a), Asia and Africa (Saari and Wilcoxson, 1974). In the U.S., SNB was reported as a common disease in the Southeastern wheat-growing area (Shaner and Buechley, 1995) and under favorable conditions, SNB has been shown to cause 30% yield loss in wheat (Bhathal et al., 2003). In the southeastern U.S., yield loss caused by SNB achieved 30-50% for some vulnerable wheat cultivars (Scharen and Krupinsk, 1969; Nelson et al., 1974). SNB has also been reported to cause 31% yield loss in Australia (Bhathal et al., 2003) and 50% in Europe (Karjalainen et al., 1983).

Symptom development

In SNB disease, infected leaves are initially water soaked with small chlorotic lesions. As the disease develops, the lesions expand to become lens shaped and turn from yellow to red-brown. Finally, more lesions with gray-brown color coalesce resulting in whole tissue death. Pin-point brown specks (pycnidia) are shown on the center of lesions, a sign of SNB disease. On the glumes, lesions develop from the tip and then cover the whole glume becoming dark brown to dark purple, resulting in a completely dried appearance. The infected leaves and glumes may result in shriveled kernels (Liu, 2006).

Causal organism

The causal agent of SNB disease is the necrotrophic fungus, *Parastagonospora* (syn. *Septoria, Leptosphaeria, Stagonospora*) *nodorum* (teleomorph: *Phaeosphaeria nodorum*), which attacks both common wheat (*Triticum aestivum* L.) and durum wheat (*Triticum turgidum* L.). It belongs to the order Pleosporales which is under the Dothideomycete class of the Ascomycetes. The asexual state was first described as *Septoria nodorum* in the 1850s by Miles Berkeley (Eyal, 1987). In 2001, *Septoria nodorum* was moved from the genus *Septoria* to *Stagonospora*, based on ITS sequence analysis (Goodwin and Zismann, 2001). Quaedvlieg et al. (2013) analyzed the sequences of the partial 28S nuclear ribosomeal DNA and RPB2 genes of 347 isolates representing 170 species in the genus *Stagonospora* and found several cereal pathogens, including *P. nodorum*, were distinguished from other species. The morphology of *Parastagonospora* and *Stagonospora* differ in that the conidia spores of *Parastagonospora* are cylindrical, granular to multi-guttulate, while that of *Stagonospora* are subcylindrical to fusoid-ellipsoidal. The Sexual stage of *Parastagonospora* are phaeosphaeria-like, while that of *Stagonospora* are didymella-like (Quaedvlieg et al., 2013). Therefore, *P. nodorum* was move to the genus *Parastagonospora* and renamed as *Parastagonospora nodorum*.

Pathogen biology and epidemiology

P. nodorum is a heterothallic fungus, therefore the sexual reproduction of *P. nodorum* needs two mating types, MAT-1-1 and MAT-1-2. Isolates carrying the two mating types develop pseudothecia which is the sexual fruiting body. The sexual spores, ascospores, are born in asci which are produced in the pseudothecia (Eyal, 1987; Fitt et al., 1989). Ascospores of *P. nodorum* are wind-dispersed and have long-distance travel capability (Solomon et al., 2006a). Ascospores have thick dark cell walls which can protect the spores from desiccation under extreme

conditions (Eyal, 1987; Fitt et al., 1989). The asexual spores are produced in pycnidia, a spherical, dark-brown fruiting body containing pycnidiospores. The pycnidiospores are protected by a mucilaginous matrix (Eyal, 1987). In dry weather conditions, proteins and sugars are produced from the mucilage that protect the pycnidiospores from desiccation. The concentrated mucilage can inhibit the germination of pycnidiospores (Fitt et al., 1989). In humid conditions, the mucilage absorbs water, causing swelling inside the pycnidium and induction of spore germination (Brennan et al., 1985; Fitt et al., 1989).

The source of primary inoculum for SNB is typically ascospores (Rapilly et al., 1973). However, the infected wheat straw or stubble carrying pycnidia and the infected seed carrying mycelium or pycnidiospores are also an important source of primary inoculum (Machacek, 1945; Cunfer, 1978; Cunfer, 1983). *P. nodorum* overwinters as pseudothecia, vegetative mycelium or pycnidia in wheat straw, seed, or grasses. In the early growing season, the sexual fruiting bodies produce airborne ascospores that are dispersed by wind as primary inoculum (Solomon et al., 2006b). The pycnidia form on leaf tissue and pycnidiospores (conidia) are dispersed by rain-splash (Solomon et al., 2006b). Conidia act as secondary inoculum in a repeating cycle (Solomon et al., 2006a) throughout the growing season. Two to four cycles of asexual reproduction can infect wheat and cause significant disease losses (Solomon et al., 2006b). Severe SNB disease is favored by long wet periods at temperatures between 20°C and 28°C (Scharen, 1964a; Djurle et al., 1996). The overwintering structure can survive in infected residue for 2-3 years (Scharen, 1964b).

Disease management

Cultural practice

The primary inoculum can be reduced by crop rotation and burying the infected wheat stubbles (Harrower, 1974; Eyal, 1981). Tillage is necessary to reduce the source of inoculum because the overwintering structures can survive for 2-3 years (Leath et al., 1993). The primary inoculum can also be reduced by removing some grass species that serve as alternative hosts for *P. nodorum* (Leath et al., 1993).

Seed treatment

Infected seed can be an important source of primary inoculum; therefore, seed treatment is useful for disease control. Lagerberg et al. (1996) developed serological methods to identify the pathogen in seeds. Based on the detection information, fungicide is applied to the seed before planting.

Chemical control

Systemic fungicides such as triazole ergosterol biosynthesis inhibitors were widely used for SNB control (Solomon et al., 2006a). Difenoconazole and triadimenol were reported to be more effective (Sundin et al., 1999). The latest family of fungicides to be introduced were the strobilurins. Strobilurins inhibit mitochondrial respiration of fungi, so the direct antifungal effect is important. In addition, strobilurins increase the lifespan of the leaf, thereby reducing sporulation on dead tissue (Solomon et al., 2006a). However, the fourth and fifth generations of *P. nodorum* were shown to be less susceptible to the main ingredient of strobilurin, azoxystrobin (Morzfeld et al., 2004). In addition, other wheat pathogens can develop resistance to strobilurin (Solomon et al., 2006a), therefore the application of strobilurin must be done with caution.

Genetic control of resistance

Sources of resistance to SNB have been found in many wheat cultivars (Xu et al., 2004a). In bread wheat, Krupinsky et al. (1972) identified 16 cultivars with high levels of seedling resistance to SNB. Liu et al. (2004) reported wheat cultivars BR34 and Erik had high levels of SNB resistance at the seedling stage. In synthetic wheat, Friesen et al. (2003) reported 39 synthetic hexaploid wheat lines showing seedling resistance to SNB disease. In durum wheat, resistance to SNB is less common (Xu et al., 2004a) and SNB has become a major problem worldwide. Ma and Hughes (1993) evaluated 100 durum wheat genotypes and found only four genotypes having seedling resistance to three *P. nodorum* isolates. Mullaney et al. (1983) observed that some durum wheat lines showed resistance at the seedling stage but were highly susceptible to SNB in the adult stage. Resistance to SNB has been reported to be quantitative in most cases but qualitative resistance has also been reported (reviewed in Xu et al., 2004b). In the past years, resistance associated with SNB on both the leaf and glume has occasionally been shown to be qualitative (reviewed in Friesen et al., 2009b; Friesen et al., 2009a), but most studies have indicated that resistance to both is quantitatively inherited (Xu et al., 2004b; Friesen et al., 2008a). Czembor et al. (2003) identified four quantitative trait loci (QTL) on chromosomes 2B, 3B, 5B and 5D. Schnurbusch et al. (2003) found resistance QTL on 4BL and 3BS. Arseniuk et al. (2004) identified a QTL associated with SNB resistance on 6AL and a putative QTL on 6D. In 2004, Liu et al. used the International Triticeae Mapping Initiative (ITMI) mapping population to identify a major QTL on chromosome 1BS and minor QTL on 3AS, 4AL, 5AL, 4BL, 7BL and 5DL for seedling resistance to SNB. Toubia-Rahme and Buerstmayr (2003) also identified five QTL on choromosome 2A, 3A, 5A, 2B and 1B for glume blotch resistance. Markers associated with partial resistance to SNB were also identified in durum wheat (Cao et al., 2001). More

recently, necrotrophic effectors (NEs) were found to be critical for SNB disease development, and wheat susceptibility genes corresponding to individual NEs were found to be dominant (Friesen et al., 2008a). Therefore, removal of sensitivity to NEs is critical to solving the problem of SNB.

Necrotrophic effectors

Classification of fungal pathogens

Plant pathogens are often classified into two groups, the biotrophic pathogens and the necrotrophic pathogens. Biotrophic pathogens feed on the living tissue of plants. They do not kill the host cell immediately, because they need the undamaged cells to provide metabolism as a source of nutrition (Prell and Day, 2001). Some pathogens behave as hemi-biotrophs, that is, they may live on the host as biotrophs in the early infection and later on as necrotrophs (Glazebrook, 2005). The attack of most biotrophic pathogens on plants consists of spore germination, hyphal penetration, development of a feeding structure such as a haustoria or intercellular hyphae, and sporulation (Reuber et al., 1998; Vogel and Somerville, 2000). Some other fungal pathogens can penetrate plants through stomata or wounds to get nutrient (Prell and Day, 2001). Defense against many biotrophic pathogens follows a gene-for-gene model. A host resistance gene (R gene) recognizes an avirulence effector gene (Avr gene) product of the pathogen to evoke R gene-mediated resistance. This type of resistance is usually associated with the accumulation of reactive oxygen species (ROS) which is required for a hypersensitive response (HR) resulting in the elimination of the nutrient source for the biotrophic pathogen.

Necrotrophic pathogens derive food from dead and dying cells by killing the host cell quickly after infection and feeding on the nutrients (Glazebrook, 2005). Killing occurs through extracellular enzymes or toxin production. The toxins produced by phytopathogenic fungi that

are toxic to plants are called phytotoxins. The two classes of phytotoxins include non-host-specific toxins (NHST) and host-specific-toxins or host-selective-toxins (HST). NHSTs are toxic to a broader range of plant species, not just to the host species and are rarely the primary determinant of host range (Prell and Day, 2001).

Host-selective toxins

In contrast to NHSTs, HSTs are toxic only to the plants that serve as hosts for the pathogen and have little or no toxicity against non-susceptible plants. HSTs are therefore determinants for host specificity (Prell and Day, 2001). It was reported that a total of 20 pathogens have been found to produce HSTs. Among the HSTs that have been described, some are low-molecular-weight metabolites, and some others are proteins (Wolpert et al., 2002). In most cases, HSTs are the cause for disease. Some studies have shown that disease does not occur if the fungal isolate does not produce the toxins. Therefore, HSTs are often considered pathogenicity factors (Wolpert et al., 2002). Some well described HSTs include victorin, AAL-toxins, T-toxin, HC-toxin, the Ptr toxins, and the necrotrophic effectors (formerly HSTs) produced in *P. nodorum*, all of which are produced by necrotrophic fungal pathogens.

Victorin, a family of cyclized pentapeptides, is produced by the fungus *Cochliobolus victoriae*, the causal agent of Victoria blight of oat (Meehan and Murphy, 1946). Victorin is required for pathogenicity, because the isolates not producing victorin cannot cause disease while all the isolates producing the toxin are pathogenic on oat lines containing the corresponding sensitivity gene (Scheffer et al., 1967). Sensitivity to victorin in oat is conferred by the dominant allele at the host *Vb* locus. The homozygous recessive genotypes (vb vb) are insensitive to the toxin and resistant to Victoria blight of oat (Wolpert et al., 2002). The interaction of victorin with oat causes mitochondrial dysfunction resulting in immediate loss of

electrolytes so that the photo respiratory cycle is broken (Curtis and Wolpert, 2002). In Arabidopsis, victorin sensitivity and disease susceptibility was found to be conferred by LOV1, a coiled-coil nucleotide-binding-leucine-rich repeat (CC-NB-LRR) protein (Lorang et al. 2007). Dysfunction of *LOV1* mutants in victorin insensitive lines were found to be due to mutation in the conserved motifs which are required for resistance. Therefore, *LOV1* was proposed to function as a resistance gene to the naturally occurring pathogens of Arabidopsis (Sweat et al., 2008). Lorang et al. (2012) found that a defense-associated thioredoxin TRX-h5 was involved in the interaction of LOV1 and victorin. In the absence of LOV1, victorin inhibits TRX-h5, resulting in resistance. While in the presence of LOV1, victorin binds with TRX-h5 to activate LOV1 and induce a resistance-like response to cause disease susceptibility.

AAL- toxins including AAL-toxin TA and TB, are a group of HSTs sharing similar structure produced by *Alternaria alternata*, the causal agent of Alternaria stem canker of tomato (Gilchrist and Grogan, 1976). Like victorin, AAL-toxins also dictate the pathogenicity of the pathogen. Sensitivity to AAL- toxin is conditioned by the homozygous recessive alleles at the *asc* locus (Clouse and Gilchrist, 1987). The homozygous dominant genotype (*Asc/ Asc*) is insensitive to the toxin and resistant to the disease (Grogan et al., 1975), whereas the heterozygous genotype (*Asc/asc*) is intermediate for sensitivity (Gilchrist and Grogan, 1976). This group of toxins may be involved in the ceramide signaling pathway to inhibit ceramide syntheses and disrupt the life cycle of cells (Gilchrist et al., 1995).

T-toxin is produced by *Cochliobolus heterostrophus* race T (Levings III et al., 1995). *C. heterostrophus* is the fungal pathogen causing southern corn leaf blight. This disease occurs on maize carrying the Texas cytoplasm for male sterility (*cms-T*) (Levings III et al., 1995). The *cms-T* genotype maize is selectively sensitive to T-toxin. However this does not mean T-toxin is

required for pathogenicity. The T-toxin producing isolates are more virulent than race O, but race O is still pathogenic on T-cytoplasm maize (Yoder et al., 1997). The sensitivity to T-toxin is determined by a 13-kDa protein (URF13) which is encoded by the *T-urf13* gene in the *cms-T* mitochondria (Dewey et al., 1986). This protein is located in the inner mitochondrial membrane. Directly binding to T-toxin leads to a hydrophilic pore formation that permeabilizes the inner mitochondrial membrane (Levings III et al., 1995; Rhoads et al., 1998).

HC-toxin is a cyclic tetrapeptide produced by the fungus *Cochliobolus carbonum*, the pathogen causing northern leaf spot and ear rot of maize (Gross et al., 1982). Among the three races of the pathogen, only race 1 produces this toxin and induces more serious disease symptoms than races 2 and 3 (Scheffer and Ullstrup, 1965). The dominant allele at the host locus *Hm1* encodes the HC-toxin reductase which can inactivate the toxin and lead to resistance to the pathogen (Johal and Briggs, 1992). If the homozygous recessive mutant genotype (*hm1/hm1*) occurs, the host will be fully sensitive to the toxin (Multani et al., 1998). The site of action of HC-toxin is the enzyme histone deacetylase (HDAC) (Brosch et al., 1995). HC-toxin inhibits the activity of HDAC when the core histone H3 and H4 are assembled in chromatin. As a result, the synthesis of the protein involved in the host defense responses is suppressed (Ciuffetti et al., 1995).

Ptr toxins are produced by *Pyrenophora tritici-repentis*, the causal agent of tan spot of wheat. Currently, at least 8 races have been identified and distinguished based on their production of one or more of three HSTs (Ptr ToxA, B, and C) (Lamari et al., 2003). Each of these HSTs provides pathogenicity on susceptible wheat lines. Ptr ToxA, produced by race 1, 2, 7 and 8, was the first proteinaceous HST to be described (Ref). Sensitivity to Ptr ToxA is governed by the *Tsn1* locus (Faris et al., 1996) allowing Ptr ToxA to accumulate within sensitive

cells (Ciuffetti et al., 2010). The toxin is localized to the chloroplast of sensitive wheat mesophyll cells. When *Tsn1* is present, the accumulation of Ptr ToxA leads to the increase of reactive oxygen species resulting in cell death (Manning and Ciuffetti, 2005).

Ptr ToxB is produced by *P. tritici-repentis* races 5, 6, 7 and 8. This toxin is a 6.5 kDa protein with a 23-aa signal peptide (Strelkov et al., 2001; Lamari et al., 2003). Race 3 and race 4 have also been found to carry Ptr ToxB homologs (Strelkov and Lamari, 2003). For Ptr ToxA, a single copy of the gene is sufficient for pathogenicity, however, Ptr ToxB requires more than one copy to cause significant symptoms on susceptible wheat. At least five copies of the Ptr ToxB gene have been found in race 5 (Martinez et al., 2004). Virulence triggered by Ptr ToxB is variable based on the number of gene copies. Numerous studies have indicated that higher copy number increases the virulence of the pathogen (Ciuffetti et al., 2010). The possible mode of action of Ptr ToxB is to trigger a decrease in chlorophyll *a*, *b* and increase the production of ROS (Ciuffetti et al., 2010).

Although all of the HSTs discussed above have different modes of action, and the sensitivities to them are conferred by different gene allele modes of the host (some are governed by homozygous dominant alleles, some by semi-dominant, and some by recessive alleles), many of them trigger PCD or responses that are hallmarks of the classic resistance response induced by avirulence effectors. For example, the oat varieties sensitive to Victorin were all found to be resistant to crown rust disease caused by *Puccinia coronata* due to the dominant *Pc2* crown rust resistance gene in Victoria oat (Litzenberger, 1949; Wolpert et al., 2002). As mentioned above, victorin sensitivity is conferred by the dominant *Vb* gene, and it has been hard to separate the *Vb* gene and the *Pc2* gene (Luke and Wheeler, 1955; Luke et al., 1966). All of these facts indicate that these two gene loci are tightly linked or more likely they are the same gene. However, the

oat – crown rust interaction is a classic gene-for-gene interaction (Luke et al., 1966), that is, an Avr gene product activates the host R gene pathway to trigger a resistance response. Some other studies showed that victorin can induce many plant responses similar to that induced by avirulence effectors, including callose deposition, respiratory burst, and lipid peroxidation (Romanko, 1959; Walton and Earle, 1985; Navarre and Wolpert, 1999). In addition, victorin can induce a PCD-like response including DNA laddering, cell shrinkage and heterochromatin condensation which are similar to animal apoptosis (Singh et al., 1968; Navarre and Wolpert, 1999; Yao et al., 2001). The AAL-toxins can also induce an apoptotic-like response such as DNA laddering and formation of apoptotic-like bodies in the toxin-sensitive hosts (Wang et al., 1996a). The similar responses were also observed in the monkey kidney cells which express AAL-toxins (Wang et al., 1996b; Jones, 2000). Both Victorin and T-toxin can cause dysfunction of the mitochondria. It is known that mitochondria are important in the regulation of the PCD process both in animals and plants (Jones, 2000; Wolpert et al., 2002). Microarray analysis provided evidence that Ptr ToxA was involved in the early up-regulation of PR protein genes and the enzyme genes which play key roles in the phenylpropanoid, jasmonic acid and ethylene biosynthesis pathways (Pandelova et al., 2009). These HST-induced host-pathogen interactions share similar host defense responses to those in the Avr effector-induced host-pathogen interactions. Therefore, HSTs can utilize the host resistance responses to confer a compatible reaction between hosts and pathogens.

Evidence presented so far indicate that HSTs are complicated and are not generally toxic but often act as effectors to elicit a host response. As mentioned above, in some cases, HSTs evoke host induced cell death, indicating that HSTs do not kill the host cells but rather elicit the host to kill its own cells via PCD. Since all HSTs found to be produced by necrotrophic fungi act

as effectors and play a key role in disease development, here we refer to them as necrotrophic effectors (NEs).

Necrotrophic effectors in *P. nodorum*

Like some other plant fungal pathogens, *Parastagonospora. nodorum* has been reported to produce cell wall degrading enzymes such as xylanase, polygalacturonase, cellulase and butyrate esterase that could be involved in disease (Lalaoui et al., 2000). The cell wall degrading enzymes may be critical for penetration and infection of the pathogen. In addition, a low molecular weight cationic acid (Kent and Strobel, 1976) and a toxic compound, septorine (Devys et al., 1978) produced from *P. nodorum* were found to be toxic to wheat. However, none of these toxic compounds mentioned above were found to be host-selective (Bousquet and Skajennikoff, 1974). Keller (1994) found that a crude extract of *P. nodorum* had a selective action in vitro to wheat embryos of different varieties. Wicki (1999) found the crude extract may contain one or more HSTs, and that wheat cultivars with different resistance levels correlated with responses to the crude extracts.

Due in part to a lack of understanding of the disease, Septoria nodorum blotch (SNB) was still a significant problem in the U.S. Resistance associated with SNB on both the leaf and glume has occasionally been shown to be qualitative (reviewed in Friesen et al., 2009b), but most studies have indicated that the resistance to both is quantitatively inherited (Xu et al., 2004b; Friesen et al., 2008a). Since the first *P. nodorum* NE interaction was identified in 2004 (Liu et al., 2004a; 2004b), it has been shown that the wheat-*P. nodorum* pathosystem is dependent on the production of NEs which are recognized by and interact with dominant host sensitivity genes to induce a virulent reaction (Liu et al., 2004a; 2004b; 2006; 2006; Friesen et al., 2007; 2008b). In some cases, NEs in *P. nodorum* can act additively as virulence factors to cause more serious

disease (Friesen et al., 2007). NEs are characterized as determinants of host specificity and are critical to the virulence or pathogenicity of necrotrophic fungal pathogens (Walton, 1996; Friesen et al., 2008a). NEs produced from some necrotrophic pathogens are directly or indirectly recognized by a corresponding dominant host sensitivity gene to cause a susceptible (compatible) reaction (Lamari et al., 2003; Manning and Ciuffetti, 2005; Friesen et al., 2007). This interaction is similar to the classic gene-for-gene model (Flor, 1956), in which the Avr effectors secreted by biotrophic pathogens are recognized by dominant R-gene products in the host, leading to a resistant (incompatible) interaction. Therefore, the NE interaction is described as an inverse gene-for-gene model. If either the NE gene or the host dominant sensitivity gene is absent, the compatible reaction will not occur, leading to resistance.

Currently, nine *P. nodorum* produced NEs have been reported (reviewed in Friesen et al., 2010; Friesen et al., 2012; Zhang et al., 2010; Shi et al., 2015; Gao et al., 2015). Each NE corresponds to a sensitivity gene in wheat that triggers a susceptible reaction which follows an inverse gene-for-gene model.

SnTox1-*Snn1*

SnTox1 was the first NE detected from *P. nodorum*. It was shown to be a secreted protein between 10 and 30kDa in size (Liu et al., 2004a). Host sensitivity to SnTox1 was governed by a single dominant gene designated *Snn1* (Liu et al., 2004b). It was physically and genetically mapped to a gene-rich region on the distal end of the short arm of chromosome 1B using the Chinese Spring wheat chromosome deletion lines and the International Triticeae Mapping Initiative (ITMI) mapping population (Liu et al., 2004b). *Snn1* accounted for 58% of the disease variation across the ITMI population at the 5 day evaluation when inoculating with SnTox1 producing isolates, indicating that SnTox1 plays an important role in SNB disease development

(Liu et al., 2004b). Liu et al. (2012) found the SnTox1-*Snn1* interaction was light-dependent, and both are necessary for pathogen penetration and host cell death. In the *Snn1* wheat genotype, SnTox1 triggers a series of classic defense responses including H_2O_2 production, the up-regulation of PR genes and obvious DNA laddering. To elucidate its molecular nature, *Snn1* was located to a 0.46 cM interval by high-resolution mapping (Reddy et al., 2008). Two EST-based markers which had high homology to NBS-LRR resistance-like genes were found to co-segregate with *Snn1* in 8501 gametes. Two microsatellite markers Xfcp618 and Xpsp3000 were found to delineate *Snn1* to a 0.9cM interval and were consider as particularly diagnostic for *Snn1* (Friesen and Faris, 2010).

SnToxA-*Tsn1*

The SnToxA-*Tsn1* interaction was the second NE-host interaction identified in the wheat-SNB system (Friesen et al., 2006). ToxA was the first proteinaceous NE found in any pathosystem (Friesen and Faris, 2010) and was first purified from the tan spot fungus, *Pyrenophora tritici-repentis* (Tomas and Bockus, 1987; Ballance et al., 1989), another necrotrophic pathogen of wheat and durum, and was designated Ptr ToxA (Ciuffetti et al., 1997; Ballance et al., 1996). The *PtrToxA* gene encodes a 178 amino acid pre-pro-protein containing a signal peptide (Ballance et al., 1996; Ciuffetti et al., 1997), a pro-region or N-domain (residues 23 to 60) and a 13.2 kDa mature peptide (residues 61-178) (Tuori et al., 2000). A 3-dimensional structure analysis of Ptr ToxA revealed that a cell attachment RGD motif (Arg-Gly-Asp) is present in a hydrophilic loop (Sarma et al., 2005). The RGD motif is likely responsible for internalizing Ptr ToxA into the cytoplasm where it localizes to the chloroplast (Sarma et al., 2005). When a GFP-ToxA fusion protein was transformed to wheat by biolistic bombardment, cell death was found in both sensitive and insensitive wheat genotypes (Manning and Ciuffetti,

2005). It is possible that ToxA can trigger some intracellular machinery to cause cell death in both genotypes, but the internalization of Ptr ToxA occurs only in the wheat genotype carrying the corresponding sensitivity gene, *Tsn1* (Manning and Ciuffetti, 2005; Manning et al., 2008). The *SnToxA* gene was shown to be more than 99% identical to the *PtrToxA* gene (Friesen et al., 2006). These two genes were also found to be functionally identical (Liu et al., 2006). The *ToxA* gene has likely been present longer in *P. nodorum* due to the presence of 11 *SnToxA* haplotypes in the *P. nodorum* population, compared to only a single *ToxA* haplotype being present in the *P. tritici-repentis* population (Friesen et al., 2006). The 11kb flanking region of *ToxA* contains a transposase-like gene, which gave a hint of possible movement of *ToxA* from *P. nodorum* to *P. tritici-repentis* (Friesen et al., 2006). Approximately, 40% of a global collection of *P. nodorum* isolates have the *SnToxA* gene (McDonald et al., 2013). Sensitivity to SnToxA is also governed by the dominant *Tsn1* gene, which maps to the long arm of wheat chromosome 5B (Faris et al., 1996). With the work of saturation mapping and BAC contig flanking sequences of the *Tsn1* locus, two microsatellite markers *Xfcp1* and *Xfcp2* were developed which flanked *Tsn1* at genetic distances of 0.3 and 0.5 cM (Haen et al., 2004; Liu et al., 2006). Zhang et al. (2009) developed two additional microsatellite markers *Xfcp394* and *Xfcp620* which delineated *Tsn1* to a 0.07 cM genetic interval. The SnToxA-*Tsn1* interaction accounts for as much as 95% of the SNB variation (Faris and Friesen, 2009). This interaction is light dependent and can cause disruption of host photosynthesis and cell death (Manning and Ciuffetti, 2005; Manning et al., 2009). *Tsn1* contains a serine/threonine protein kinase and NBS-LRR like regions, indicating that *Tsn1* is a disease resistance-like gene (Faris et al., 2010). Tsn1 is not an integrin-like protein or an extracellular receptor-like protein, therefore Tsn1 is likely not the receptor for Ptr ToxA/SnToxA

(Faris et al., 2010). This indicates that ToxA may enter the cell by another mechanism before it is recognized by Tsn1.

SnTox2-*Snn2*

The third NE identified from *P. nodorum* was SnTox2 (Friesen et al., 2007). SnTox2 is also a small secreted protein and is in the size range of 7 to 10 kDa, causing necrosis on wheat genotypes harboring the *Snn2* gene which was located to the short arm of wheat chromosome 2D. A wheat recombinant inbred (RI) population derived from BR34×Grandin segregating for *Snn2* and *Tsn1* was inoculated with *P. nodorum* isolates which produced both SnTox2 and SnToxA. The SnTox2-*Snn2* interaction accounted for 47% of the disease variation, and the SnToxA-*Tsn1* interaction accounted for 20% of the disease variation (Friesen et al., 2007). These two interactions were shown to have additive effects and together they accounted for 65% of the variation in SNB susceptibility. The additive level of disease variation explains that the wheat resistance to SNB is quantitatively inherited, and that *P. nodorum* can produce multiple NEs to cause disease. Zhang et al. (2009) developed an EST-based marker *XTC253803* and a microsatellite marker *Xcfd51*, mapping *Snn2* to a 4.0 cM interval.

SnTox3-*Snn3*

SnTox3 is a 693 bp intron-free gene encoding an immature protein of 230 amino acids containing a 20 amino acid signal peptide, and a 30 amino acid predicted pro-sequence resulting in an 18 kDa mature protein. The six cysteine residues in the mature SnTox3 sequence likely form three disulfide bridges which are important to structure stability and function of the protein (Liu et al., 2009). The host locus conferring sensitivity to SnTox3 locates near the telomere end of the short arm of chromosome 5B (Friesen et al., 2008b) and was designated *Snn3*. The SnTox3-*Snn3* interaction accounted for at most 18% of the disease variation (Friesen et al.,

2008b). In addition, it is less important for disease development, because it is found to be significant only in the absence of the SnToxA-*Tsn1* interaction. The SnToxA-*Tsn1* interaction is epistatic to the SnTox3-*Snn3* interaction, and the SnTox2-*Snn2* interaction was shown to have a relatively stronger effect (Friesen et al., 2008b). Disruption of SnTox3 resulted in elimination of a significant QTL on *Snn3*, but the significant QTL at the other loci such as *Snn2* remained, indicating the SnTox3-*Snn3* interaction is independent of the other NE-host sensitivity gene interactions (Liu et al., 2009; Oliver et al., 2012). A microsatellite marker *Xcfd20* has been identified that is tightly linked to *Snn3* at 0.5 cM. More recently, a gene from *Aegilops tauschii* (Coss.) (2n = 2x = 14, DD genomes), the D-genome donor of hexaploid wheat, has been found to confer SnTox3 sensitivity (Zhang et al., 2010). Zhang et al. (2010) reported this gene to be likely homeologous with *Snn3* and was mapped to the distal end of chromosome arm 5DS. Zhang et al. (2010) designated *Snn3* on 5BS as *Snn3-B1* and the recently reported gene on 5DS as *Snn3-D1*. The subsequent high-resolution mapping work led to observations of the microsatellite markers *Xcfd18* and *Xhbg337*, which delimited *Snn3* to a 1.44 cM interval.

SnTox4-*Snn4*

SnTox4 was estimated to be 10–30 kDa in size and proteinaceous in nature (Abeysekara et al., 2009b). Sensitivity to SnTox4 is conferred by the single dominant gene *Snn*4, which was mapped to the short arm of chromosome 1A. The SnTox4-*Snn4* interaction resulted in a mottled necrotic reaction and accounted for as much as 41% of the disease variation. The EST-based markers *XBG262267* and *XBG262975* and the microsatellite marker *Xcfd58* delineated *Snn4* to a 2.5 cM interval.

SnTox5-*Snn5*

The sixth NE-wheat interaction reported was the SnTox5-*Snn5* interaction. The size of SnTox5 is in the range of 10-30kDa (Friesen et al. 2012). The dominant sensitivity gene *Snn5* mapped to the long arm of wheat chromosome 4B. The SnTox5-*Snn5* interaction conferred 37-63% of the SNB disease variation. The SnTox5-*Snn5* interaction is epistatic to the SnTox3-*Snn3* interaction, while the interactions of SnTox5-*Snn5* and SnToxA-*Tsn1* together increase the level of SNB disease (Friesen et al. 2012).

SnTox6-*Snn6*

The seventh identified interaction was SnTox6-*Snn6* which is also light dependent like several other NE-wheat sensitivity gene interactions (Gao et al., 2015). SnTox6 is a small secreted protein whose size is about 12kDa. The corresponding sensitivity gene *Snn6* was mapped to the long arm of wheat chromosome 6A. The compatible SnTox6-*Snn6* interaction accounted for 27% of the SNB disease variation (Gao et al. 2015) (see Chapter 2).

SnTox7-*Snn7*

The latest reported interaction was SnTox7-*Snn7*. Like the other identified *P. nodorum* NEs, SnTox7 is a small secreted protein with an estimated size of less than 30 kDa. Additionally, SnTox7 was resistant to heat and chemical degradation (Shi et al., 2015). The wheat gene conferring sensitivity to SnTox7 (*Snn7*) mapped to a 2.7-cM interval on the long arm of wheat chromosome 2D. The SnTox7-*Snn7* interaction explained 33% of the SNB disease variation in a population segregating for *Snn7*. The *Snn7* sensitivity allele was evaluated on a set of 52 hexaploid wheat lines with diverse genetic origins. Only a few lines likely carried the *Snn7* allele, showing that *Snn7* is relatively rare.

Genome wide association study

Linkage disequilibrium (LD)

Association mapping, also known as linkage disequilibrium (LD) mapping, is a relatively new genetic method used to analyze complex traits in natural populations (Mackay and Powell, 2007). Association mapping exploits the recombination events at the population level to map markers associated with traits onto genomic regions (Varshney and Tuberosa, 2008). Linkage disequilibrium is (LD) the non-random association of specific alleles at different genetic loci for traits in a natural population (Abdurakhmonov and Abdukarimov, 2008). LD can be affected by many factors such as population size, population structure, recombination rates, mutations, and genetic variation between lineages (Gupta et al., 2005; Mackay and Powell, 2007). In the marker trait association (MTA) analysis, LD correlates the phenotypic variation with the genotype (Borba et al., 2010) and identifies markers associated with traits (Thornsberry et al., 2001; Hirschhorn and Daly, 2005).

Population structure

Population structure, an important component which can reduce false positive association between markers and traits of interest (Kennedy et al., 1992), is a consequence of departure of random mating, resulting in some individuals that are more related than others in a nature population(Breseghello and Sorrells, 2006). Population structure is made of non-random mating within a species, resulting in change of allele frequencies (Ersoz et al., 2008). Non-random mating can be caused by genetic drift or events in domestication. These events may affect the presence ratio of certain markers causing false association with a phenotype (Pritchard et al., 2000b). To account for population structure, statistical approaches including genomic control (GC) and structured association (SA) are exploited to calculate the non-independence of loci and

thereby adjusting for population structure (Ersoz et al., 2008). In association mapping, the program STRUCTURE is designed to calculate the degree of population admixture of every individual using random unlinked markers (Pritchard et al., 2000a). The program STRUCTURE assumes that all individuals are unrelated and keep Hardy-Weinberg equilibrium in a population. Individuals are clustered into subpopulations by calculating the proportion of each individual genome that are derived from different inferred groups using an MCMC Bayesian algorithm, and the association statistics are calculated by stratifying by cluster (Pritchard et al., 2000a). Another approach to compute population structure is principle component analysis (PCA). Principle components (PCs) not only reflect population structure, but also reflect family relatedness (Patterson et al., 2006) and long range LD (Clayton et al., 2005). By computing PCs, these effects can be eliminated by removing related samples, regions of long range LD and low-quality data. In order to account for population structure, PCs capture the genetic ancestry of each individual and fix this effect in a regression-based association test (Price et al., 2006; Price et al., 2010). In PCA, the genotype data is used to infer continuous axes of genetic variation to reduce the data to a small number of dimensions. The top eigenvectors can be inferred as a covariance matrix between individuals. Through computing residuals of linear regression, the genotypes and phenotypes are continuously adjusted by counting the attribution to ancestry along each axis. The ancestry-adjusted genotypes and phenotypes are used for association statistical analysis (Price et al., 2006).

Steps and models of association mapping

The process of association mapping includes (1) Selection of individuals with wide genetic diversity to form a natural population, (2) measuring the phenotypic data of each individual for traits of interest, (3) genotyping each individual using molecular markers, (4)

analyzing the population structure and the relatedness between pairs of each individual and (5) correlating the phenotypic data with genotypic data to identify markers associated with traits of interest (Reich et al., 2001). The models of association mapping include a general linear model (GLM) and a mixed linear model (MLM). GLM models use the subpopulations (Q matrix) as covariates to regress the genotype with phenotype (Thornsberry et al., 2001). The GLM model cannot reduce false positives and have low statistical power (Yu et al., 2006). The MLM model or Q+K model combines population structure (Q-matrix) and relatedness of pairwise individuals, kinship (K matrix) as covariates in regression (Yu et al., 2006). In the Q+K model, random markers are used to estimate the Q and K matrix and then fit them into a mixed model which can cross the boundary of family-based and population-based variance (Yu et al., 2006). Another method is to replace the Q matrix with PCA to consider population structure and family relatedness as the covariances (Zhao et al., 2007; Weber et al., 2008). In the MLM model, genetic similarity of each individual and the heritability of the phenotype are used as covariances between each pair of individuals. This covariance is fixed and the phenotype is regressed with principal components of the genotype matrix or Q matrix (Kang et al., 2010). Therefore, in some cases the MLM model is more effective than the GLM model because the MLM model corrects more false association of the population and relatedness in association (Zhao et al., 2007). Hoffman (2013) introduced the effective degree of freedom to measure MLM complexity and the influence of each PC on the fit of the MLM. By leveraging the MLM framework and the effective degrees of freedom, a novel model, the low rank linear mixed model (LRLMM) was proposed using an algorithm describe by Lippert et al. (2011) to learn the dimensionality of the correction for population structure and kinship. LRLMM produces a low-dimensional fit to the

data and is less affected by a high degree of uncertain strength of the population and kinship correction.

References

Abdurakhmonov, I.Y., and Abdukarimov, A. 2008. Application of association mapping to understanding the genetic diversity of plant germplasm resources. International Journal of Plant Genomics 2008:574927-574927.

Abeysekara, N.S., Friesen, T.L., Keller, B., and Faris, J.D. 2009a. Identification and characterization of a novel host-toxin interaction in the wheat-*Stagonospora nodorum* pathosystem. Theoretical and Applied Genetics 120:117-126.

Abeysekara, N.S., Friesen, T.L., Keller, B., and Faris, J.D. 2009b. Identification and characterization of a novel host-toxin interaction in the wheat-*Stagonospora nodorum* pathosystem. Theoretical and Applied Genetics 120:117-126.

Agrios, G. 1997. Plant pathology. 4th Edition. Academic Press, New York.

Ahmad, S., Gordon-Weeks, R., Pickett, J., and Ton, J. 2010. Natural variation in priming of basal resistance: from evolutionary origin to agricultural exploitation. Molecular Plant Pathology 11:817-827.

Arseniuk, E., Czembor, P.C., Czaplicki, A., Song, Q.J., Cregan, P.B., Hoffman, D.L., and Ueng, P.P. 2004. QTL controlling partial resistance to Stagonospora nodorum leaf blotch in winter wheat cultivar Alba. Euphytica 137:225-231.

Ballance, G., Lamari, L., and Bernier, C. 1989. Purification and characterization of a host-selective necrosis toxin from *Pyrenophora tritici-repentis*. Physiological and Molecular Plant Pathology 35:203-213.

Ballance, G., Lamari, L., Kowatsch, R., and Bernier, C. 1996. Cloning, expression and occurrence of the gene encoding the Ptr necrosis toxin from *Pyrenophora tritici-repentis*. Molecular Plant Pathology.

Bhathal, J.S., Loughman, R., and Speijers, J. 2003. Yield reduction in wheat in relation to leaf disease from yellow (tan) spot and septoria nodorum blotch. European Journal of Plant Pathology 109:435-443.

Bolot, S., Abrouk, M., Masood-Quraishi, U., Stein, N., Messing, J., Feuillet, C., and Salse, J. 2009. The 'inner circle'of the cereal genomes. Current Opinion in Plant Biology 12:119-125.

Borba, d.O., Tereza, C., Brondani, R.P.V., Breseghello, F., Coelho, A.S.G., Mendonca, J.A., Rangel, P.H.N., and Brondani, C. 2010. Association mapping for yield and grain quality traits in rice (Oryza sativa L.). Genetics and Molecular Biology 33:515-524.

Bousquet, J.F., and Skajennikoff, M. 1974. Isolement et mode d'action d'une phytotoxine produite en culture par *Septoria nodorum* Berk. Phytopathology. Zeitsch 80:355-360.

Brennan, R.M., Fitt, B.D.L., Taylor, G.S., and Colhoun, J. 1985. Dispersal of *Septoria nodorum* pycnidiospores by simulated raindrops in still air. Phytopathologische Zeitschrift-Journal of Phytopathology 112:281-290.

Breseghello, F., and Sorrells, M.E. 2006. Association mapping of kernel size and milling quality in wheat (*Triticum aestivum* L.) cultivars. Genetics 172:1165-1177.

Brosch, G., Ransom, R., Lechner, T., Walton, J.D., and Loidl, P. 1995. Inhibition of maize histone deacetylases by HC toxin, the host-selective toxin of Cochliobolus carbonum. The Plant Cell Online 7:1941-1950.

Cao, W., Hughes, G.R., Ma, H., and Dong, Z. 2001. Identification of molecular markers for resistance to Septoria nodorum blotch in durum wheat. Theoretical and Applied Genetics 102:551-554.

Charmet, G. 2011. Wheat domestication: Lessons for the future. Comptes Rendus Biologies.

Ciuffetti, L., Yoder, O., and Turgeon, B. 1992. A microbiological assay for host-specific fungal polyketide toxins. Fungal Genetics Newsl 39:18-19.

Ciuffetti, L., Kim, S.D., Knoche, H., and Dunkle, L. 1995. Maize DNA alkylation and genotype-specific alterations in protein synthesis induced by the host-selective toxin produced by Cochliobolus carbonum. Physiological and Molecular Plant Pathology 46:61-70.

Ciuffetti, L.M., Tuori, R.P., and Gaventa, J.M. 1997. A single gene encodes a selective toxin causal to the development of tan spot of wheat. The Plant Cell Online 9:135-144.

Ciuffetti, L.M., Manning, V.A., Pandelova, I., Betts, M.F., and Martinez, J.P. 2010. Host-selective toxins, Ptr ToxA and Ptr ToxB, as necrotrophic effectors in the *Pyrenophora tritici-repentis*-wheat interaction. New Phytologist 187:911-919.

Clayton, D.G., Walker, N.M., Smyth, D.J., Pask, R., Cooper, J.D., Maier, L.M., Smink, L.J., Lam, A.C., Ovington, N.R., Stevens, H.E., Nutland, S., Howson, J.M.M., Faham, M., Moorhead, M., Jones, H.B., Falkowski, M., Hardenbol, P., Willis, T.D., and Todd, J.A. 2005. Population structure, differential bias and genomic control in a large-scale, case-control association study. Nature Genetics 37:1243-1246.

Clouse, S., and Gilchrist, D. 1987. Interaction of the asc locus in F8 paired lines of tomato with Alternaria alternata f. sp. lycopersici and AAL-toxin. Phytopathology 77:80.

Cunfer, B.M. 1978. The incidence of *Septoria nodorum* in wheat seed. Phytopathology 68:832-835.

Cunfer, B.M. 1983. Epidemiology and control of seed-born *Septoria nodorum* on wheat. Seed Science and Technology 11:707-718.

Curtis, M.J., and Wolpert, T.J. 2002. The oat mitochondrial permeability transition and its implication in victorin binding and induced cell death. The Plant Journal 29:295-312.

Czembor, P.C., Arseniuk, E., Czaplicki, A., Song, Q.J., Cregan, P.B., and Ueng, P.P. 2003. QTL mapping of partial resistance in winter wheat to Stagonospora nodorum blotch. Genome 46:546-554.

Devys, M., Bousquet, J.F., Kollmann, A., and Barbier, M. 1978. La septorine, nouvelle pyrazine substitiuée, isolée du milieu de culture de *Septoria nodorum* Berk. Champignon phytopathogéne. Comptes Rendu Hebdomadaires des Séances de L' Académie des Sciences, Série C 286:457-458.

Dewey, R., Levings, C., and Timothy, D. 1986. Novel recombinations in the maize mitochondrial genome produce a unique transcriptional unit in the Texas male-sterile cytoplasm. Cell 44:439-449.

Djurle, A., Ekbom, B., and Yuen, J.E. 1996. The relationship of leaf wetness duration and disease progress of glume blotch, caused by *Stagonospora nodorum*, in winter wheat to standard weather data. European Journal of Plant Pathology 102:9-20.

Dubcovsky, J., and Dvorak, J. 2007. Genome plasticity a key factor in the success of polyploid wheat under domestication. Science 316:1862.

Dvorak, J., di Terlizzi, P., Zhang, H.B., and Resta, P. 1993. The evolution of polyploid wheats: identification of the A genome donor species. Genome 36:21-31.

Ersoz, E.S., Yu, H., and Buckler, E.S. 2008. Applications of linkage disequilibrium and association mapping in crop plants. Springer Series on Biofilms 2:97-119.

Eulgem, T., Rushton, P.J., Schmelzer, E., Hahlbrock, K., and Somssich, I.E. 1999. Early nuclear events in plant defence signalling: rapid gene activation by WRKY transcription factors. Embo Journal 18:4689-4699.

Eyal, Z. 1981. Integrated control of septoria diseases of wheat. Plant Disease 65:763-768.

Eyal, Z. 1987. The Septoria diseases of wheat: concepts and methods of disease management. CIMMYT, Mexico.

Eyal, Z. 1999. The Septoria tritici and Stagonospora nodorum blotch diseases of wheat. European Journal of Plant Pathology 105:629-641.

Faris, J., Anderson, J., Francl, L., and Jordahl, J. 1996. Chromosomal location of a gene conditioning insensitivity in wheat to a necrosis-inducing culture filtrate from *Pyrenophora tritici-repentis*. Phytopathology 86:459-463.

Faris, J.D., and Friesen, T.L. 2009. Reevaluation of a tetraploid wheat population indicates that the Tsn1-ToxA interaction is the only factor governing Stagonospora nodorum blotch susceptibility. Phytopathology 99:906-912.

Faris, J.D., Friebe, B., and Gill, B.S. 2002. Wheat genomics: Exploring the polyploid model. Current Genomics 3:577-591.

Faris, J.D., Zhang, Z., Lu, H., Lu, S., Reddy, L., Cloutier, S., Fellers, J.P., Meinhardt, S.W., Rasmussen, J.B., and Xu, S.S. 2010. A unique wheat disease resistance-like gene governs effector-triggered susceptibility to necrotrophic pathogens. Proceedings of the National Academy of Sciences 107:13544-13549.

Feldman, M. 2000. Origin of cultivated wheat. The World Wheat Book, A history of wheat breeding:W.J. pp. 3–56.

Fitt, B.D.L., McCartney, H.A., and Walklate, P.J. 1989. The role of rain in dispersal of pathogen inoculum. Annual Review of Phytopathology 27:241-270.

Flor, H. 1956. The complementary genic systems in flax and flax rust. Advances in genetics 8:29-54.

Flors, V., Ton, J., Jakab, G., and Mauch-Mani, B. 2005. Abscisic acid and callose: Team players in defence against pathogens? Journal of Phytopathology 153:377-383.

Fried, P., and Meister, E. 1987. Inheritance of leaf and head resistance of winter wheat to *Septoria nodorum* in a diallel cross. Phytopathology 77:1371-1375.

Friesen, T.L., and Faris, J.D. 2010. Characterization of the wheat-*Stagonospora nodorum* disease system: what is the molecular basis of this quantitative necrotrophic disease interaction? Canadian Journal of Plant Pathology 32:20-28.

Friesen, T.L., Meinhardt, S.W., and Faris, J.D. 2007. The *Stagonospora nodorum*-wheat pathosystem involves multiple proteinaceous host-selective toxins and corresponding host sensitivity genes that interact in an inverse gene-for-gene manner. The Plant Journal 51:681-692.

Friesen, T.L., Faris, J.D., Solomon, P.S., and Oliver, R.P. 2008a. Host-specific toxins: effectors of necrotrophic pathogenicity. Cellular Microbiology 10:1421-1428.

Friesen, T.L., Chu, C.G., Xu, S.S., and Faris, J.D. 2012. SnTox5-*Snn5*: a novel *Stagonospora nodorum* effector-wheat gene interaction and its relationship with the SnToxA-*Tsn1* and SnTox3-*Snn3-B1* interactions. Molecular Plant Pathology 13:1101-1109.

Friesen, T.L., Zhang, Z., Solomon, P.S., Oliver, R.P., and Faris, J.D. 2008b. Characterization of the interaction of a novel *Stagonospora nodorum* host-selective toxin with a wheat susceptibility gene. Plant Physiology 146:682-693.

Friesen, T.L., Xu, S.S., Faris, J.D., Rasmussen, J.B., Miller, J.D., and Harris, M.D. (2003). In Proceedings of the 10th International Wheat Genetics Symposium, N.E. Pogna, M. Romano, E.A. Pogna, and G. Galterio, eds (Pasetum, Italy: Istituto Sperimentale per la Cerealicoltura, Rome, Italy), pp. 1133-1135.

Friesen, T.L., Chu, C.G., Liu, Z.H., Xu, S.S., Halley, S., and Faris, J.D. 2009a. Host-selective toxins produced by *Stagonospora nodorum* confer disease susceptibility in adult wheat plants under field conditions. Theoretical and Applied Genetics 118:1489-1497.

Friesen, T.L., Chu, C.G., Liu, Z., Xu, S., Halley, S., and Faris, J. 2009b. Host-selective toxins produced by *Stagonospora nodorum* confer disease susceptibility in adult wheat plants under field conditions. Theoretical and Applied Genetics 118:1489-1497.

Friesen, T.L., Stukenbrock, E.H., Liu, Z., Meinhardt, S., Ling, H., Faris, J.D., Rasmussen, J.B., Solomon, P.S., McDonald, B.A., and Oliver, R.P. 2006. Emergence of a new disease as a result of interspecific virulence gene transfer. Nature Genetics 38:953-956.

Gao, Y., Faris, J.D., Liu, Z., Kim, Y.M., Syme, R.A., Oliver, R.P., Xu, S.S., and Friesen, T.L. 2015. Identification and Characterization of the SnTox6-*Snn6* Interaction in the *Parastagonospora nodorum*-Wheat Pathosystem. Molecular Plant-Microbe Interactions 28:615-625.

Gaut, B.S. 2002. Evolutionary dynamics of grass genomes. New phytologist 154:15-28.

Gilchrist, D., and Grogan, R. 1976. Production and nature of a host-specific toxin from *Alternaria alternata* f. *sp. lycopersici.* Phytopathology 66:165.

Gilchrist, D.G., Bostock, R.M., and Wang, H. 1995. Sphingosine-related mycotoxins in plant and animal diseases. Canadian Journal of Botany 73:459-467.

Glazebrook, J. 2005. Contrasting mechanisms of defense against biotrophic and necrotrophic pathogens. Annual Review of Phytopathology 43:205-227.

Goodwin, S.B., and Zismann, V.L. 2001. Phylogenetic analyses of the ITS region of ribosomal DNA reveal that *Septoria passerinii* from barley is closely related to the wheat pathogen *Mycosphaerella graminicola*. Mycologia 93:934-946.

Grogan, R., Kimble, K., and Misaghi, I. 1975. A stem canker disease of tomato caused by *Alternaria alternata* f. *sp*. *lycopersici*. Phytopathology 65:880-886.

Gross, M.L., McCrery, D., Crow, F., Tomer, K.B., Pope, M., Ciuffetti, L., Knoche, H., Daly, J., and Dunkle, L. 1982. The structure of the toxin from *Helminthosporium carbonum*. Tetrahedron Letters 23:5381-5384.

Gupta, P.K., Rustgi, S., and Kulwal, P.L. 2005. Linkage disequilibrium and association studies in higher plants: Present status and future prospects. Plant Molecular Biology 57:461-485.

Haen, K.M., Lu, H., Friesen, T.L., and Faris, J.D. 2004. Genomic targeting and high-resolution mapping of the Tsn1 gene in wheat. Genome 45:706-718.

Harrower, K.M. 1974. Survival and regeneration of *Leptoshaeria nodorum* in wheat debris. Transactions of the British Mycological Society 63:527-533.

Heil, M., and Ton, J. 2008. Long-distance signalling in plant defence. Trends in Plant Science 13:264-272.

Heun, M., Schafer-Pregl, R., Klawan, D., Castagna, R., Accerbi, M., Borghi, B., and Salamini, F. 1997. Site of einkorn wheat domestication identified by DNA fingerprinting. Science 278:1312.

Hirschhorn, J.N., and Daly, M.J. 2005. Genome-wide association studies for common diseases and complex traits. Nature Reviews Genetics 6:95-108.

Hoffman, G.E. 2013. Correcting for population structure and kinship using the linear mixed model: theory and extensions. Plos One 8: e75707.

Huang, S., Sirikhachornkit, A., Su, X., Faris, J., Gill, B., Haselkorn, R., and Gornicki, P. 2002. Genes encoding plastid acetyl-CoA carboxylase and 3-phosphoglycerate kinase of the Triticum/Aegilops complex and the evolutionary history of polyploid wheat. Proceedings of the National Academy of Sciences 99:8133.

Johal, G.S., and Briggs, S.P. 1992. Reductase activity encoded by the HM1 disease resistance gene in maize. Science 258:985.

Jones, A. 2000. Does the plant mitochondrion integrate cellular stress and regulate programmed cell death? Trends in Plant Science 5:225-230.

Jones, J.D.G., and Dangl, J.L. 2006. The plant immune system. Nature 444:323-329.

Kang, H.M., Sul, J.H., Service, S.K., Zaitlen, N.A., Kong, S.-y., Freimer, N.B., Sabatti, C., and Eskin, E. 2010. Variance component model to account for sample structure in genome-wide association studies. Nature Genetics 42:348-U110.

Karjalainen, R., Laitinen, A., and Juuti, T. 1983. Effects of *Septoria nodorum* Berk. on yield and yield components of spring wheat. Journal of the Scientific Agricultural Society of Finland 55:333-344.

Keller, B., Winzeler, H., Winzeler, M., and Fried, P. 1994. Differential sensitivity of wheat embryos against extracts containing toxins of *Septoria nodorum*: First steps towards in vitro selection. Journal of Phytopathology 141:233-240.

Kellogg, E.A. 2001. Evolutionary history of the grasses. Plant Physiology 125:1198-1205.

Kennedy, B.W., Quinton, M., and Vanarendonk, J.A.M. 1992. Estimation of effects of single genes on quantitative traits. Journal of Animal Science 70:2000-2012.

Kent, S.S., and Strobel, G.A. 1976. Phytotoxin from *Septoria nodorum*. Transactions of the British Mycological Society 67:354-358.

Kihara, H. 1944. Discovery of the DD-analyser, one of the ancestors of Triticum vulgare. Agric. Hortic 19:13-14.

Kihara, H. 1966. Factors affecting the evolution of common wheat. The Indian Journal of Genetics & Plant Breeding 26A:14-28.

King, J., Cook, R., and Melville, S. 1983. A review of Septoria diseases of wheat and barley. Annals of Applied Biology 103:345-373.

Krupinsk, J. M., Scharen, A.L., and Schillin.Ja. 1972. Resistance in wheat to *Septoria nodorum*. Crop Science 12:528-530.

Lagerberg, C., Gripwall, E., and Wiik, L. 1996. Detection and quantification of seed-borne *Septoria nodorum* in naturally infected grains of wheat with polyclonal ELISA. Seed Science and Technology 23:609-615.

Lalaoui, F., Halama, P., Dumortier, V., and Paul, B. 2000. Cell wall-degrading enzymes produced in vitro by isolates of *Phaeosphaeria nodorum* differing in aggressiveness. Plant Pathology 49:727-733.

Lamari, L., Strelkov, S., Yahyaoui, A., Orabi, J., and Smith, R. 2003. The identification of two new races of *Pyrenophora tritici-repentis* from the host center of diversity confirms a one-to-one relationship in tan spot of wheat. Phytopathology 93:391-396.

Leath, S., Scharen, A.L., Dietzholmes, M.E., and Lund, R.E. 1993. Factors associated with global occurrences of Septoria nodorum blotch and Septoria tritici blotch of wheat. Plant Disease 77:1266-1270.

Levings III, C.S., Rhoads, D.M., and Siedow, J.N. 1995. Molecular interactions of *Bipolaris maydis* T-toxin and maize. Canadian Journal of Botany 73:483-489.

Lippert, C., Listgarten, J., Liu, Y., Kadie, C.M., Davidson, R.I., and Heckerman, D. 2011. FaST linear mixed models for genome-wide association studies. Nature Methods 8:833-U894.

Litzenberger, S. 1949. Nature of susceptibility to *Helminthosporium victoriae* and resistance to *Puccinia coronata* in Victoria oats. Phytopathology 39:300-318.

Liu, Z. 2006. Genomic mapping of toxin sensitivity and quantitative trait loci for seedling resistance to Stagonospora nodorum blotch in wheat. In Plant pathology (Fargo, North Dakota: North Dakota State University).

Liu, Z., Faris, J., Meinhardt, S., Ali, S., Rasmussen, J., and Friesen, T. 2004a. Genetic and physical mapping of a gene conditioning sensitivity in wheat to a partially purified host-selective toxin produced by *Stagonospora nodorum*. Phytopathology 94:1056-1060.

Liu, Z., Friesen, T., Rasmussen, J., Ali, S., Meinhardt, S., and Faris, J. 2004b. Quantitative trait loci analysis and mapping of seedling resistance to Stagonospora nodorum leaf blotch in wheat. Phytopathology 94:1061-1067.

Liu, Z., Faris, J.D., Oliver, R.P., Tan, K.C., Solomon, P.S., McDonald, M.C., McDonald, B.A., Nunez, A., Lu, S., and Rasmussen, J.B. 2009. SnTox3 acts in effector triggered susceptibility to induce disease on wheat carrying the *Snn3* gene. PLoS Pathogens 5:e1000581.

Liu, Z., Zhang, Z., Faris, J.D., Oliver, R.P., Syme, R., McDonald, M.C., McDonald, B.A., Solomon, P.S., Lu, S., and Shelver, W.L. 2012. The Cysteine Rich Necrotrophic Effector SnTox1 Produced by *Stagonospora nodorum* Triggers Susceptibility of Wheat Lines Harboring *Snn1*. PLoS Pathogens 8:1-24.

Liu, Z.H., Friesen, T.L., Ling, H., Meinhardt, S.W., Oliver, R.P., Rasmussen, J.B., and Faris, J.D. 2006. The Tsn1-ToxA interaction in the wheat-*Stagonospora nodorum* pathosystem parallels that of the wheat-tan spot system. Genome 49:1265-1273.

Luke, H., and Wheeler, H. 1955. Toxin production by *Helminthosporium victoriae*. Phytopathology 45:453-458.

Luke, H., Murphy, H., and Peter, F. 1966. Inheritance of spontaneous mutations of the Victoria locus in oats. Phytopathology 56:210-212.

Ma, H., and Hughes, G.R. 1993. Resistance to Septoria nodorum blotch in several Tricitum species. Euphytica 70:151-157.

Machacek, J.E. 1945. The prevalence of septoria on cereal seed in Canada. Phytopathology 35:51-53.

Mackay, I., and Powell, W. 2007. Methods for linkage disequilibrium mapping in crops. Trends in Plant Science 12:57-63.

Manning, V.A., and Ciuffetti, L.M. 2005. Localization of Ptr ToxA produced by *Pyrenophora tritici-repentis* reveals protein import into wheat mesophyll cells. The Plant Cell Online 17:3203-3212.

Manning, V.A., Hamilton, S.M., Karplus, P.A., and Ciuffetti, L.M. 2008. The Arg-Gly-Asp-containing, solvent-exposed loop of Ptr ToxA is required for internalization. Molecular Plant-Microbe Interactions 21:315-325.

Manning, V.A., Chu, A.L., Steeves, J.E., Wolpert, T.J., and Ciuffetti, L.M. 2009. A host-selective toxin of *Pyrenophora tritici-repentis*, Ptr ToxA, induces photosystem changes and reactive oxygen species accumulation in sensitive wheat. Molecular Plant-Microbe Interactions 22:665-676.

Martinez, J.P., Oesch, N.W., and Ciuffetti, L.M. 2004. Characterization of the multiple-copy host-selective toxin gene, ToxB, in pathogenic and nonpathogenic isolates of *Pyrenophora tritici-repentis*. Molecular Plant-Microbe Interactions 17:467-474.

Matsuoka, Y. 2011. Evolution of polyploid Triticum Wheats under cultivation: the role of domestication, natural hybridization and allopolyploid speciation in their diversification. Plant and Cell Physiology 52:750.

McDonald, M.C., Oliver, R.P., Friesen, T.L., Brunner, P.C., and McDonald, B.A. 2013. Global diversity and distribution of three necrotrophic effectors in *Phaeosphaeria nodorum* and related species. New Phytologist 199:241-251.

McFadden, E., and Sears, E. 1944. The artificial synthesis of Triticum spelta. Records of the Genetics Society of America 13:26-27.

McMullen, M., Rasmussen, J.B., Friesen, T.L., and Ali, S. 2002. Prevalence and severity of tan spot and the Septoria leaf disease complex on wheat and relationship to previous crop, North Dakota 1998-2001. In In Proceedings of Fourth International Wheat Tan Spot and Spot Blotch Workshop (Bemidji, Minnesota, USA: Agricultural Experiment Station, North Dakota State University, 2003), pp. 1-7.

Meehan, F., and Murphy, H. 1946. A new Helminthosporium blight of oats. Science (New York, NY) 104:413.

Morzfeld, J., Koopmann, B., and Hoppe, H.H. 2004. Development of fungicide resistance of wheat and barley pathogens against strobilurins: A methodological approach. Zeitschrift Fur Pflanzenkrankheiten Und Pflanzenschutz-Journal of Plant Diseases and Protection 111:105-114.

Mullaney, E.J., Scharen, A.L., and Bryan, M.D. 1983. Resistance to *Septoria nodorum* in a durum wheat cultivar as determined by stage of host development. Canadian Journal of Botany-Revue Canadienne De Botanique 61:2248-2250.

Multani, D., Meeley, R., Paterson, A., Gray, J., Briggs, S., and Johal, G. 1998. Plant-pathogen microevolution: molecular basis for the origin of a fungal disease in maize. Proceedings of the National Academy of Sciences 95:1686.

Navarre, D.A., and Wolpert, T.J. 1999. Victorin induction of an apoptotic/senescence-like response in oats. The Plant Cell Online 11:237-250.

Nelson, L.R., Morey, D.D., and Brown, A.R. 1974. Wheat cultivar responses to severe glume blotch in Georgia. Plant Disease Reporter 58:21-23.

Oliver, R., Friesen, T.L., Faris, J.D., and Solomon, P.S. 2012. *Stagonospora nodorum*: From Pathology to Genomics and Host Resistance. Annual Review of Phytopathology.

Pandelova, I., Betts, M.F., Manning, V.A., Wilhelm, L.J., Mockler, T.C., and Ciuffetti, L.M. 2009. Analysis of transcriptome changes induced by Ptr ToxA in wheat provides insights into the mechanisms of plant susceptibility. Molecular Plant 2:1067-1083.

Patterson, N., Price, A.L., and Reich, D. 2006. Population structure and eigenanalysis. Plos Genetics 2:2074-2093.

Peng, J.H., Sun, D., and Nevo, E. 2011. Domestication evolution, genetics and genomics in wheat. Molecular Breeding:1-21.

Petersen, G., Seberg, O., Yde, M., and Berthelsen, K. 2006. Phylogenetic relationships of Triticum and Aegilops and evidence for the origin of the A, B, and D genomes of common wheat (*Triticum aestivum*). Molecular Phylogenetics and Evolution 39:70-82.

Prell, H.H., and Day, P.R. 2001. Plant-fungal pathogen interaction: a classical and molecular view. Springer Verlag.

Price, A.L., Zaitlen, N.A., Reich, D., and Patterson, N. 2010. New approaches to population stratification in genome-wide association studies. Nature Reviews Genetics 11:459-463.

Price, A.L., Patterson, N.J., Plenge, R.M., Weinblatt, M.E., Shadick, N.A., and Reich, D. 2006. Principal components analysis corrects for stratification in genome-wide association studies. Nature Genetics 38:904-909.

Pritchard, J.K., Stephens, M., and Donnelly, P. 2000a. Inference of population structure using multilocus genotype data. Genetics 155:945-959.

Pritchard, J.K., Stephens, M., Rosenberg, N.A., and Donnelly, P. 2000b. Association mapping in structured populations. American Journal of Human Genetics 67:170-181.

Quaedvlieg, W., Verkley, G.J.M., Shin, H.D., Barreto, R.W., Alfenas, A.C., Swart, W.J., Groenewald, J.Z., and Crous, P.W. 2013. Sizing up Septoria. Studies in Mycology:307-390.

Rapilly, F., Foucault, B., and Lacazedieux, J. 1973. Study of the inoculum of *Septoria nodorum* Berk.(*Leptosphaeria nodorum* Muller) agent of glume blotch of wheat. I. Ascospores. Annales de Phytopathologie.

Reddy, L.F., Meinhardt, T.L., Chao, S.W., Faris, S., and Justin, D. 2008. Genomic analysis of the *Snn1* locus on wheat chromosome arm 1BS and the identification of candidate genes. The Plant Genome 1:55.

Reich, D.E., Cargill, M., Bolk, S., Ireland, J., Sabeti, P.C., Richter, D.J., Lavery, T., Kouyoumjian, R., Farhadian, S.F., Ward, R., and Lander, E.S. 2001. Linkage disequilibrium in the human genome. Nature 411:199-204.

Reuber, T.L., Plotnikova, J.M., Dewdney, J., Rogers, E.E., Wood, W., and Ausubel, F.M. 1998. Correlation of defense gene induction defects with powdery mildew susceptibility in Arabidopsis enhanced disease susceptibility mutants. The Plant Journal 16:473-485.

Rhoads, D., Brunner-Neuenschwander, B., Levings III, C., and Siedow, J. 1998. Characterization of the interaction between fungal pathotoxins and Urf13, the cms-T maize mitochondrial T-toxin receptor. Developments in Plant Pathology 13.

Romanko, R. 1959. A physiological basis for resistance of oats to victoria blight. Phytopathology 49:32-36.

Saari, E.E., and Wilcoxson, R.D. 1974. Plant disease situation of high yielding dwarf wheats in Asia and Africa. Annual Review of Phytopathology 12:49-68.

Salamini, F., Ozkan, H., Brandolini, A., Schafer-Pregl, R., and Martin, W. 2002. Genetics and geography of wild cereal domestication in the Near East. Nature Reviews Genetics 3:429-441.

Sarma, G.N., Manning, V.A., Ciuffetti, L.M., and Karplus, P.A. 2005. Structure of Ptr ToxA: An RGD-containing host-selective toxin from *Pyrenophora tritici-repentis*. The Plant Cell Online 17:3190-3202.

Scharen, A.L. 1964a. Environmental influences on development of glume blotch in wheat. Phytopathology 54:300.

Scharen, A.L. 1964b. Environmental influences on development of glume blotch in wheat. Phytopathology 54:300-&.

Scharen, A.L., and Krupinsk, J. M. 1969. Effect of *Septoria nodorum* infection of CO_2 absorption and yield of wheat. Phytopathology 59:1298-1301.

Scheffer, R., and Ullstrup, A. 1965. A host-specific toxic metabolite from *Helminthosporium carbonum*. Phytopathology 55:1037-1038.

Scheffer, R., Nelson, R., and Ullstrup, A. 1967. Inheritance of toxin production and pathogenicity in *Cochliobolus carbonum* and *Cochliobolus victoriae*. Phytopathology 57:1288-1291.

Schnurbusch, T., Paillard, S., Fossati, D., Messmer, M., Schachermayr, G., Winzeler, M., and Keller, B. 2003. Detection of QTLs for Stagonospora glume blotch resistance in Swiss winter wheat. Theoretical and Applied Genetics 107:1226-1234.

Shaner, G., and Buechley, G. 1995. Epidemiology of leaf blotch of soft red winter wheat caused by *Septoria tritici* and *Stagonospora nodorum*. Plant Disease 79:928-938.

Shewry, P. 2009. Wheat. Journal of Experimental Botany 60:1537-1553.

Shi, G., Friesen, T.L., Saini, J., Xu, S.S., Rasmussen, J.B., and Faris, J.D. 2015. The Wheat *Snn7* Gene Confers Susceptibility on Recognition of the *Parastagonospora nodorum* Necrotrophic Effector SnTox7. Plant Genome 8. doi:10.3835/plantgenome2015.02.0007

Singh, R., Wallace, A., and Browning, R. 1968. Mitotic inhibition and histological changes induced by Helminthosporium victoriaetoxin in susceptible oats (Avena byzantina C. Koch). Crop Science 8:143-146.

Slageren, M.W.S.J.M., and Areas, I.C.f.A.R.i.t.D. 1994. Wild Wheats: A Monograph of Aegilops L. and Amblyopyrum (Jaub. & Spach) Eig (Poaceae): a Revision of All Taxa Closely Related to Wheat, Excluding Wild Triticum Species, with Notes on Other Genera in the Tribe Triticcae, Especially Triticum. Wageningen Agricultural University.

Solomon, P.S., Lowe, R.G.T., Tan, K.C., Waters, O.D.C., and Oliver, R.P. 2006a. *Stagonospora nodorum*: cause of Stagonospora nodorum blotch of wheat. Molecular Plant Pathology 7:147-156.

Solomon, P.S., Wilson, T.J.G., Rybak, K., Parker, K., Lowe, R.G.T., and Oliver, R.P. 2006b. Structural characterisation of the interaction between *Triticum aestivum* and the dothideomycete pathogen *Stagonospora nodorum*. European Journal of Plant Pathology 114:275-282.

Strelkov, S., and Lamari, L. 2003. Host-parasite interactions in tan spot [*Pyrenophora tritici-repentis*] of wheat. Canadian Journal of Plant Pathology 25:339-349.

Strelkov, S.E., Lamari, L., Sayoud, R., and Smith, R.B. 2001. Comparative virulence of chlorosis-inducing races of *Pyrenophora tritici-repentis*. Canadian Journal of Plant Pathology 24:29-35.

Sundin, D.R., Bockus, W.W., and Eversmeyer, M.G. 1999. Triazole seed treatments suppress spore production by *Puccinia recondita*, *Septoria tritici*, and *Stagonospora nodorum* from wheat leaves. Plant Disease 83:328-332.

Thornsberry, J.M., Goodman, M.M., Doebley, J., Kresovich, S., Nielsen, D., and Buckler, E.S. 2001. Dwarf8 polymorphisms associate with variation in flowering time. Nature Genetics 28:286-289.

Tomas, A., and Bockus, W. 1987. Cultivar-specific toxicity of culture filtrates of *Pyrenophora tritici-repentis*. Phytopathology 77:1337-1340.

Torres, M.A., Jones, J.D.G., and Dangl, J.L. 2006. Reactive oxygen species signaling in response to pathogens. Plant Physiology 141:373-378.

Toubia-Rahme, H., and Buerstmayr, H. (2003). Molecular mapping of QTLs for Stagonospora nodorum blotch resistance in the spring wheat line CM-82036. In Proceedings of the 6th International Symposium on Septoria and Stagonospora Diseases of Cereals., G.H.J. Kema, M. van Ginkel, and H. M., eds (Tunis, Tunisia: Global insights into the Septoria and Stagonospora Diseases of Cereals), pp. 143-147.

Tsunewaki, K. 2009. Plasmon analysis in the Triticum-Aegilops complex. Breeding Science 59:455-470.

Tuori, R.P., Wolpert, T.J., and Ciuffetti, L.M. 2000. Heterologous expression of functional Ptr ToxA. Molecular Plant-Microbe Interactions 13:456-464.

Varshney, R.K., and Tuberosa, R. 2008. Genomics-assisted crop improvement: An overview. Springer Series on Biofilms 2:1-12.

Vogel, J., and Somerville, S. 2000. Isolation and characterization of powdery mildew-resistant Arabidopsis mutants. Proceedings of the National Academy of Sciences 97:1897.

Walton, J.D. 1996. Host-selective toxins: agents of compatibility. The plant cell 8:1723.

Walton, J.D., and Earle, E.D. 1985. Stimulation of extracellular polysaccharide synthesis in oat protoplasts by the host-specific phytotoxin victorin. Planta 165:407-415.

Wang, H., Li, J., Bostock, R.M., and Gilchrist, D.G. 1996a. Apoptosis: a functional paradigm for programmed plant cell death induced by a host-selective phytotoxin and invoked during development. The Plant Cell Online 8:375-391.

Wang, W., Jones, C., Ciacci-Zanella, J., Holt, T., Gilchrist, D.G., and Dickman, M.B. 1996b. Fumonisins and Alternaria alternata lycopersici toxins: sphinganine analog mycotoxins induce apoptosis in monkey kidney cells. Proceedings of the National Academy of Sciences 93:3461.

Weber, A.L., Briggs, W.H., Rucker, J., Baltazar, B.M., de Jesus Sanchez-Gonzalez, J., Feng, P., Buckler, E.S., and Doebley, J. 2008. The Genetic Architecture of Complex Traits in Teosinte (Zea mays ssp parviglumis): New Evidence From Association Mapping. Genetics 180:1221-1232.

Weber, G.F. 1992. Septoria diseases of cereals. II. Septoria diseases of Wheat. Phytopathology 12:537-585.

Wicki, W., Winzeler, M., Schmid, J., Stamp, P., and Messmer, M. 1999. Inheritance of resistance to leaf and glume blotch caused by *Septoria nodorum* Berk. in winter wheat. Theoretical and Applied Genetics 99:1265-1272.

Wolpert, T.J., Dunkle, L.D., and Ciuffetti, L.M. 2002. Host-Selective Toxins and Avirulence Determinants: What's in a Name? Annual Review of Phytopathology 40:251-285.

Xu, S., Friesen, T., and Cai, X. 2004a. Sources and genetic control of resistance to Stagonospora nodorum blotch in wheat. Recent Research Developments in Genetics & Breeding 1:449-469.

Yao, N., Tada, Y., Park, P., Nakayashiki, H., Tosa, Y., and Mayama, S. 2001. Novel evidence for apoptotic cell response and differential signals in chromatin condensation and DNA cleavage in victorin-treated oats. The Plant Journal 28:13-26.

Yoder, O., Macko, V., Wolpert, T., and Turgeon, B. 1997. *Cochliobolus spp*. and their host-specific toxins. The Mycota 5:145-166.

Yu, J.M., Pressoir, G., Briggs, W.H., Bi, I.V., Yamasaki, M., Doebley, J.F., McMullen, M.D., Gaut, B.S., Nielsen, D.M., Holland, J.B., Kresovich, S., and Buckler, E.S. 2006. A unified mixed-model method for association mapping that accounts for multiple levels of relatedness. Nature Genetics 38:203-208.

Zhang, Z., Friesen, T.L., Simons, K.J., Xu, S.S., and Faris, J.D. 2009. Development, identification, and validation of markers for marker-assisted selection against the *Stagonospora nodorum* toxin sensitivity genes *Tsn1* and *Snn2* in wheat. Molecular Breeding 23:35-49.

Zhang, Z., Friesen, T.L., Xu, S.S., Shi, G., Liu, Z., Rasmussen, J.B., and Faris, J.D. 2011. Two putatively homoeologous wheat genes mediate recognition of SnTox3 to confer effector-triggered susceptibility to *Stagonospora nodorum*. The Plant Journal 65:27-38.

Zhao, K., Aranzana, M.J., Kim, S., Lister, C., Shindo, C., Tang, C., Toomajian, C., Zheng, H., Dean, C., Marjoram, P., and Nordborg, M. 2007. An Arabidopsis example of association mapping in structured samples. Plos Genetics 3.

CHAPTER 2. IDENTIFICATION AND CHARACTERIZATION OF THE SNTOX6-*SNN6* INTERACTION IN THE *PARASTAGONOSPORA NODORUM* - WHEAT PATHOSYSTEM

Abstract

Parastagonospora nodorum is a necrotrophic fungal pathogen that causes Septoria nodorum blotch (SNB) on wheat. *P. nodorum* produces necrotrophic effectors (NE) that are recognized by dominant host sensitivity gene products resulting in disease development. To date, nine NE-host sensitivity gene interactions have been identified. Here, I used a wheat mapping population that segregated for sensitivity to two previously characterized interactions (SnTox1-*Snn1* and SnTox3-*Snn3-B1*) to identify and characterize a new interaction involving the NE (SnTox6) and the host sensitivity gene (*Snn6*). SnTox6 is a small secreted protein that induces necrosis on wheat lines harboring *Snn6*. The SnTox6-*Snn6* interaction was light dependent and underlay a major disease susceptibility QTL. No other QTL were identified even though the *P. nodorum* isolate used in this study harbored both the *SnTox1* and *SnTox3* genes. This work expands our knowledge of the wheat-*P. nodorum* interaction and further establishes this system as a model for necrotrophic specialist pathosystems.

Introduction

Fungal pathogens are divided into classes including biotrophs, necrotrophs, and hemi-biotrophs based on their pathogenic lifestyle. Resistance to biotrophic pathogens typically follows the classical gene-for-gene model (Flor, 1956), where pathogen-produced effectors are thought to suppress PAMP-triggered-immunity in the early stages of resistance, but in turn are recognized directly or indirectly by corresponding dominant host resistance gene products to evoke a resistant (incompatible) reaction, termed effector-triggered immunity (ETI) (Flor, 1956;

Chisholm et al., 2006; Jones and Dangl, 2006). Once recognition of an effector takes place, a series of host responses are induced (Nurnberger et al., 2004).

Necrotrophic pathogens can be divided into two groups including necrotrophic generalists that typically attack several host species and necrotrophic specialists that typically attack a single or closely related host species (Andrew et al., 2012). Necrotrophic specialist pathogens such as *Parastagonospora nodorum* often secrete necrotrophic effectors (NEs) (formerly called host-selective toxins or HSTs) that induce necrotrophic effector-triggered susceptibility (NETS) (Friesen et al., 2008a). More than 20 necrotrophic specialist fungal pathogens have been shown to produce NEs, which are determinants of pathogenicity or virulence and often determine host specificity of a pathogen (Wolpert et al., 2002; Stergiopoulos et al., 2013). In many cases, NEs are recognized directly or indirectly by a corresponding host sensitivity gene product resulting in a susceptible (compatible) interaction (Wolpert et al., 2002; Lamari et al., 2003; Manning and Ciuffetti, 2005; Friesen et al., 2007; Oliver and Solomon, 2010). Disease is reduced if either the pathogen does not produce an NE or the host does not carry the corresponding sensitivity gene (Wolpert et al., 2002; Friesen et al., 2008a). Therefore, the NE-host susceptibility gene interaction has been described as an inverse gene-for-gene model (Friesen et al., 2007).

Parastagonospora nodorum (Synonyms: *Phaeosphaeria nodorum, Stagonospora nodorum*) is a necrotrophic filamentous fungal pathogen causing Septoria nodorum blotch (SNB) (formerly Stagonospora nodorum blotch) on common wheat (*Triticum aestivum*) and durum wheat (*T. turgidum*) and is capable of affecting both leaves and glumes. SNB has occurred in most wheat-growing regions and often has negative impact on yield and grain quality (King et al., 1983; Fried and Meister, 1987; Wicki et al., 1999). An effective way to control SNB is

through the development of resistant cultivars. The inheritance of SNB resistance is often complex, and conferred by multiple quantitative trait loci (QTL) throughout the wheat genome, whereas qualitative resistance to SNB has rarely been reported (Xu et al., 2004; Friesen et al., 2008a).

In the last decade, genetic dissection of the wheat-*P. nodorum* system has revealed that *P. nodorum* produces multiple NEs (Friesen et al., 2008a; Friesen and Faris, 2010; Oliver et al., 2012) and the recognition of *P. nodorum* NEs by corresponding wheat sensitivity genes leads to the induction of necrosis, a result of programmed cell death (PCD) and eventually SNB disease through the mechanisms associated with NETS. To date, nine NE-host sensitivity gene interactions have been identified in the *P. nodorum*-wheat pathosystem, each of which follows a NETS model (Reviewed in Friesen and Faris, 2010; Oliver et al., 2012). These nine interactions include SnTox1-*Snn1* (Liu et al., 2004a), SnToxA-*Tsn1* (Friesen et al., 2006; Faris et al., 2010), SnTox2-*Snn2* (Friesen et al., 2007), SnTox3-*Snn3-B1* (Friesen et al., 2007; Liu et al., 2009), SnTox3-*Snn3-D1* (Zhang et al., 2011), SnTox4-*Snn4* (Abeysekara et al., 2009), SnTox5-*Snn5* (Friesen et al., 2012), SnTox6-*Snn6* (Gao et al., 2015, this study)SnTox7-*Snn7* (Shi et al., 2015) which were shown to explain from 18 to 95% of the disease variation. These NE-host interactions have been implicated in both seedling and adult plant field susceptibility (Friesen et al., 2009).

Here a novel proteinaceous NE produced by *P. nodorum* which has been designated SnTox6 is characterized. Additionally, the corresponding host gene *Snn6*, which confers sensitivity to SnTox6 on the long arm of wheat chromosome 6A was identified and it was shown that a compatible SnTox6-*Snn6* interaction played a significant role in the development of SNB in wheat.

Materials and methods

Plant materials and *P. nodorum* strains

I used 106 RILs of the ITMI population, which was developed from a cross between the synthetic hexaploid wheat W-7984 (SNB moderately resistant) and the hard red spring wheat cultivar Opata 85 (SNB moderately susceptible) (Nelson et al., 1995). To date, over 2,000 molecular markers have been placed on the genetic linkage maps developed in this population (http://wheat.pw.usda.gov/GG2/index.shtml). Opata 85 is sensitive to the *P. nodorum* NEs SnTox3, and the novel NE reported here, SnTox6. W-7984 is sensitive only to SnTox1 (Liu et al., 2004a). We used the ITMI population to map the *Snn6* locus and characterize the SnTox6-*Snn6* interaction. The RIL ITMI37 is insensitive to SnTox1 and SnTox3, but was shown to be sensitive to the novel NE SnTox6 and was therefore used as a differential line in characterizing the SnTox6 protein.

The *P.* nodorum isolate Sn6 has been reported to produce multiple NEs including SnToxA, SnTox2, and SnTox3, (Friesen et al., 2007; Friesen et al., 2008a; Friesen et al., 2012) that interact with *Tsn1*, *Snn2*, and *Snn3*, respectively. Sn6 and the SnTox3 disruption strain Sn6Δ*SnTox3* (see below for description) was used to identify and partially purify SnTox6 and to characterize the SnTox6-*Snn6* interaction. Because the ITMI population segregates for *Snn1* and *Snn3-B1*, but the SnTox1-*Snn1* and SnTox3-*Snn3-B1* interactions were not associated with disease, we investigated transcriptional expression of the *SnTox1* and *SnTox3* genes in Sn6 during infection. The RILs ITMI6 and ITMI10, which are each sensitive to SnTox1, SnTox3 and SnTox6, were used to perform reverse transcription (RT)-PCR after being inoculated with Sn6. Because isolates Sn2000 and Sn4 were used to report the cloning of *SnTox1* (Liu et al., 2012)

and *SnTox3* (Liu et al., 2009) respectively, these two isolates were used to inoculate ITMI6 and ITMI10 for the evaluation of *SnTox1* and *SnTox3* expression as positive controls.

Because SnTox3 was produced abundantly in culture and it was difficult to separate SnTox3 from SnTox6 by chromatography methods, we generated a strain of Sn6 in which we disrupted *SnTox3*. This strain, Sn6Δ*SnTox3*, was used for mapping the SnTox6 sensitivity gene *Snn6* and for characterization of the SnTox6-*Snn6* interaction.

The *SnTox3* gene was disrupted using a split marker strategy as described by Liu et al. (2009). The *SnTox3* gene was disrupted by inserting the hygromycin phosphotransferase gene (*hph*) expression cassette, which confers resistance to hygromycin, into a *Sal*I restriction site of the *SnTox3* gene. The disruption fragments containing the *hph* cassette in the middle of the *SnTox3* open reading frame were transformed into Sn6 using PEG-mediated transformation methods following fungal protoplasting as described by Liu and Friesen (2012). The transformed colonies were screened by PCR. The primers SnTox3g0F and HY (Table 2.1) were used to amplify a fragment extending from the *SnTox3* 5' flanking region into the middle of the *hph* gene. The primers SnTox3cF and SnTox3cR (Table 2.1) were used to amplify the disrupted *SnTox3* fragment containing the *hph* expression cassette. The primers SnActinF and SnActinR (Table 2.1) were used to amplify the *P. nodorum* actin gene (*Act1*; Genbank accession number EAT90788) as an internal control to monitor RT-PCR efficiency and cDNA quality. PCR reaction mix without DNA (H_2O) was used as a negative control to make sure that all reagents were free of contamination. PCR was run using the following parameters: 94℃ 4 min; 30 cycles of 94 ℃ for 30 sec, 60 ℃ for 30 sec, and 72 ℃ for 3 min, followed by 72 ℃ 10 min. The SnTox3 disrupted strain Sn6Δ*SnTox3*, was used for CF infiltration to map *Snn6* (see below). The

wild type isolate Sn6 and Sn6ΔSnTox3 were used in conidial inoculations to evaluate the SnTox6-*Snn6* interaction (see below).

Table 2.1. Primers used in Chapter 2 for the amplification of SnTox1 (top), SnTox3 (middle) and the *Parastagonospora nodorum* actin gene, SnActin (bottom).

Primer pair	Sequence	Amplicon size (bp)
SnTox1cF SnTox1cR	ATGAAGCTTACTATGGTCTTGT TGTGGCAGCTAACTAGCACA	356
SnTox3cF SnTox3cR	CTCGAACCACGTGGACCCGGA CTCCCCTCGTGGGATTGCCCCATATG	600 from wild type Sn6, ~ 3200 from Sn6ΔSnTox3
SnTox3g0F HY	ATCCCAGACATCCCACTCAA GGATGCCTCCGCTCGAAGTA	~ 2900
SnActinF SnActinR	CTGCTTTGAGATCCACAT GTCACCACTTTCAACTCC	255

Purification of SnTox6

CFs of *P. nodorum* isolate Sn6 and the *SnTox3* disrupted strain Sn6ΔSnTox3 were grown and harvested as described by Friesen and Faris (2012). The bioactivity of SnTox6 was tested weekly by infiltrating leaves of the differential line ITMI37. Three replications were completed with each replication consisting of seven ITMI37 seedlings. SnTox6 was partially purified from the CFs of Sn6 and Sn6ΔSnTox3 using low pressure and high pressure liquid chromatography techniques (Friesen and Faris, 2012). A total of 200 ml of Sn6 CF was dialyzed overnight against water in 3,500 MWCO dialysis tubing (Fisher Scientific) and then loaded onto a 5 ml Hitrap SPXL ion exchange column using an AKTA Prime plus system (GE healthcare). The column was equilibrated with a 20 mM sodium acetate buffer (pH 5.0). The active NE was eluted using 20 mM sodium acetate (pH 5.0) plus a gradient elution of 0-300 mM NaCl over 150 ml at a flow

rate of 5 ml/min. The eluted proteins were separated into 28 fractions of 5 ml each. The fractions were tested by infiltration on the SnTox6 differential line ITMI37. The active fractions were combined and concentrated to 10 ml by freeze drying and were loaded onto a HiLoad 16/60 Superdex 30 prep-grade gel filtration column (GE Healthcare) for purification by size exclusion chromatography. Size standards, blue dextran (2,000 kDa), cytochrome C (12.3 kDa), and aprotinin (6.5 kDa) were added to identify the approximate molecular weight of SnTox6. The sample was run in a buffer of 20 mM sodium acetate plus 100 mM NaCl (pH 5.0) at a flow rate of 1 ml/min. A total of thirty-six 5 ml fractions were collected.

The fractions *were* assayed again by infiltration on ITMI37. The active fractions were combined and frozen at -20℃ overnight. The frozen fractions were freeze dried followed by re-dissolving in 500 µl distilled water. The concentrated fractions were loaded onto an analytical grade high-performance liquid chromatography (HPLC) BioSep SEC-S2000 column for the final size-exclusion purification. Carbonic anhydrase (30 kDa), cytochrome C and aprotinin were used as size standards to estimate the approximate size of SnTox6. The sample was run in a buffer consisting of 20 mM sodium acetate plus 500 mM NaCl (pH5.0) at a flow rate of 1 ml/min. The 1 ml fractions were collected and assayed by infiltration on ITMI37.

The *infiltrated* leaves were scored three days post-infiltration using a 0-3 scale (0 = no reaction, 1 = mottled chlorosis, 2 = chlorosis/necrosis without tissue collapse, 3 = necrosis with complete tissue collapse) (Friesen and Faris, 2012). The HPLC gel filtration fractions having SnTox6 activity were separated using SDS-PAGE gel electrophoresis as described by Liu *et al.* (2009). In brief, the fractions were loaded into a precast 16.5% tris-tricine polyacrylamide gel and subjected to electrophoresis in a Bio-Rad Mini PROTEAN 3 system (Bio-Rad, Hercules,

CA). The separated samples were stained with Coomassie blue solution (0.2% Coomassie Blue R250, 7.5% acetic acid and 50% ethanol) to show the protein bands.

2-DGE separation of SnTox6 produced by Sn6

Sn6 proteins in the final HPLC gel filtration fraction 20 were separated by isoelectric focusing (IEF) in the first dimension and SDS-PAGE in the second dimension as described by Sharma *et al.* (2007). In brief, 500 µg of total protein in 125 µl of ReadyPrep 2-D starter kit rehydrated buffer (Bio-Rad) was loaded overnight into 7 cm IPG strips (pH 3-10, nonlinear, Bio-Rad). IEF was conducted in the Ettan IPGphor 3 system (GE healthcare). After IEF, the IPG strips were equilibrated in 5 mL equilibration buffer 1 (6 M urea, 2% w/v SDS, 0.375 M Tris-HCl, pH 8.8, 20% v/v glycerol, and 130 mM DTT) twice and equilibration buffer 2 (6 M urea, 2% w/v SDS, 0.375 M Tris-HCl, pH 8.8, 20% v/v glycerol, and 135 mM iodoacetamide) an additional two times. SDS-PAGE was performed in the mini PROTEAN system (Bio-Rad) as described by Laemmli (1970) on 13% polyacrylamide gels at a constant voltage (100 V). The PAGE gel was fixed in 50% methanol and 7% acetic acid for 30 min, stained in SYPRO Ruby gel stain solution overnight and de-stained in 10% methanol and 7% acetic acid for 30 min.

Mass spectrometry of SnTox6

Spots in the SDS-PAGE gel were cut and subjected to in-gel tryptic digestion as described by Shevchenko et al. (1996). Lyophilized tryptic peptides were desalted according to Rappsilber et al. (2003). Eluted peptides were dried in vacuo and reconstituted in 98:2:0.1 water:acetonitrile:trifluoroacetic acid. Approximately 0.2 µg of each gel spot was analyzed by capillary LC-MS as previously described (Lin-Moshier et al., 2013) on a Velos Orbitrap mass spectrometer (Thermo Fisher Scientific, Inc., Waltham, MA) with higher energy collision

induced dissociation (HCD) activation at the Center for Mass Spectrometry and Proteomics, University of Minnesota.

Mass spectral database search

Peaks® Studio (Ma et al., 2003) 6.0 build 20120620 (Bioinformatics Solutions, Inc, Waterloo, ON CA) software package was used for interpretation of tandem MS (mass spectra) and protein inference. Database searches included the *P. nodorum* SN15 protein database (http://genome.jgi.doe.gov/Stano2/Stano2.home.html), as well as six frame translation databases of SN15 and Sn4. The six way translation databases of SN15 and Sn4 were generated by translating the genomic DNA sequences (Hane et al., 2007; Syme et al., 2013) between stop codons for all six frames using CLC Genomic Workbench (CLC Bio). All the protein databases were concatenated with the common lab contaminant proteins from http://www.thegpm.org/crap/. Search parameters included parent mass error tolerance 20.0 ppm; fragment mass error tolerance 0.1 Da; precursor mass search type monoisotopic; enzyme trypsin with max missed cleavages 2 and non-specific trypsin cleavage; variable modifications methionine oxidation; fixed modifications carbamidomethyl cysteine; maximum variable modifications per peptide 5; false discovery rate calculation On; spectra merge options: 0.2 minutes within 10.0 ppm mass window; charge correction on for charge states 2 – 8; spectral filter quality >0.65. Support for the detection of peptides from each supporting tandem MS data was based on: 1) high confidence Peaks® Peptide Score (minimum -10 logP35); 2) a minimum of 3 consecutive b- or y-type peptide fragment ions; 3) high precursor mass accuracy (<7 ppm) and a maximum 30 kDa molecular weight (Zhang et al., 2012).

SnTox6 protease sensitivity

SnTox6 from HPLC was treated with 1 mg/ml Pronase (EMD Biosciences Inc., San Diego, CA, USA), a mixture of endo- and exo-proteases, for 4 h at room temperature. The Pronase treated sample, the non-Pronase treated sample (positive control), and the Pronase only (negative control) were then infiltrated on ITMI37. In order to show that the protease (Pronase) was not affecting the receptor or downstream signaling of SnTox6 recognition, we combined SnTox6 and Pronase and immediately infiltrated the mixture on ITMI37. Additionally, we pretreated leaves of ITMI37 by infiltrating with Pronase at a concentration of 1 mg/ml, waited 4 h and then infiltrated the same leaf area with SnTox6. All five treatments involving Pronase sensitivity were performed using a total of three replicates. Leaf necrosis was evaluated 3 days post-infiltration (Fig. 3).

Light dependence of the SnTox6-*Snn6* interaction

The partially purified SnTox6 from HPLC was used to infiltrate ITMI37 and plants were subjected to either a 12 h photoperiod or 24 h dark conditions. Three replicates were completed for both treatments with each replication consisting of seven ITMI37 plants. Necrotic activity was evaluated 3 days post-infiltration.

Identification of the *Snn6* locus

CFs of Sn6 were infiltrated into the second leaf of W-7984, Opata 85, and 106 RILs of the ITMI population. Approximately 25 µl of the active CFs were infiltrated using a 1 ml needleless syringe. The infiltrated region was labeled using a non-toxic felt marker. The infiltrated plants were grown in a growth chamber at 21℃ under a 12 h photoperiod. At least three replications were completed for each line with each replication consisting of two plants organized in racks of 98 (Stuewe and Sons Inc., Corvallis, OR, USA). The infiltrated leaves were

scored three days post-infiltration using a 0-3 scale where 0 = no reaction, 1 = mottled chlorosis, 2 = chlorosis/necrosis without tissue collapse, 3 = necrosis with complete tissue collapse (Friesen and Faris, 2012).

A total of 505 genetic markers previously mapped in the ITMI population were downloaded from the Graingenes website (http://wheat.pw.usda.gov/GG2/index.shtml) and used to reassemble the linkage maps of all 21 chromosomes. The average infiltration data of three replications was regressed on the 505 genetic markers using simple interval-regression as described by Liu et al. (2004a). A LOD (logarithm (base 10) of odds) threshold of approximately 3.0 at an experiment-wise error (α) level of 0.05 was determined by executing a permutation test with 5,000 permutations.

Mapping of the *Snn6* locus and additional molecular markers

CFs of Sn6ΔSnTox3 were infiltrated into the second leaf of the parents and 106 RILs of the ITMI population. The infiltrated leaves were scored three days post-infiltration using a 0-3 scale (Friesen and Faris, 2012). Plants scored as 0 were insensitive, meaning that these plants inherited the *snn6* allele from W-7984, whereas plants scored as 1, 2 and 3 were sensitive and possessed the *Snn6* allele from Opata 85.

The insensitivity/ sensitivity data were converted to genotypic scores to place the *Snn6* locus on the ITMI map using the software program Mapmaker v2.0 (Lander et al., 1987). The 'try' command was used to place the *Snn6* locus in the most likely position relative to the molecular markers that made up the linkage map of chromosome 6A. Genetic distances were calculated using the Kosambi mapping function (Kosambi, 1944).

Nine additional markers were placed on the 6A linkage map in the vicinity of the *Snn6* locus. These included the two microsatellite markers *Xhbe385* and *Xhbg402* previously shown

by Torada et al. (2006) to identify loci in the distal region of the wheat chromosome arm 6AL. PCR conditions followed those of Torada et al. (2006). The other seven markers were developed from wheat ESTs (GenBank accession numbers BF145792, BE494057, BE591377, BF428729, BE424987, BE403326, and BE590952) that were previously shown to detect loci within the most distal bin of the long arm of the chromosome 6A physical map (Qi et al., 2004). PCR amplification and visualization of amplified products was done as described in Lu et al. (2006). The microsatellite and EST-based markers were added to the ITMI chromosome 6A linkage map as described above for *Snn6*.

SNB disease evaluation

The *P. nodorum* isolates Sn6 and Sn6ΔSnTox3 were cultured on V8-potato dextrose agar (PDA) for 6-7 days as described by (Friesen and Faris, 2012). Conidia (pycnidiospores) served as inoculum and were adjusted to a concentration of 1×10^6 spores/ml and sprayed onto juvenile plants at the two to three leaf stage as described by Friesen and Faris (2012). The inoculated plants were subjected to 100% relative humidity in the light for 24 h in a mist chamber and then grown in a growth chamber at 21ºC under a 12 h photoperiod for 6 additional days. The disease on the second leaf of each inoculated plant was scored 7 days post-inoculation using a 0-5 rating scale based on lesion type (Liu et al., 2004b). Three replications were completed with each replication consisting of two cones per line with two plants per cone with a single cone border of the susceptible wheat variety Alsen to reduce any edge effect.

To determine the effects of host NE sensitivity genes on the development of SNB (i.e. the effects of the SnTox6-*Snn6* interaction), the average 7-day disease phenotypic data of three replications was regressed on the data for the 514 genetic markers with composite interval-regression mapping using the software QGene v4.0 (Joehanes and Nelson, 2008). A LOD

threshold of approximate 3.0 at an experiment-wise error (α) level of 0.05 was determined by executing a permutation test with 5,000 permutations.

Expression analysis of *SnTox3* and *SnTox1*

Total RNA of ITMI6 and ITMI10 was extracted using the RNeasy plant Mini Kit (QIAGEN) 3 days after inoculating with Sn6, Sn2000 and Sn4. Because Sn2000 and Sn4 were used to clone *SnTox1* and *SnTox3* respectively, we used cDNA of Sn2000 and Sn4 inoculated ITMI6 and ITMI10 as positive controls for *SnTox1* and *SnTox3* amplification, respectively. The three day time point was used because both SnTox3 and SnTox1 have been shown to be produced most abundantly at 3 days post inoculation (Liu et al., 2009; Liu et al., 2012). The total RNA was reverse transcribed using TaqMan Reverse Transcription Reagents (Roche) and the resulting cDNA was used as template to conduct reverse transcription-PCR (RT-PCR). The primers SnTox1cF and SnTox1cR (Table 2.1) were used to amplify *SnTox1* (*Snog_20078*; Genebank accession number XM_001797453.1). The primers SnTox3cF and SnTox3cR (Table 2.1) were used to amplify *SnTox3* (*Snog_08981*; Genbank accession number XM_001799232.1). The primers SnActinF and SnActinR (Table 2.1) were used to amplify the *P. nodorum* actin gene (*Act1*; Genbank accession number EAT90788) as an internal control. A PCR reaction mix without DNA (H_2O) was used as a negative control. PCR was run using the following parameters: 94℃ 4 min; 30 cycles of 94 ℃ for 30 sec, 60 ℃ for 30 sec, and 72 ℃ for 30 sec, followed by 72 ℃ 10 min.

Results

The identification of a novel NE-wheat gene interaction

Culture filtrate (CF) of the *P. nodorum* fungal isolate Sn6 was used to infiltrate leaves of wheat lines W-7984 and Opata 85, the parents of the International Triticeae Mapping Initiative

(ITMI) population. W-7984 was insensitive to Sn6 CF whereas Opata 85 was sensitive, indicating at least one NE other than SnTox1 was being produced by Sn6, because W-7984 is sensitive only to SnTox1 and Opata 85 is insensitive to SnTox1 (Liu et al., 2004a). To determine if the NE produced by Sn6 was different from the other NEs that have been reported, we used the CF of isolate Sn6 to infiltrate several of the SNB differential lines with known NE sensitivities including BG223 (SnTox2), BG220 (SnTox3), AF89 (SnTox4) and LP29 (SnTox5), as well as the ITMI population. Sn6 had previously been shown by Friesen et al. (2007) to produce SnToxA. Previous work and current Sn6 culture filtrate infiltration of these differential lines showed that Sn6 produced SnToxA, SnTox2, and SnTox3, but not SnTox4 or SnTox5 (Table 2.2). However, neither SnToxA nor SnTox2 sensitivity segregated in the ITMI population. Interval regression analysis of Sn6 CF infiltration data on the ITMI population marker data revealed two loci, one at the distal end of the short arm of chromosome 5BS, which is the same location of *Snn3-B1* identified in the BG population (Friesen et al., 2008b; Zhang et al., 2011), and a novel locus on chromosome 6A (Figure 2.1). We designated the novel NE produced by isolate Sn6 as SnTox6, and the wheat gene conferring sensitivity to SnTox6 as *Snn6*.

Table 2.2. Culture filtrate (CF) infiltration reactions of *P. nodorum* isolate Sn6 in SNB differential lines which are sensitive to SnToxA, SnTox1, SnTox2, SnTox3, SnTox4 and SnTox5, respectively

SNB differential lines	Sn6 CF reaction
[1]BG261 (SnToxA)	+
M6 (SnTox1)	-
BG223 (SnTox2)	+
BG220 (SnTox3)	+
AF89 (SnTox4)	-
LP29 (SnTox5)	-

[1](Friesen et al., 2007)

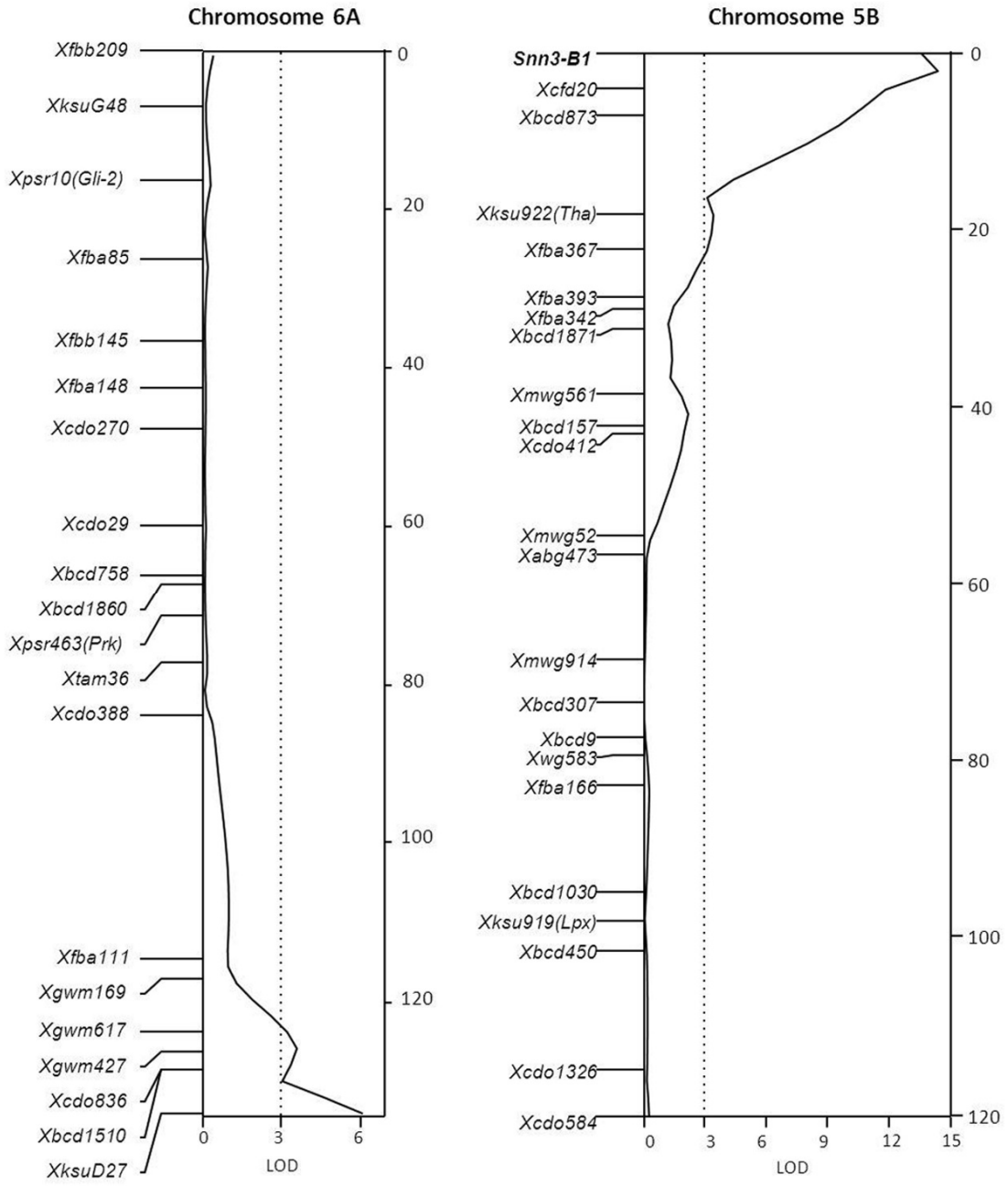

Figure 2.1. QTL analysis of sensitivity induced by the *P. nodorum* isolate Sn6 onto the ITMI population.

Interval-regression map of wheat chromosomes 6A (left) and 5B (right) generated using the average 3-day reaction to culture filtrates of *P. nodorum* isolate Sn6 in the ITMI recombinant inbred population. A centiMorgan (cM) scale is indicated to the right of the maps and the markers are indicated on the left. LOD scales are shown across the bottoms of the maps, and the significant QTL threshold is shown by the dotted line.

To evaluate the genetics of the wheat gene conferring sensitivity to SnTox6 alone, we generated and confirmed (Figure 2.2) an SnTox3-disrupted mutant, which was named Sn6ΔSnTox3. Because the *SnTox3* gene was disrupted in Sn6ΔSnTox3, and Sn6ΔSnTox3 was confirmed to show similar SnTox6 activity as the wild type (Figuer 2.4), the CF of Sn6ΔSnTox3 was used to infiltrate the ITMI population resulting in a 58:48 sensitive: insensitive ratio, which was not significantly different from the expected 1:1 ratio ($\chi^2_{df=1} = 0.943$, P = 0.3315), indicating that sensitivity to SnTox6 is controlled by the single host gene, *Snn6*.

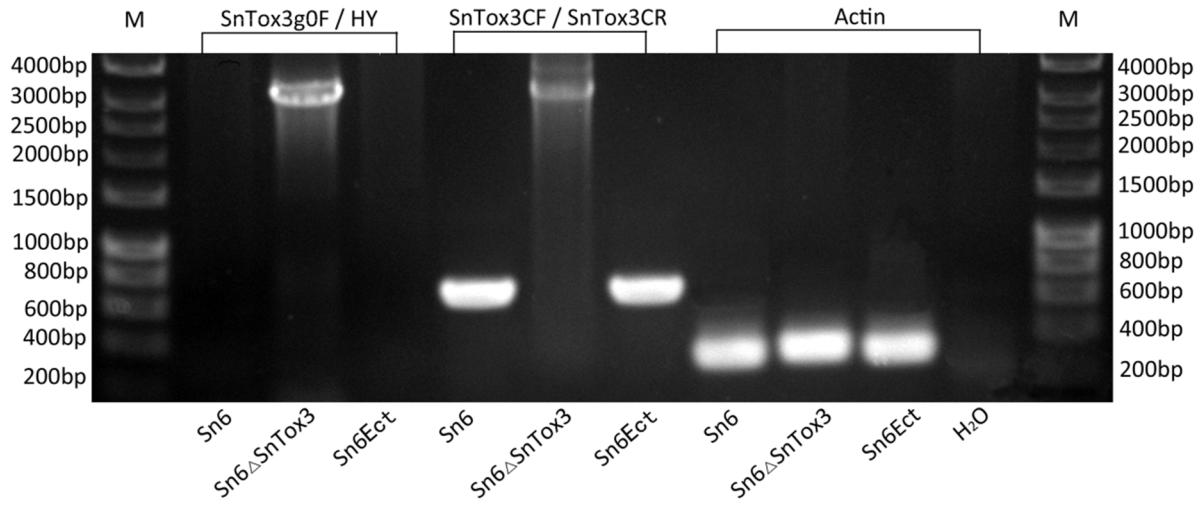

Figure 2.2. PCR screening and confirmation of the SnTox3 disruption in the Sn6ΔSnTox3 strain.

The primers SnTox3g0F and HY amplify a 1.2kb 5' *SnTox3* gene region plus a 1.2 kb partial *hph* gene region to generate a total fragment size of 2.9 kb (SnTox3g0F-HY) from Sn6ΔSnTox3, the *SnTox3* disruption strain. No amplification is observed in the wild type (Sn6) or the ectopic insertion strain (Sn6Ect). The primers SnTox3CF and SnTox3CR amplify a 600 bp fragment (SnToxCF-SnToxCR) in the wild type and ectopic strains indicating that the SnTox3 gene remains intact, while they amplify a 3.2 kb fragment (600 bp of SnTox3 plus 2.6 kb of the *hph* expression cassette) in the *SnTox3*-disrupted strains. The *P. nodorum* actin gene was amplified as an internal control. The PCR reaction mix without DNA (H_2O) was used as a negative control.

Snn6 mapped to the long arm of chromosome 6A

Reactions of the ITMI recombinant inbred lines (RILs) to the CF infiltration of Sn6ΔSnTox3 were converted to genotypic scores to allow linkage analysis of *Snn6* relative to the molecular markers. Due to the disruption of SnTox3, the interaction of SnTox3-*Snn3-B1* was eliminated, allowing the evaluation of only the gene (*Snn6*) conferring sensitivity to SnTox6. The *Snn6* gene mapped near the distal end of the long arm of chromosome 6A (Figure 2.3).

Because most of the markers near *Snn6* were restriction fragment length polymorphism (RFLP) markers, which are not user-friendly or suitable for high-throughput genotyping or marker-assisted selection, we placed nine additional PCR-based markers on the ITMI 6A map. Two of the nine markers were microsatellite markers *Xhbe385.2* and *Xhbg402*, which were previously developed by Torada et al. (2006). We developed the remaining seven PCR-based markers (*XBF145792, XBE494057, XBE591377, XBF428729, XBE424987, XBE403326*, and *XBE590952*) from wheat expressed sequence-tagged (EST) sequences (http://wheat.pw.usda.gov/NSF/). Four of the nine PCR-based markers mapped within 10 cM of *Snn6,* with markers *XBE424987* and *XBE403326* immediately flanking the gene and delineating it to a 3.2 cM interval (Figure 2.3).

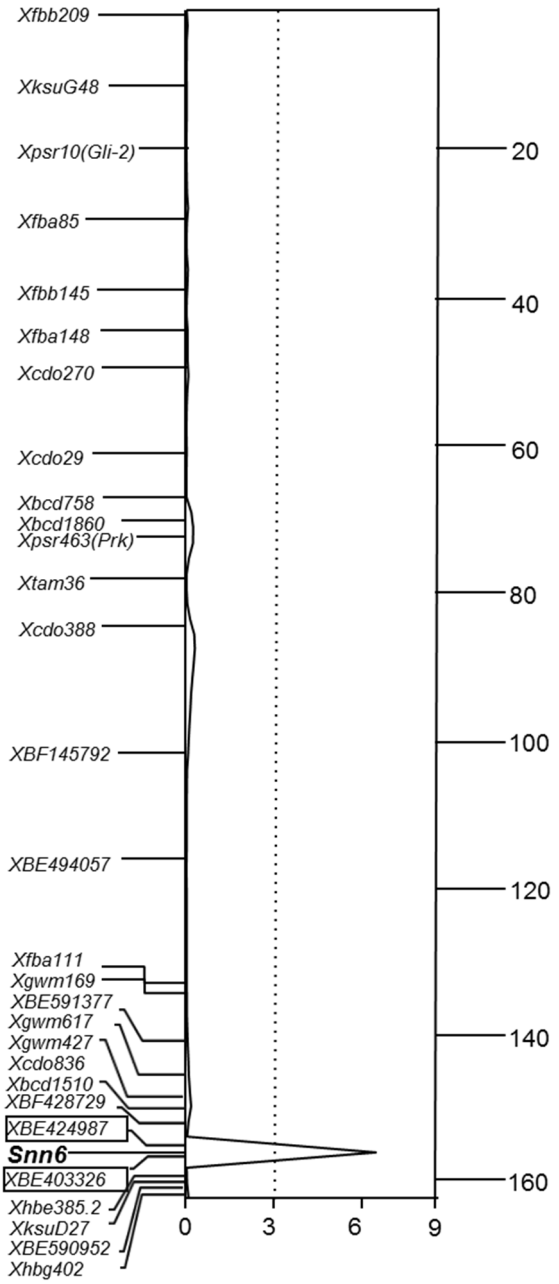

Figure 2.3. QTL analysis of disease susceptibility induced by the *P. nodorum* isolate Sn6 onto the ITMI population.

Composite interval-regression map of wheat chromosomes 6A generated by the average 7-day disease reaction scores using *P. nodorum* isolate Sn6 on the ITMI recombinant inbred population. A centiMorgan (cM) scale is indicated to the right of the map and the markers are indicated on the left of the map. A LOD scale is indicated on the *x*-axis, and the significant QTL threshold is shown by the dotted line. The marker conferring the largest QTL is shown in bold, and the two flanking markers are shown in boxes.

SnTox6 is a small, secreted, necrosis-inducing protein

The wheat line ITMI37 was chosen as a differential line to characterize the SnTox6 protein because it contained only one known sensitivity gene, *Snn6*, which confers sensitivity to SnTox6. ITMI37 was shown to be insensitive to the *Pichia pastoris* heterologous expression cultures of SnTox1 and SnTox3, as well as all other known NEs based on *P. nodorum* culture filtrate infiltrations.

When infiltrated on ITMI37, three-week old CFs of Sn6 and Sn6ΔSnTox3 induced strong necrosis and therefore we used these cultures to purify SnTox6. Initial purification was done by low-pressure ion exchange chromatography using a 5 ml Hitrap SPXL cation exchange column (GE Healthcare). The SnTox6 activity on ITMI37 eluted between 75 and 270 mM NaCl (fractions 6 to 19) with the strongest NE activity identified in the fractions eluting between 135 and 225 mM NaCl (fractions 10 to 15) and showing type 2 and 3 reactions (0 = no reaction, 1 = mottled chlorosis, 2 = chlorosis/necrosis without tissue collapse, 3 = necrosis with complete tissue collapse) as described in Friesen and Faris (2012) (Figure 2.4. A, D, G). Tissue necrosis/damage at the infiltration point was not associated with the NE interaction and therefore the region between the infiltration point and the black marked lines was used for scoring. Fractions before 6 and after 19 did not show SnTox6 activity (reaction type 0) on ITMI37 (data not shown).

The active fractions (fraction 10 to 15) were combined and further separated by size exclusion chromatography using a HiLoad 16/60 Superdex 30 prep-grade gel filtration column. The eluted fractions were assayed by infiltration on ITMI37, and activity eluted between blue dextran (2000 kDa) and aprotinin (6.5 kDa) (fractions 8 to 18). Fractions before 8 and after 18 showed no SnTox6 activity (reaction type 0) on ITMI37 (data not shown). The strongest NE

activity (type 2 and 3 reactions) was identified in fractions 12 and 13 from Sn6 (Figure 2.4. B, E) and 11, 12 and 13 from Sn6ΔSnTox3 (Figure 2.4 B, H). Cytochrome C (12.3 kDa) eluted in fraction 12 indicating the size of the eluted fractions 11, 12 and 13, which contained the strongest NE activity, were close to the size of cytochrome C.

Fractions 11, 12 and 13 were then subjected to a final purification by size exclusion HPLC. The eluted fractions between 17 and 23 were assayed by infiltration on ITMI37. The fractions 19, 20 and 21 showed 2 or 3 type reactions, indicating these fractions contained the most significant SnTox6 activity (Figure 2.4. C, F, I). Fractions before 17 and after 23 did not have SnTox6 activity (reaction type 0) on ITMI37 (data not shown). Fractions 19 and 20 eluted between cytochrome C (12.3 kDa) and aprotinin (6.5 kDa), and fraction 21 eluted after aprotinin (Figure 2.4. C, F, I). The infiltration of fraction 19, 20 and 21 from Sn6ΔSnTox3 showed type 2, 3, 2 reactions, respectively (Figure 2.4. I), indicating fraction 20 from Sn6ΔSnTox3 had the strongest SnTox6 activity. This result provided evidence for the molecular mass of SnTox6 being at or less than that of cytochrome C.

To further investigate the molecular size of SnTox6 from Sn6, the HPLC gel filtration fractions 19, 20 and 21 (Figure 2.4. F) were subjected to sodium dodecyl sulfate-polyacrylamide gel electrophoresis (SDS-PAGE) analysis. Fractions 19, 20 and 21 showed a strong band around 12 kDa. Fractions 20 and 21 showed another band around 8 kDa which was not visible in fraction 19 (Figure 2.5). Because all three fractions had SnTox6 activity, we hypothesized that the larger band with a size around 12 kDa contained SnTox6.

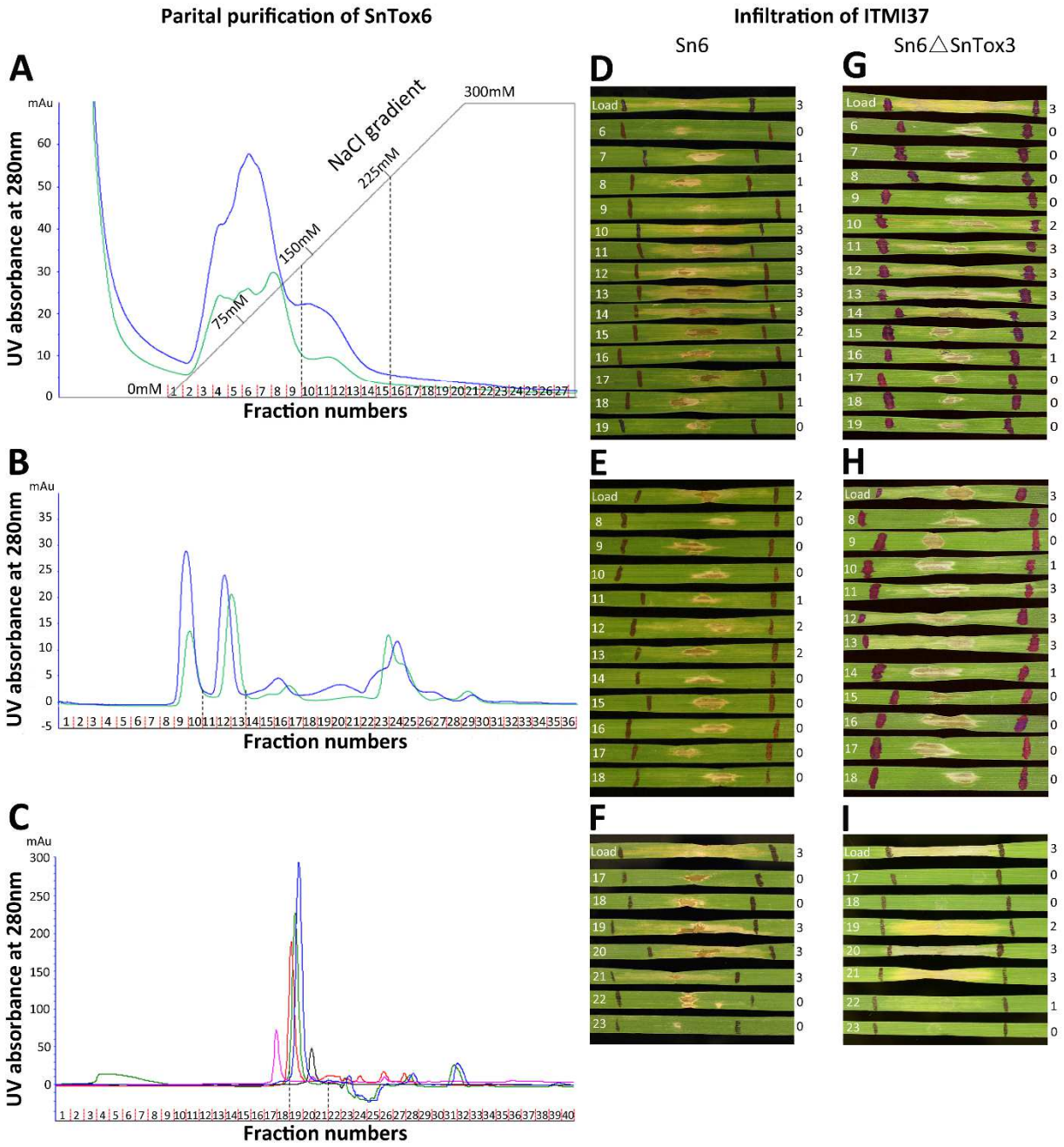

Figure 2.4. Partial purification of SnTox6 (**A, B, C**), and NE bioassays of SnTox6 from Sn6 (**D, E, F**) and Sn6ΔSnTox3 (**G, H, I**).

(**A**) Cation exchange chromatography with a 0 to 300 mM NaCl gradient elution of dialyzed Sn6 and Sn6ΔSnTox3 culture filtrates. The *y*-axis indicates the UV absorbance at 280 nm (blue curve Sn6, green curve Sn6ΔSnTox3) with the *x*-axis indicating the fraction number. The salt gradient is indicated by the gray line. The fraction range with NE activity is indicated by the vertical black dashed lines. The activity of SnTox6 was observed by infiltrating the differential line

ITMI37 with the eluted fractions from Sn6 (**D**) and Sn6ΔSnTox3 (**G**). (**B**) Size exclusion purification of SnTox6 separated by gel filtration chromatography (left). The *y*-axis shows the UV absorbance (blue curve for Sn6, green curve for Sn6ΔSnTox3) with the *x*-axis showing the fraction number. The fractions with NE activity are indicated by the vertical black dashed lines. The NE bioassay of SnTox6 was observed by infiltrating the differential line ITMI37 with the eluted fractions from Sn6 (**E**) and Sn6ΔSnTox3 (**H**). (**C**) A final size exclusion purification of SnTox6 separated by HPLC gel filtration chromatography. The *y*-axis shows the UV absorbance and the *x*-axis shows the eluted fraction numbers. The absorbance of the Sn6 sample is indicated by the blue line, and Sn6ΔSnTox3 is indicated by the green line. The size standards cytochrome C (12.3 kDa), aprotinin (6.5 kDa) and carbonic anhydrase (30 kDa) are indicated by the red, black, and pink lines, respectively. The fractions with NE activity are indicated by the vertical black dashed lines. The presence of SnTox6 observed by infiltrating the differential line ITMI37 with the eluted fractions from Sn6 (**F**) and Sn6ΔSnTox3 (**I**). The eluted fraction numbers are indicated on the left side of each infiltrated ITMI37 leaf of panels (**D**) - (**I**). The relative activity of all the eluted fractions were scored on a 0 to 3 scale where 0 = no reaction, 1 = mottled chlorosis, 2 = chlorosis/necrosis without tissue collapse, 3 = necrosis with complete tissue collapse (Friesen and Faris, 2012). 0 to 3 scores are indicated to the right of each corresponding ITMI37 leaf.

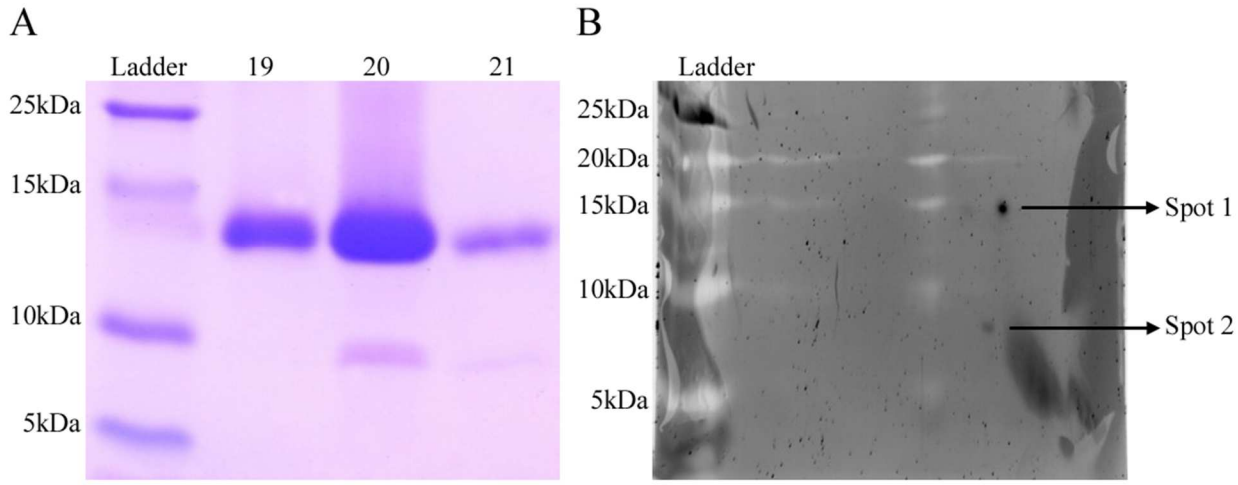

Figure 2.5. SDS-PAGE image of the final HPLC gel filtration chromatography fractions 19-21 and (**A**) a 2DGE image of the final HPLC gel filtration fraction 20 which contained the highest SnTox6 activity (**B**).

(**A**) Ladder consists of a Genscript Smart His Tagged protein standard (Genscript, Piscataway, NJ USA). The molecular weight (kDa) of each protein standard is labeled. Lanes labeled 19, 20, and 21 contain protein samples from HPLC gel filtration fractions 19, 20, and 21. (**B**) The Precision Plus Protein™ Dual Xtra size standard is on the left. Spot 1 and 2 were excised and subjected to mass spectrometry.

In an attempt to isolate SnTox6, we performed 2DGE of the final gel filtration HPLC fraction 20 which contained the strongest SnTox6 activity (Figure 2.4. F). Two spots (~12 kDa and 8 kDa) were identified (Figure 2.5) and excised from the gel to identify the proteins using mass spectrometry. Protein hits with a maximum molecular weight of 30 kDa and a minimum of three peptide hits were used. By using the *P. nodorum* protein database (http://genome.jgi.doe.gov/Stano2/Stano2.home.html), one strong hit from the 12 kDa spot SNOG_16063 (Figure 2.5. B, Spot 1) was identified which had been previously ruled out as an NE (Liu et al., 2009). One hit from the 8 kDa spot (Figure 2.5. B, Spot 2) SNOG_06667 (ubiquitin) was also identified, which was not likely SnTox6.

We then used 6-way translation databases generated from the SN15 and Sn4 genomic sequences (Hane et al., 2007; Syme et al., 2013) to identify genomic regions (identified by three peptide hits) with no previously annotated genes. In addition to the genomic regions harboring SNOG_16063 and SNOG_06667, a single three peptide hit from a genomic region that had no previously annotated genes in either Sn4 or SN15 was identified in both the Sn4 and SN15 6-way translation databases. Further work is needed to validate the possibility that this genomic region harbors *SnTox6*.

To determine if the purified fraction associated with *Snn6* sensitivity was a protein, fractions 19, 20 and 21 from HPLC gel filtration were combined and digested with Pronase (Sigma) and then tested by infiltration on ITMI37. The sample treated with Pronase had no activity on ITMI37, whereas the sample without Pronase treatment (positive control) maintained strong NE activity (Figure 2.6. A). The Pronase-only infiltration (negative control) showed no activity on ITMI37. Additionally, to prove that the Pronase was not acting on the host receptor of SnTox6 or affecting downstream signaling, leaves were either infiltrated with SnTox6 that had

just been mixed with Pronase or infiltrated with SnTox6 samples after leaves had been pre-treated for four hours by infiltrated Pronase. Neither treatment reduced the NE activity indicating that Pronase did not render the plant insensitive to SnTox6, and that the necrosis induced on ITMI37 was induced by a protein (Figure 2.6. A).

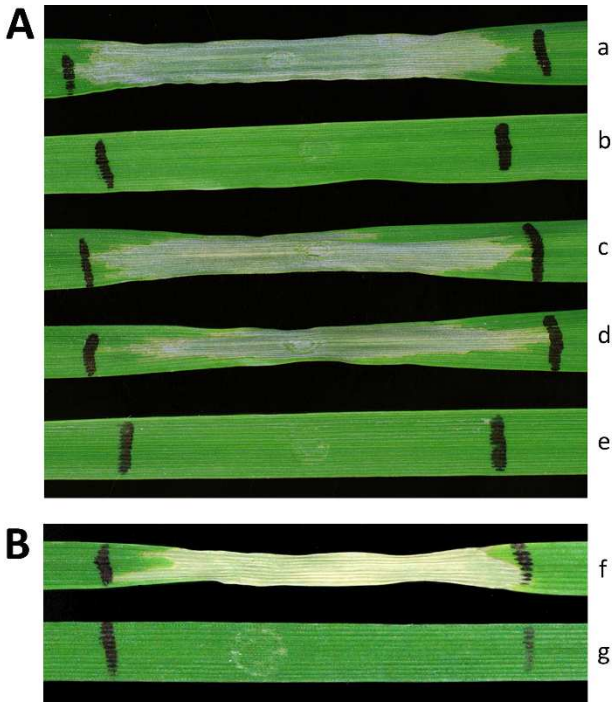

Figure 2.6. Protease analysis (**A**) and light dependency testing (**B**) of the SnTox6-*Snn6* interaction using partially purified SnTox6 infiltrated on ITMI37.

(**A**) ITMI37 leaves were infiltrated with untreated SnTox6 (a), SnTox6 treated with Pronase for 4 h (b), SnTox6 treated with Pronase for 0 h (c), Pronase only followed by SnTox6 infiltration 4 hours later (d) and Pronase only (e). (**B**) ITMI37 leaves were infiltrated with SnTox6 and grown under a 12 h photoperiod (f), and 24 h dark conditions (g) for 72 h.

Sensitivity to SnTox6 is light dependent

Previous studies have shown that other *P. nodorum* and *Pyrenophora tritici-repentis* NE interactions are light-dependent (Oliver et al., 2012). To determine if the SnTox6-*Snn6*

interaction was light dependent, fractions 19, 20 and 21 from HPLC gel filtration were combined and infiltrated on ITMI37. The infiltrated plants were subjected to either a 12 h photoperiod or 24 h dark conditions. Strong necrosis occurred on leaves of plants grown under a 12 h photoperiod, but no necrosis was evident on plants grown under 24 h dark conditions (Figure 2.6. B), indicating that the SnTox6-*Snn6* interaction is dependent on light.

The SnTox6-*Snn6* interaction contributes significantly to SNB disease

Three replications of the ITMI population were inoculated with conidia of isolate Sn6. A Bartlett's Chi-squared test indicated the three replicates were homogeneous ($\chi^2_{df=2} = 0.0807$, $P = 0.960$) and therefore were pooled for further analysis. Disease reactions were scored using a scale of 0-5 (0 = highly resistant; 5 = highly susceptible) (Liu et al., 2004a; Liu et al., 2004b). Average disease reaction types for Opata 85 and W-7984 were 3.0 and 1.5, respectively (Table 2.3; Figure 2.7). The average disease reaction types of the ITMI population showed a normal distribution in a range of 0-4. The mean reaction type of the population was 2.5. SnTox6 sensitive RILs (*Snn6Snn6* genotype) had a mean reaction type of 2.8 with a range of 2.0 to 4.0, whereas insensitive RILs (*snn6snn6* genotype) had a mean reaction type of 2.1 with a range of 1.0 to 3.5 (Table 2.3; Figure 2.7). Interval regression analysis revealed a significant association (LOD = 7.1) between the *Snn6* locus and the disease reaction types (Figure 2.3), which explained 27% of the disease variation. No other markers in the dataset were associated with SNB caused by Sn6 in this population.

Table 2.3. Average and range of SNB disease reaction types of parents and RILs of the ITMI population for the two genotypes of the *Snn6* locus 7 days post inoculation using isolate Sn6

Genotype	Average disease reaction type	Reaction type range
Opata85	3.0	2.5-3.5
W-7984	1.5	1.0-2.0
Snn6Snn6	2.8[a]	2.0-4.0
snn6snn6	2.1[a]	1.0-3.5

[a] Average disease reaction of the RILs with an *Snn6Snn6* genotype is significantly different from that of RILs with an *snn6snn6* genotype at the 0.01 level of probability

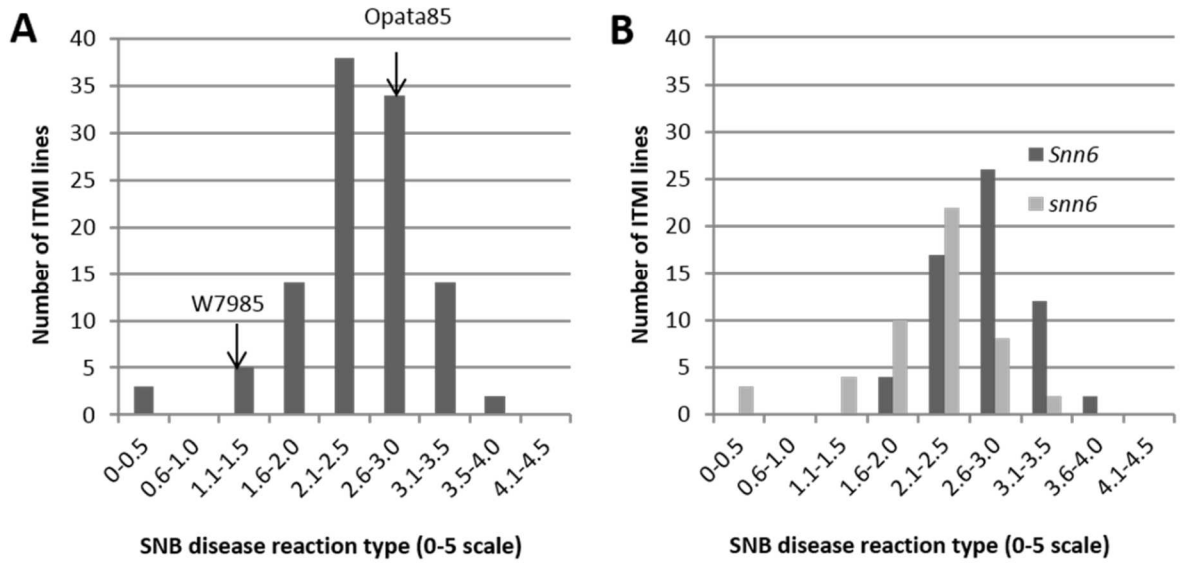

Figure 2.7. Histograms of the average SNB disease reaction type induced by Sn6 conidial inoculation.

(**A**) Average SNB disease reaction types of the ITMI population. (**B**) Average SNB disease reaction types of the SnTox6 sensitive (*Snn6*, black) and insensitive (*snn6*, gray) ITMI RIL lines.

The ITMI population also segregated for the NE sensitivity genes *Snn1* and *Snn3-B1*, but these genetic loci, which lie on chromosome arms 1BS and 5BS, respectively, were not significantly associated with disease caused by Sn6. Therefore, we used conidia of Sn6 to

inoculate ITMI6 and ITMI10, both of which are sensitive to SnTox6, SnTox1 and SnTox3 (*Snn1Snn1*/*Snn3-B1Snn3-B1*/*Snn6Snn6* genotype), and conducted RT-PCR using RNA collected three days after inoculation to check the expression levels of the *SnTox1* and *SnTox3* genes. Also, RNA collected from ITMI6 and ITMI10 three days after inoculation with isolates Sn2000 and Sn4 were used as controls, because Sn2000 and Sn4 are known to have and express the *SnTox1* and *SnTox3* genes, respectively (Liu et al., 2009; Liu et al., 2012). No *SnTox1* transcript was identified in the Sn6 inoculated plants (Figure 2.8), indicating that the SnTox1-*Snn1* interaction was not significant in disease because SnTox1 was not produced by this isolate. On the contrary, abundant transcript of *SnTox3* was identified in Sn6 (Figure 2.8), even though the SnTox3-*Snn3-B1* interaction was not significant in disease.

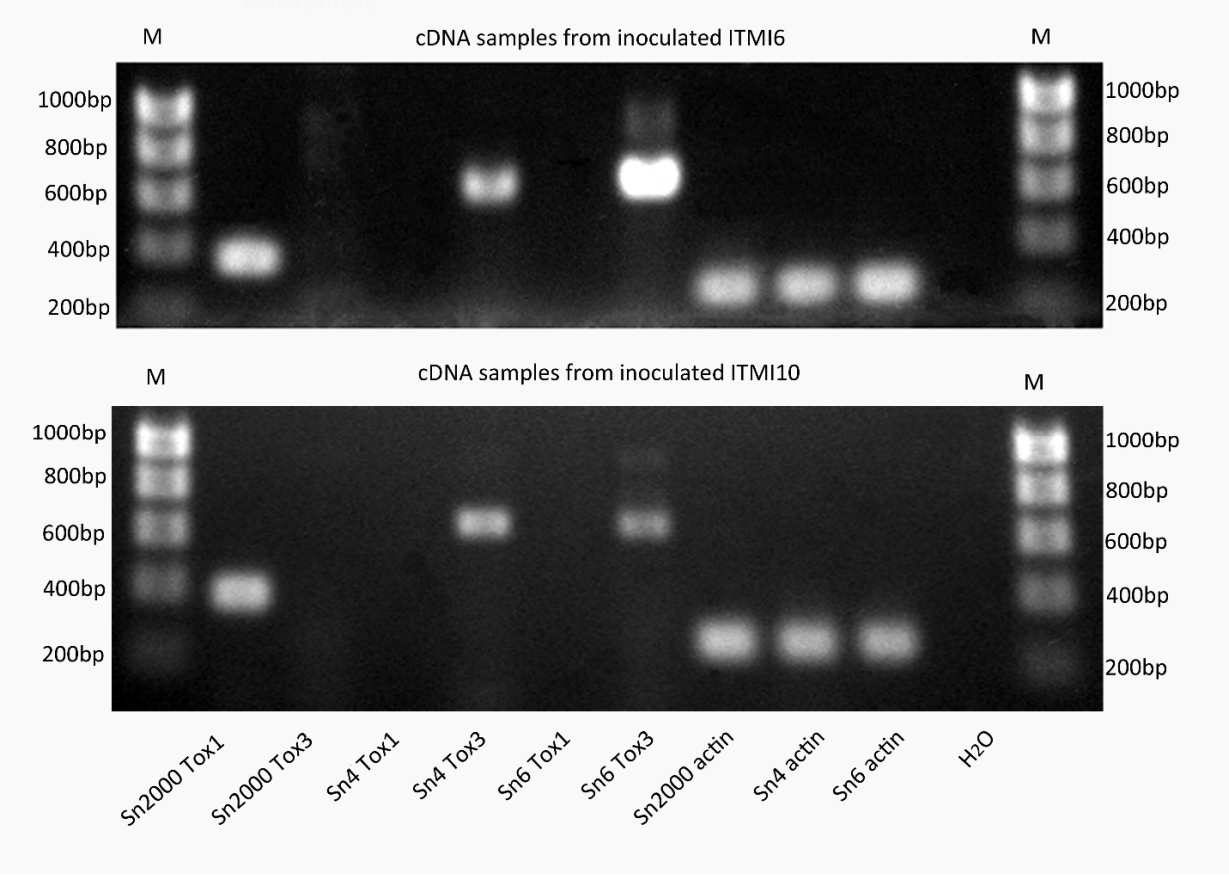

Figure 2.8. Reverse transcriptase expression of the SnTox3 and SnTox1 genes.

Reverse transcriptase PCR were performed using cDNA generated from plant inoculations of ITMI6 (top) and ITMI 10 (bottom) using *P. nodorum* isolates Sn2000, Sn4 and Sn6. Leaf tissue was harvested 3 days post inoculation. The *P. nodorum* actin gene was amplified as an internal control. PCR reaction mix without DNA (H_2O) was used as a negative control. Size standards (M) were loaded on the right and left boarders.

Discussion

The SnTox6-*Snn6* interaction is a novel NE-host gene interaction important in the *P. nodorum*-wheat pathosystem. Our previous studies showed that the *P. nodorum* isolate Sn6 harbored the genes *SnToxA*, *SnTox1*, and *SnTox3*, and it produces additional NEs including, but not limited to, SnTox2 (Friesen et al., 2007). Opata 85, a parent of the ITMI population, was moderately susceptible to isolate Sn6 and harbors *Snn3-B1* (sensitivity to SnTox3), *Snn6* and

likely *Snn5* (Abeysekara et al., 2009), while the other ITMI parent, W-7984, was moderately resistant to Sn6 and harbors only *Snn1* (sensitivity to SnTox1) (Liu et al., 2004b). Therefore the ITMI RIL population segregated for susceptibility to isolate Sn6. However, the other reported NE-sensitivity gene interactions such as the SnTox2-*Snn2* and SnTox4-*Snn4* interactions are not present in the ITMI population because neither ITMI parent harbors the sensitivity genes *Snn2* (sensitivity to SnTox2) or *Snn4* (sensitivity to SnTox4). A disease QTL on wheat chromosome 4B at a similar location as that reported for *Snn5* was reported in the ITMI population using isolate Sn2000 (Friesen et al., 2012). However, based on infiltration on the SnTox5 differential line LP29, the isolate Sn6 does not produce SnTox5. Additionally, if the SnTox5-*Snn5* interaction was contributing to disease, we should have seen a significant QTL on chromosome 4BL in the Sn6 culture filtrate infiltration and/or spore inoculation, which we did not.

The sensitivity gene *Snn6* mapped to chromosome 6A in the ITMI population and accounted for 27% of the SNB disease variation. Previously, a single QTL, *QSnl.ihar-6A* associated with partial resistance to SNB was identified on the long arm of chromosome 6A (Arseniuk et al., 2004), however, a comparison of common markers indicated that *QSnl.ihar-6A* is in a different region of 6AL, which would suggest that *Snn6* is not the gene responsible for the effect of the *QSnl.ihar-6A* QTL.

QTL analysis of infiltration data of CFs produced by isolate Sn6 on the ITMI population led to the identification of two loci, *Snn3-B1* (Zhang et al., 2011) and the novel locus on chromosome 6A (Figure 2.1) that were significantly associated with the development of necrosis. Although the ITMI population is known to segregate for sensitivity to SnTox1 (Liu et al., 2004a; Liu et al., 2012), SnTox3 (Zhang et al., 2011) and SnTox6 (current study), only the SnTox3-*Snn3-B1* and SnTox6-*Snn6* interactions were detected by CF infiltrations, and only the SnTox6-

Snn6 interaction was significant in disease caused by Sn6 conidial inoculations. SnTox1-*Snn1* was previously shown to produce a strong interaction accounting for as much as 63% of the disease variation in the ITMI population when inoculated with *P. nodorum* isolate Sn2000 (Liu et al., 2004a; Liu et al., 2004b). However, in the current work, no significance was associated with the *Snn1* locus either by CF infiltrations or by spore inoculations even though it is known that isolate Sn6 harbors the *SnTox1* gene.

Previous work in our lab has shown that the relative level of gene expression of NE genes has a significant impact on the level of disease explained by a particular NE-host gene interaction (Faris et al., 2011). The height of *in planta* gene expression for *SnTox1* (Liu et al., 2012) and *SnTox3* (Liu et al., 2009) as well as other *P. nodorum* NEs has been shown to be around 72 hours post inoculation (Friesen et al., 2006; Liu et al., 2009; Liu et al., 2012), indicating the importance of these effectors in disease development. We therefore evaluated the expression of *SnTox1* and *SnTox3 in planta* 72 hours post inoculation to see if expression levels could explain the lack of significance in disease across the ITMI population. *In planta* expression of *SnTox1* strongly indicated that expression levels of SnTox1 were responsible for the lack of significance for the SnTox1-*Snn1* interaction since no detectable transcript of SnTox1 was identified at the 72 hour time point indicating that regulation of the SnTox1 gene is different between isolates of *P. nodorum*. The failure to detect *SnTox1* transcript in Sn6-inoculated/infiltrated plants provides an explanation for the lack of significance in disease associated with the SnTox1-*Snn1* interaction.

Faris et al. (2011) showed that, in the case of the SnToxA-*Tsn1* interaction, decreased expression levels of *SnToxA* resulted in a decrease in significance of the SnToxA-*Tsn1* interaction in the presence of other NE interactions and consequently a decrease in average

disease across the population. Our results agree with those of Faris et al. (2011) in that, like *SnToxA*, regulation of *SnTox1* varies between different isolates of *P. nodorum* allowing it to play a more significant role in SNB for some isolates (e.g. Sn2000) (Liu et al., 2004a; Liu et al., 2004b; Liu et al., 2012) but less so for others (e.g. Sn6). On the contrary, SnTox3 showed high levels of expression both *in planta* and in culture (data not shown) indicating that the limiting factor for the SnTox3-*Snn3-B1* interaction lies on the host side and likely in the *Snn3-B1* gene or pathway.

Unlike SnTox1, SnTox3 was produced in sufficient quantities in Sn6 CFs to induce necrosis upon infiltration. For this reason, and because separation of SnTox3 from SnTox6 by chromatography was difficult, we disrupted the *SnTox3* gene in isolate Sn6. Infiltration of Sn6ΔSnTox3 CFs on the ITMI population verified that the *SnTox3*-disrupted strain did not produce SnTox3 (data not shown). Sensitive:insensitive ratios to Sn6ΔSnTox3 CF of the ITMI population segregated 1:1 indicating a single gene conferred sensitivity to SnTox6. This data also allowed us to precisely locate *Snn6* to the long arm of wheat chromosome 6A.

SnTox3 was produced both in culture and *in planta* during disease development. RT-PCR also showed that transcript of SnTox3 was present during infection therefore the lack of significance of the SnTox3-*Snn3-B1* interaction was not explained by lack of *SnTox3* expression or SnTox3 production. The SnTox3-*Snn3-B1* interaction was previously shown to be a relatively weak interaction compared to other reported interactions (Friesen et al., 2008a) and predominately masked by stronger interactions including SnToxA-*Tsn1* and SnTox2-*Snn2* (Friesen et al., 2008a). Friesen et al. (2007) showed that Sn6 produced SnToxA and SnTox2, but did not observe the production of SnTox3. All these results indicate that the SnTox3-*Snn3-B1* interaction can be weak in some populations relative to the other interactions, and even if both

host and pathogen components are present, it may not be significant either due to masking by other interactions, or due to the small sizes of the populations used in these studies and therefore the interaction does not meet the significance threshold used in statistical analysis. Additionally it is possible that more than one allele of *Snn3-B1* exists. Evidence of different alleles of *Snn3-B1* has been observed where different wheat lines show different levels of sensitivity to the same concentration of purified SnTox3 (Faris and Friesen, unpublished data).

Because a relatively small population (106 lines) was used here to evaluate disease produced by isolate Sn6, it is possible that other interactions with relatively minor effects in addition to the SnTox3-*Snn3-B1* interaction were not statistically significant even though collectively these interactions likely contribute to disease. The use of a larger mapping population would increase the power to detect interactions with relatively minor effects and likely lead to the identification of multiple loci associated with disease development, which together would account for more of the variation in SNB.

SnTox6 is similar to several other small secreted protein effectors produced by necrotrophs, hemi-biotrophs, and biotrophs including similar size, secretion, and function in terms of conferring rapid induction of programmed cell death (PCD) (Stergiopoulos and de Wit, 2009; Stergiopoulos et al., 2013). Based on size exclusion chromatography, SDS-PAGE, and 2DGE, the estimated size of SnTox6 is likely around 12 kDa, comparable to the estimated sizes of the other six *P. nodorum* NEs including SnToxA (13.2 kDa) (Tuori et al., 2000; Friesen et al., 2006), SnTox1 (10.33 kDa) (Liu et al., 2012), SnTox3 (18 kDa) (Liu et al., 2009), SnTox2 (7-10 kDa) (Friesen et al., 2007), SnTox4 (10 - 30 kDa) (Abeysekara et al., 2009), and SnTox5 (10 - 30 kDa) (Friesen et al., 2012). From the HPLC gel filtration chromatography, the size of SnTox6

was not perfectly clear but based on size standards was likely around that of cytochrome C (12.3 kDa).

Mass-spectrometry was performed on the two 2DGE spots obtained from the most active HPLC gel filtration fraction and used an SN15 protein database (Hane et al., 2007) to identify candidate proteins. None of the hits obtained from the SN15 protein database were obvious candidates for SnTox6. Therefore, using 6-way translation databases that we generated from the SN15 and Sn4 genome sequences (Syme et al., 2013), a single region with three peptide hits was identified corresponding to the 12 kDa spot. The genomic region matching this peptide region had not been annotated previously (Hane et al., 2007). Additional work to validate this gene/protein is underway.

Like several other *P. nodorum* (Oliver et al., 2012) and *P. tritici-repentis* (Pandelova et al., 2012) NE interactions, the SnTox6-*Snn6* interaction is dependent on light. Therefore, SnTox6 is likely to utilize a similar downstream mechanism as SnToxA/Ptr ToxA, SnTox1, SnTox2, SnTox4 and SnTox5 to induce necrosis/chlorosis. Currently we are working toward isolating SnTox6 and cloning the *SnTox6* gene in order to further characterize the SnTox6-*Snn6* interaction.

SnTox3 induces necrosis (PCD) using two, likely homeologous, genes *Snn3-B1* and *Snn3-D1* (Zhang et al., 2011) which have been shown to account for as much as 18% and more than 90% of the disease variation, respectively. The ITMI population segregates for *Snn3-B1* and likely carries a weaker allele than that present at the *Snn3-D1* locus. We are currently evaluating several sources of the *Snn3-B1* gene as well as attempting to clone both the *Snn3-B1* and *Snn3-D1* loci to evaluate the possibility of alleles conferring different intensities of PCD.

The *P. nodorum*-wheat interaction has been studied as a model to reveal the host-pathogen interaction between necrotrophic specialist pathogens and plant hosts. Unlike the biotrophic pathogen-host interactions that follow the classic gene-for-gene model, *P. nodorum* secretes NEs as determinants to trigger a compatible interaction (susceptible) on the host genotypes that carry the corresponding sensitivity genes in an inverse gene-for-gene manner. Because the NEs produced by *P. nodorum* are critical to the development of SNB, the identification of novel NE-host susceptible gene interactions is significant. This information can be used by breeders to identify SNB resistance sources by evaluating breeding lines using each NE. Also, the molecular markers identified in this research that flank the *Snn6* locus can be used in marker-assisted selection schemes to expedite the removal of SnTox6 sensitivity from breeding materials and varieties.

References

Abeysekara, N.S., Friesen, T.L., Keller, B., and Faris, J.D. 2009. Identification and characterization of a novel host-toxin interaction in the wheat-*Stagonospora nodorum* pathosystem. Theoretical and Applied Genetics 120:117-126.

Andrew, M., Barua, R., Short, S.M., and Kohn, L.M. 2012. Evidence for a Common Toolbox Based on Necrotrophy in a Fungal Lineage Spanning Necrotrophs, Biotrophs, Endophytes, Host Generalists and Specialists. Plos One 7:e29943.

Arseniuk, E., Czembor, P.C., Czaplicki, A., Song, Q.J., Cregan, P.B., Hoffman, D.L., and Ueng, P.P. 2004. QTL controlling partial resistance to Stagonospora nodorum leaf blotch in winter wheat cultivar Alba. Euphytica 137:225-231.

Chisholm, S.T., Coaker, G., Day, B., and Staskawicz, B.J. 2006. Host-microbe interactions: shaping the evolution of the plant immune response. Cell 124:803-814.

Faris, J.D., Zhang, Z.C., Rasmussen, J.B., and Friesen, T.L. 2011. Variable Expression of the *Stagonospora nodorum* Effector SnToxA Among Isolates Is Correlated with Levels of Disease in Wheat. Molecular Plant-Microbe Interactions 24:1419-1426.

Faris, J.D., Zhang, Z., Lu, H., Lu, S., Reddy, L., Cloutier, S., Fellers, J.P., Meinhardt, S.W., Rasmussen, J.B., and Xu, S.S. 2010. A unique wheat disease resistance-like gene governs effector-triggered susceptibility to necrotrophic pathogens. Proceedings of the National Academy of Sciences 107:13544-13549.

Flor, H. 1956. The complementary genic systems in flax and flax rust. Advances in genetics 8:29-54.

Fried, P., and Meister, E. 1987. Inheritance of leaf and head resistance of winter wheat to *Septoria nodorum* in a diallel cross. Phytopathology 77:1371-1375.

Friesen, T.L., and Faris, J.D. 2010. Characterization of the wheat-*Stagonospora nodorum* disease system: what is the molecular basis of this quantitative necrotrophic disease interaction? Canadian journal of plant pathology 32:20-28.

Friesen, T.L., and Faris, J.D. 2012. Characterization of plant-fungal interactions involving necrotrophic effector-producing plant pathogens. Methods in Molecular Biology. 835:191-207.

Friesen, T.L., Meinhardt, S.W., and Faris, J.D. 2007. The *Stagonospora nodorum*-wheat pathosystem involves multiple proteinaceous host-selective toxins and corresponding host sensitivity genes that interact in an inverse gene-for-gene manner. The Plant Journal 51:681-692.

Friesen, T.L., Faris, J.D., Solomon, P.S., and Oliver, R.P. 2008a. Host-specific toxins: effectors of necrotrophic pathogenicity. Cellular microbiology 10:1421-1428.

Friesen, T.L., Chu, C.G., Xu, S.S., and Faris, J.D. 2012. SnTox5-*Snn5*: a novel *Stagonospora nodorum* effector-wheat gene interaction and its relationship with the SnToxA-*Tsn1* and SnTox3-*Snn3-B1* interactions. Molecular Plant Pathology 13:1101-1109.

Friesen, T.L., Zhang, Z., Solomon, P.S., Oliver, R.P., and Faris, J.D. 2008b. Characterization of the interaction of a novel *Stagonospora nodorum* host-selective toxin with a wheat susceptibility gene. Plant physiology 146:682-693.

Friesen, T.L., Chu, C.G., Liu, Z.H., Xu, S.S., Halley, S., and Faris, J.D. 2009. Host-selective toxins produced by *Stagonospora nodorum* confer disease susceptibility in adult wheat plants under field conditions. Theoretical and Applied Genetics 118:1489-1497.

Friesen, T.L., Stukenbrock, E.H., Liu, Z., Meinhardt, S., Ling, H., Faris, J.D., Rasmussen, J.B., Solomon, P.S., McDonald, B.A., and Oliver, R.P. 2006. Emergence of a new disease as a result of interspecific virulence gene transfer. Nature genetics 38:953-956.

Hane, J.K., Lowe, R.G.T., Solomon, P.S., Tan, K.C., Schoch, C.L., Spatafora, J.W., Crous, P.W., Kodira, C., Birren, B.W., Galagan, J.E., Torriani, S.F.F., McDonald, B.A., and Oliver, R.P. 2007. Dothideomycete-plant interactions illuminated by genome sequencing and EST analysis of the wheat pathogen *Stagonospora nodorum*. Plant Cell 19:3347-3368.

Joehanes, R., and Nelson, J.C. 2008. QGene 4.0, an extensible Java QTL-analysis platform. Bioinformatics 24:2788-2789.

Jones, J.D.G., and Dangl, J.L. 2006. The plant immune system. Nature 444:323-329.

King, J., Cook, R., and Melville, S. 1983. A review of Septoria diseases of wheat and barley. Annals of applied biology 103:345-373.

Kosambi, D.D. 1944. The estimation of map distances from recombination values. Annals of Eugenics 12:172-175.

Laemmli, U. 1970. Cleavage of structural proteins during the assembly of the head of bacteriophage T4. Nature 227:680-685.

Lamari, L., Strelkov, S., Yahyaoui, A., Orabi, J., and Smith, R. 2003. The identification of two new races of *Pyrenophora tritici-repentis* from the host center of diversity confirms a one-to-one relationship in tan spot of wheat. Phytopathology 93:391-396.

Lander, E.S., Green, P., Abrahamson, J., Barlow, A., Daly, M.J., Lincoln, S.E., Newberg, L.A., and Newburg, L. 1987. MAPMAKER: an interactive computer package for constructing primary genetic linkage maps of experimental and natural populations. Genomics 1:174-181.

Lin-Moshier, Y., Sebastian, P.J., Higgins, L., Sampson, N.D., Hewitt, J.E., and Marchant, J.S. 2013. Re-evaluation of the Role of Calcium Homeostasis Endoplasmic Reticulum Protein (CHERP) in Cellular Calcium Signaling. Journal of Biological Chemistry 288:355-367.

Liu, Z., and Friesen, T.L. 2012. Polyethylene Glycol (PEG)-Mediated Transformation in Filamentous Fungal Pathogens. Plant Fungal Pathogens: Methods and Protocols 835:365-375.

Liu, Z., Faris, J., Meinhardt, S., Ali, S., Rasmussen, J., and Friesen, T. 2004a. Genetic and physical mapping of a gene conditioning sensitivity in wheat to a partially purified host-selective toxin produced by *Stagonospora nodorum*. Phytopathology 94:1056-1060.

Liu, Z., Friesen, T., Rasmussen, J., Ali, S., Meinhardt, S., and Faris, J. 2004b. Quantitative trait loci analysis and mapping of seedling resistance to Stagonospora nodorum leaf blotch in wheat. Phytopathology 94:1061-1067.

Liu, Z., Faris, J.D., Oliver, R.P., Tan, K.C., Solomon, P.S., McDonald, M.C., McDonald, B.A., Nunez, A., Lu, S., and Rasmussen, J.B. 2009. SnTox3 acts in effector triggered susceptibility to induce disease on wheat carrying the *Snn3* gene. PLoS Pathogens 5:e1000581.

Liu, Z., Zhang, Z., Faris, J.D., Oliver, R.P., Syme, R., McDonald, M.C., McDonald, B.A., Solomon, P.S., Lu, S., and Shelver, W.L. 2012. The Cysteine Rich Necrotrophic Effector SnTox1 Produced by *Stagonospora nodorum* Triggers Susceptibility of Wheat Lines Harboring *Snn1*. PLoS Pathogens 8:1-24.

Lu, H.J., Fellers, J.P., Friesen, T.L., Meinhardt, S.W., and Faris, J.D. 2006. Genomic analysis and marker development for the *Tsn1* locus in wheat using bin-mapped ESTs and flanking BAC contigs. Theoretical and Applied Genetics 112:1132-1142.

Ma, B., Zhang, K.Z., Hendrie, C., Liang, C.Z., Li, M., Doherty-Kirby, A., and Lajoie, G. 2003. PEAKS: powerful software for peptide de novo sequencing by tandem mass spectrometry. Rapid Communications in Mass Spectrometry 17:2337-2342.

Manning, V.A., and Ciuffetti, L.M. 2005. Localization of Ptr ToxA produced by *Pyrenophora tritici-repentis* reveals protein import into wheat mesophyll cells. The Plant Cell 17:3203-3212.

Nelson, J.C., Van Deynze, A.E., Sorrells, M.E., Autrique, E., Lu, Y.H., Negre, S., Bernard, M., and Leroy, P. 1995. Molecular mapping of wheat. Homoeologous group 3. Genome 38:525-533.

Nurnberger, T., Brunner, F., Kemmerling, B., and Piater, L. 2004. Innate immunity in plants and animals: striking similarities and obvious differences. Immunological reviews 198:249-266.

Oliver, R.P., and Solomon, P.S. 2010. New developments in pathogenicity and virulence of necrotrophs. Current Opinion in Plant Biology 13:415-419.

Oliver, R.P., Friesen, T.L., Faris, J.D., and Solomon, P.S. 2012. *Stagonospora nodorum*: From Pathology to Genomics and Host Resistance. Pages 23-43 in: Annual Review of Phytopathology, Vol 50, N.K. VanAlfen, J.E. Leach, and S. Lindow, eds. Annual Reviews, Palo Alto.

Pandelova, I., Figueroa, M., Wilhelm, L.J., Manning, V.A., Mankaney, A.N., Mockler, T.C., and Ciuffetti, L.M. 2012. Host-Selective Toxins of *Pyrenophora tritici-repentis* Induce Common Responses Associated with Host Susceptibility. Plos One 7:e40240.

Qi, L.L., Echalier, B., Chao, S., Lazo, G.R., Butler, G.E., Anderson, O.D., Akhunov, E.D., Dvorak, J., Linkiewicz, A.M., Ratnasiri, A., Dubcovsky, J., Bermudez-Kandianis, C.E., Greene, R.A., Kantety, R., La Rota, C.M., Munkvold, J.D., Sorrells, S.F., Sorrells, M.E., Dilbirligi, M., Sidhu, D., Erayman, M., Randhawa, H.S., Sandhu, D., Bondareva, S.N., Gill, K.S., Mahmoud, A.A., Ma, X.F., Miftahudin, Gustafson, J.P., Conley, E.J., Nduati, V., Gonzalez-Hernandez, J.L., Anderson, J.A., Peng, J.H., Lapitan, N.L.V., Hossain, K.G., Kalavacharla, V., Kianian, S.F., Pathan, M.S., Zhang, D.S., Nguyen, H.T., Choi, D.W., Fenton, R.D., Close, T.J., McGuire, P.E., Qualset, C.O., and Gill, B.S. 2004. A chromosome bin map of 16,000 expressed sequence tag loci and distribution of genes among the three genomes of polyploid wheat. Genetics 168:701-712.

Rappsilber, J., Ishihama, Y., and Mann, M. 2003. Stop and go extraction tips for matrix-assisted laser desorption/ionization, nanoelectrospray, and LC/MS sample pretreatment in proteomics. Analytical Chemistry 75:663-670.

Sharma, N., Rahman, M.H., Strelkov, S., Thiagarajah, M., Bansal, V.K., and Kav, N.N.V. 2007. Proteome-level changes in two Brassica napus lines exhibiting differential responses to the fungal pathogen Alternaria brassicae. Plant Science 172:95-110.

Shevchenko, A., Wilm, M., Vorm, O., and Mann, M. 1996. Mass spectrometric sequencing of proteins from silver stained polyacrylamide gels. Analytical Chemistry 68:850-858.

Stergiopoulos, I., and de Wit, P. 2009. Fungal Effector Proteins. Annual Review of Phytopathology 47:233-263.

Stergiopoulos, I., Collemare, J., Mehrabi, R., and De Wit, P. 2013. Phytotoxic secondary metabolites and peptides produced by plant pathogenic Dothideomycete fungi. Fems Microbiology Reviews 37:67-93.

Syme, R.A., Hane, J.K., Friesen, T.L., and Oliver, R.P. 2013. Resequencing and Comparative Genomics of *Stagonospora nodorum*: Sectional Gene Absence and Effector Discovery. G3-Genes Genomes Genetics 3:959-969.

Torada, A., Koike, M., Mochida, K., and Ogihara, Y. 2006. SSR-based linkage map with new markers using an intraspecific population of common wheat. Theoretical and Applied Genetics 112:1042-1051.

Tuori, R.P., Wolpert, T.J., and Ciuffetti, L.M. 2000. Heterologous expression of functional Ptr ToxA. Molecular Plant-Microbe Interactions 13:456-464.

Wicki, W., Winzeler, M., Schmid, J., Stamp, P., and Messmer, M. 1999. Inheritance of resistance to leaf and glume blotch caused by *Septoria nodorum* Berk. in winter wheat. Theoretical and Applied Genetics 99:1265-1272.

Wolpert, T.J., Dunkle, L.D., and Ciuffetti, L.M. 2002. Host-selective toxins and avirulence determinants: What's in a name? Annual Review of Phytopathology 40:251-285.

Xu, S., Friesen, T., and Cai, X. 2004. Sources and genetic control of resistance to Stagonospora nodorum blotch in wheat. Recent Research Developments in Genetics & Breeding 1:449-469.

Zhang, J., Xin, L., Shan, B.Z., Chen, W.W., Xie, M.J., Yuen, D., Zhang, W.M., Zhang, Z.F., Lajoie, G.A., and Ma, B. 2012. PEAKS DB: De Novo Sequencing Assisted Database Search for Sensitive and Accurate Peptide Identification. Molecular & Cellular Proteomics 11.

Zhang, Z., Friesen, T.L., Xu, S.S., Shi, G., Liu, Z., Rasmussen, J.B., and Faris, J.D. 2011. Two putatively homoeologous wheat genes mediate recognition of SnTox3 to confer effector-triggered susceptibility to *Stagonospora nodorum*. The Plant Journal 65:27-38.

CHAPTER 3. SNTOX1 BINDS CHITIN TO PROTECT THE FUNGAL CELL WALL FROM WHEAT CHITINASE ACTIVITY

Abstract

The necrotrophic effector SnTox1 was shown to interact directly or indirectly with the wheat dominant sensitivity gene *Snn1* and induce an oxidative burst, DNA laddering, and up regulation of PR genes such as PR-1 and chitinase genes. These responses result in susceptibility rather than resistance of wheat cultivars that carry the *Snn1* gene. Interestingly, the SnTox1 protein contains chitin binding domains and was shown to bind a main component of the fungal cell wall, chitin. SnTox1 was therefore hypothesized to prevent fungal cell wall against wheat chitinases. To investigate this hypothesis, two wheat chitinases were used to treat several fungal species including *P. nodorum*, *Neuorospora crassa*, *Pyrenophora teres* f. *teres*, and *Cercospora beticola*. All strains harboring *SnTox1* grew better than the strain not harboring *SnTox1*, showing that SnTox1 not only protected *P. nodorum* but also other fungi against degradation by wheat chitinase, providing evidence for a second role in pathogenicity.

Introduction

When attacked by pathogens, plants utilize a series of strategies to induce a hypersensitive response. These strategies include programmed cell death, an oxidative burst, reinforcement of plant cell walls, secretion of pathogenesis-related (PR) proteins, and production of other secondary metabolites (van den Burg et al., 2006). Most PR proteins accumulate in the vacuoles or apoplast where fungal pathogens grow after penetration. Some PR proteins, such as fungal cell wall degraded enzymes, hydrolyze different components of the fungal cell wall to inhibit the growth of fungal pathogens (van den Burg et al., 2006). Well described PR proteins include β-1, 3-glucanases (PR-2), chitinases (PR-3, 4, 8, or 11) and some serine and cysteine

proteases (Datta and Muthukrishnan, 1999; Jorda et al., 1999; Jorda and Vera, 2000; Kruger et al., 2002). Chitinases are classified into two categories: endochitinases and exochitinases. Endochitinases randomly cleave the internal β-1, 4-glycoside bonds of chitin to produce N-acetylglucosamine. Exochitinases are divided into two subgroups, chitobiosidases which catalyze the nondeoxydizing end of the chitin microfibril with the production of di-acetylchitobioses, and β-1, 4-N-acetylglucoseaminidases which cleave oligomer products of endochitinases and chitobiosidases to produce monomer the N-acetylglucosamine. (Cohen-Kupiec and Chet, 1998). Based on structure, chitinases are grouped into at least five classes (class I-V) (Beintema, 1994). Some Class I chitinases locate to vacuoles, while other chitinases locate to the apoplastic fluid (Collinge et al., 1993). Class I chitinases are basic enzymes made up of an N-terminal chitin-binding domain followed by a chitinase domain and a C-terminal vacuolar targeting sequence. Class II chitinases are acidic extracellular enzymes showing 60-65% identity with class I chitinases but lacking the chitin-binding domain and vacuolar targeting sequence. Class IV chitinases include acidic and basic extracellular proteins that contain an N-terminal chitin-binding domain but lack a C-terminal extension. The structure of class IV chitinases show 30-35% identity with class I and class II chitinases. Classes I, II and IV chitinases belong to the glycoside hydrolase family 19 (GH-19). The GH-18 family includes chitinases found in classes III and V. Class III chitinases lack a cysteine-rich domain, are extracellular hydrolases without a chitin-binding domain and were previously described as lysozyme. The conserved catalytic-domain of class III chitinases show differences in amino acid sequence compared to the chitinases of class I or II. Class V chitinases have no homology with any of the other classes. This class does not have a chitin-binding domain but does contain a C-terminal extension (Beintema, 1994).

The recognition of pathogen derived molecules by PR proteins is known to trigger plant defense (van den Burg et al., 2006). To avoid recognition, fungal pathogens produce effectors that bind components of the fungal cell wall and block degradation. The best described example of a fungal effector that protects the fungal cell wall degradation is the *Cladosporium fulvum* effector protein Avr4, an effector protein produced by the tomato leaf mold pathogen *C. fulvum*. Avr4 can be recognized by the product of the tomato resistance gene *Cf4* to induce a hypersensitive response (HR) (Joosten et al., 1997; Thomas et al., 1997), however, the primary function of Avr4 is due to its chitin-binding-domain, which confers the ability of Avr4 to bind to the cell wall of *C. fulvum* and prevent chitin hydrolysis by tomato chitinases (van den Burg et al., 2006). In addition, Avr4 can bind with the cell walls of *Trichoderma viride* and *Fusarium solani* f. sp. *phaseoli* and protect growth of these fungi in the presence of plant chitinases (van den Burg et al., 2006).

SnTox1 was the first NE detected from *Parastagonospora nodorum* and was shown to be a secreted protein between 10 and 30kDa in size (Liu et al., 2004a). Host sensitivity to SnTox1 was governed by a single dominant gene designated *Snn1*. *Snn1* was physically and genetically mapped to a gene-rich region on the distal end of the short arm of chromosome 1B using the Chinese Spring wheat chromosome deletion lines and the International Triticeae Mapping Initiative (ITMI) mapping population (Liu et al., 2004b). *Snn1* accounted for as much as 58% of the disease variation across the ITMI population at the 5 day evaluation when inoculating with SnTox1 producing isolates, showing the importance of SnTox1 in SNB disease development (Liu et al., 2004b). Liu et al. (2012) found the SnTox1-*Snn1* interaction was light-dependent, and was involved in pathogen penetration and the induction of host cell death. In the *Snn1* wheat genotypes, SnTox1 triggered a series of classic defense responses including H_2O_2 production, the

up-regulation of PR genes and obvious DNA laddering (Liu et al., 2012). Interestingly, like Avr4, the SnTox1 protein has a chitin binding domain (CBD) at the C-terminus. The CBD region theoretically confers the ability of SnTox1 to bind with a main component of the fungal cell wall, chitin.

SnTox1 is hypothesized to bind the fungal cell wall and thereby protects the cell wall from chitinase degradation. The objective of this study was to investigate the protection function of SnTox1 in the presence of chitinases. To investigate the hypothesis, the SnTox1 binding affinity for chitin as well as for another polysaccharide, chitosan, was tested. Secondly, two wheat chitinases were cloned and the protection function of SnTox1 to these chitinases in *P. nodorum*, as well as several other non-wheat pathogens was tested.

Material and methods

Plant and fungal materials

The spring wheat cultivar Chinese Spring (CS) was used to clone the wheat chitinase IV gene *AF112966* and wheat chitinase II gene *AF112963* to perform a chitinase protection assay. The CS *Snn1* deletion line CS1BS-18 and CS were infiltrated with purified SnTox1 protein for the chitinase gene expression assay.

For the in vitro chitinase protection assay, ten fungal strains were used including virulent *P. nodorum* isolate Sn2000 wild type and its *SnTox1* knockout strain Sn2000Δ*SnTox1* (Liu et al., 2012), avirulent *P. nodorum* isolate Sn79-1087 wild type and its *SnTox1* transformed strain Sn79-1087+*SnTox1*, *Neurospora crassa* isolate *Nc*2489 wild type and its SnTox1 transformed strain *Nc*2489+*SnTox1*, *Cercospora beticola* isolate 0928 wild type and its *SnTox1* transformed strain *Cb*0928+*SnTox1*, *Pyrenophora teres* isolate 0-1 wild type and its SnTox1 transformed strain *Ptt*0-1+*SnTox1*. The transformation of *SnTox1* into the *P. nodorum* avirulent isolate Sn79-

1087 was achieved previously using the plasmid pDAN-SnTox1 which contains *SnTox1* and the hygromycin resistance gene (Liu et al., 2012). The same plasmid was used to transform *N. crassa*, *P. teres* f. *teres*, and *C. beticola* following the polyethylene glycol-mediated transformation method described in Liu and Friesen (2012). The transformants for each fungus were tested for the presence of *SnTox1* using PCR with the primer pair of SnTox1gF and SnTox1gR (Table 3.1). The positive transformants for each fungus were also tested for the production of SnTox1 by infiltrating culture filtrates prepared from each onto CS.

DNA and RNA extraction

To extracted total RNA and DNA of wheat leaf tissue, wheat leaves with different treatments were frozen in liquid nitrogen and were ground with a mortar and pestle. Total RNA of wheat leaves was extracted using the RNeasy Plant Mini Kit (QIAGEN) according to the kit manual and then reverse transcribed to cDNA. The cDNA samples were used for wheat chitinase gene cloning and quantitative measurement of wheat chitinase gene expression. DNA of wheat leaves treated with inoculation was extracted using a Biosprint 15 DNA Plant Kit (QIAGEN) and Biosprint 15 workstation (QIAGEN) according to the kit manual. The DNA samples were used to measure biomass through quantitative PCR. The quantity of DNA and RNA was estimated by the Bradford method (Kruger, 1994) using a Qubit (Invitrogen). DNA and RNA was dried by lyophilization and adjusted to 200ng/µl by adding sterilized MilliQ water according to the original quantity of each DNA or RNA sample.

Expression and purification of wheat chitinase, SnTox1, and Avr4

The wheat genes encoding the chitinase IV (Li et al., 2001) which has a chitin binding domain (CBD) and the chitinase II (Li et al., 2001) which does not have a CBD were amplified from RNA obtained from leaves of Chinese Spring. Total RNA was reverse transcribed to cDNA

using the TaqMan reverse transcription reagents (Roche). The wheat chitinase genes without the signal sequence were amplified from the cDNA with the forward primers 112963EcoNosig.F and 112963Xba+2.R for *AF112963* and primers 112966EcoNosig. F and 112966Xbai+2.R for *AF112966* (Table 3.1). The primer pairs contain *Eco*RI and *Xba*I restriction sites, respectively, for subsequent sub-cloning into the *Pichia pastoris* expression vector PGAPZα (Invitrogen). PCR was run using the following program: 94 ℃ for 4 min; 30 cycles of 94 ℃ for 30 sec, 60 ℃ for 30 sec, and 72 ℃ for 3 min, followed by 72 ℃ for 10 min. The PCR amplicon was cloned into the TopoTA vector (Invitrogen) for sequencing. After the sequence confirmation, the chitinase gene fragment was released from the TopoTA backbone by *EcoRI* and *XbaI* restriction enzymes and then was ligated into the PGAPZA*α* vector between the *Pichia α*-factor mating signal sequence and the 6× histidine tag. Since the *Cladosporium fulvum* gene *Avr4* (provided by Pierre deWit, NCBI Accession No. CAA55403) protects fungal cell walls against hydrolysis by plant chitinases (van den Burg et al., 2006), Avr4 was used as a positive control. *Avr4* without a signal peptide sequence was amplified from its plasmid using primers Avr4Eco.F and Avr4Xba.R (Table 3.1) containing EcoRI and XbaI restriction sites, respectively, and then was cloned into the PGAPZ*α* vector using the same method as above. The expression construct of the two chitinase genes, SnTox1, Avr4 and the empty PGAPZ*α* vector were transformed into *P. pastoris* strain X33 using the Pichia EasyComp Transformation Kit (Invitrogen). Positive *P. pastoris* transformant strains were confirmed by PCR using primer pairs 112963EcoNosig.F / 112963Xba+2.R, 112966EcoNosig. F / 112966Xbai+2.R, Avr4Eco.F / Avr4Xba.R, 20078CF / 20078CR_NT, and pGAPZF/ 3AOX1 to amplify *AF112963*, *AF112966*, *Avr4, SnTox1* and mutated *SnTox1* and partial sequence on the empty PGAPZ*α* vector, respectively (Table 3.1).

The PCR program was set up as 94°C 4 min; 94°C 30 sec, 60°C 30 sec, 72°C 1 min, 30 cycles; 72°C 10 min. The amplicons were further confirmed by sequencing.

To express the wheat chitinase, SnTox1 and Avr4, the transformed *P. pastoris* strains with the complete expression cassette were cultured in 2 liters of yeast peptone dextran liquid media (Invitrogen user manual) at 30 ℃ for 2 days. All culture filtrates were harvested and dialyzed overnight against binding buffer (20mM sodium phosphate, 500mM NaCl, 10mM Imidazole). The expressed proteins in culture filtrates were then purified using a Ni Sepharose 6 Fast Flow HisPrep FF 16/10 column (GE Healthcare Life Sciences) and an ÄKTA Prime Plus system (GE Healthcare Life Sciences). The eluted fractions containing the purified protein were confirmed by running a 16.5% Tricine precast gel (Bio-rad) at 100 volts for 2 h. The purified proteins were then dialyzed against water overnight and concentrated by lyophilization. The quantity of purified proteins were estimated by the Bradford method (Kruger, 1994) using a Qubit (Invitrogen).

Polysacharide binding assay

The polysaccharide-binding assay for purified SnTox1-His was performed following a protocol described in van den Burg et al. (2006) with minor modifications. Polysaccharide compounds for the assay included shrimp shell chitin (Sigma-Aldrich), chitin-beads (New England Bioscience), and chitosan (Sigma-Aldrich). Insoluble polyssacharides were hydrated in 500 µl of incubation buffer (20mM NaCl, 5mM TrisHCl, pH5.5) for 15 min with gentle shaking. After centrifugation for 3 min at 16,000 ×g (maximum speed), the buffer was removed. Hydrated polysaccharides (10 mg each) were then incubated with a total of 5 µg of purified SnTox1-His in a 500 µl solution for 2 h at room temperature with gentle shaking. The supernatants containing unbound fractions were collected by centrifugation for 3 min at 12,000g. The insoluble pellet

containing bound SnTox1-His was further washed with 500 µl of incubation buffer and then washed with water three times for 10 min each with shaking at room temperature. Bound SnTox1-His on the various polysaccharides was then eluted by adding 25 µl Tricine sample buffer (Bio-rad) plus 15 µl β-mercaptoethanol and boiled for 10 min. The same amount of SnTox3 was used as a negative control. Bound and unbound supernatant fractions of each treatment were separated on a 16.5% Tris-Tricine precast gel (Bio-rad) at 100 volts for 2 h. Precision Plus Protein Dual Color Standard (Bio-Rad) was added as the protein standard. The precast gel was stained in 0.2% Coomassie Blue overnight and destained in sterile water for 8h. The gel was scanned using CanoScan LiDE70 (Canon). Three replicates were completed for each treatment.

Testing of the SnTox1 protection mechanism in different fungi

The dried plugs of all fungal isolates/strains, including wild type, *SnTox1*-transformed strains and *SnTox1* knockout strains were regrown on V8-potato dextrose agar plates according to the culture methods described by Friesen and Faris (2012). Spores were harvested and diluted at a concentration of 10,000 spores/ml for *P. nodorum* and *N. crassa* and 2,000 spores/ml for *P. teres* f. *teres*, and *C. beticola*. Spores were inoculated into 200 µl of ½ Fries media in a 96 well ELISA plate, followed by the addition of wheat chitinase II (AF112963) or chitinase IV (AF112966) at a final concentration of 7µM or 4 µM, respectively. The purified SnTox1-His was added to the solution at 25 µM for testing the SnTox1 protection activity. Avr4 was added at the final concentration of 25 µM in the presence of wheat chitinase as the positive control. For the fungal isolate Sn2000 (containing *SnTox1*) and transformed isolates with *SnTox1*, wheat chitinases alone were added to test the chitinase protection of endogenous SnTox1. In addition, spore cultures without chitinase, SnTox1, SnTox1 mutants or Avr4 were included as controls to

ensure the viability of the spores for each fungus. All reactions were set up in a microtiter plate (Greiner bio-one) and incubated at room temperature (or 25 °C) with shaking at 20rpm for 30min and then incubated under light at room temperature. Three biological replications were completed for each treatment. The germination of spores and the growth of mycelia were examined at 24 h after the treatment using a Nikon inverted compound microscope (EclipseTE2000-U, Nikon). Photographs were taken using a Canon 70D camera attached to the microscope. Fungal growth under each treatment was also measured by optical density (OD) using an ELx800 Absorbance Microplate Reader (BIO-TEK). The OD values of mycelial densities were calculated at 0h and then every 24h for 5 days at an absorbance of 630 nm using software Gen 5 2.05.

Wheat chitinase gene expression after SnTox1 infiltration using qPCR

Two-week old secondary leaves of CS and CS1BS18 were infiltrated with purified SnTox1. Purified protein from the *P. pastoris* transformant with an empty PGAPZ*α* vector were used to infiltrate CS and CS 1BS18 as the negative control. Infiltrated leaf tissue was collected at 1, 2, 4, 8, 10, 24, 36, 48, 60 and 72 h post infiltration. Three replications were completed, with each replication consisting of four leaves. The infiltrated tissue was collected for each time point. The first strand cDNA was synthesized from total RNA, and real time PCR was performed using SsoAdvanced Universal SYBR Green Supermix (Bio-Rad) and the CFX384 Real-Time PCR system (Bio-Rad). The primer pairs AF112966qF / AF112966qR and AF112963qF / AF112963qR (Table 3.1) were used for the AF112966 and AF112963 genes, respectively, in qPCR. The primers WtActinqF and WtActinqR (Table 3.1) were used for the wheat actin gene as an internal control to normalize the relative quantities of chitinase gene expression. Quantitative PCR reactions containing three replicates at each time point for each treatment were set up in a

384 hard-shell PCR plate (Bio-Rad). Normalized relative quantities of chitinase gene expression and standard deviation were calculated using the Bio-Rad CFX Manager software.

Table 3.1. Primers used in Chapter 3

Primer ID	Sequences	Usage
112963EcoNosig.F	GAATTCGATCCCGTGGAGAGCGTCGTCACC	Amplify AF112963 gene without signal peptide sequence
112963Xbal+2.R	TCTAGATAGCAAGTGAGGTTGTTCCCCGGGT	Amplify AF112963 gene without signal peptide sequence
112966EcoNosig.F	GAATTCCAGAACTGCGGCTGCCAGCCGAAC	Amplify AF112966 gene
112966 Xbal+2.R	TCTAGATAGCAAGTGAGGTTGTTCCCTGGGTC	Amplify AF112966 gene
SnTox1cF	ATGAAGCTTACTATGGTCTTGT	Amplify SnTox1 gene
SnTox1cR_NT	TGTGGCAGCTAACTAGCACA	Amplify SnTox1 gene
Avr4Eco.F	GAATTCATGCACTACACAACCCTCCTCCTA	Amplify Avr4 gene
Avr4Xba.R	TCTAGAGCTTGCGGCGTCTTTACCGGACAC	Amplify Avr4 gene
112963qF	CAGAAGCTCGGCTTCAACGGGCTCG	Quantitative PCR for AF112963 gene expression
112963qR	GCGCGTTCCCGCCGTTGCACTCGC	Quantitative PCR for AF112963 gene expression
112966qF	CTAGCAGCACTAGTCCTATCT	Quantitative PCR for AF112963 gene expression
112966qR	ATCGCCGCTCCCGCCGCCGCTCGCCGT	Quantitative PCR for AF112963 gene expression
SnTox1gF	TACATCTAGACCTTCTTCCAT	Amplify genomic region of SnTox1 from SnTox1 transformed strains
SnTox1gR	AATCTAGACGTGTGGTCCGCTAACCTAT	Amplify genomic region of SnTox1 from SnTox1 transformed strains
WActinF	GCGGTCGAACAACTGGTATT	Used to amplify the wheat actin gene fragment as an internal control
WActinR	ACCTGACCATCAGGCATCTC	Used to amplify the wheat actin gene fragment as an internal control
pGAPZF	GTCCCTATTTCAATCAATTGAA	Amplify the partial sequences of pGAPZα vector
3AOX1	GCAAATGGCATTCTGACATCC	Amplify the partial sequences of pGAPZα vector

Results

SnTox1 has the ability to bind polysaccharides

SnTox1 contains a putative chitin binding domain (CBD) at the C-terminus (Liu et al., 2012), likely providing SnTox1 with the ability to bind chitin. To test this hypothesis, shrimp shell chitin, chitin beads, as well as chitosan were used to test the binding activity of SnTox1. SnTox1 (10.33 kDa) was found to have strong binding capacity to crab shell chitin and chitin beads, but not chitosan (Figure 3.1). The positive control Avr4 (10kDa) showed a similar binding result as SnTox1. SnTox3 (25.8kDa) (Liu et al., 2009), the negative control, did not bind with any of the polysaccharides tested (Figure 3.1).

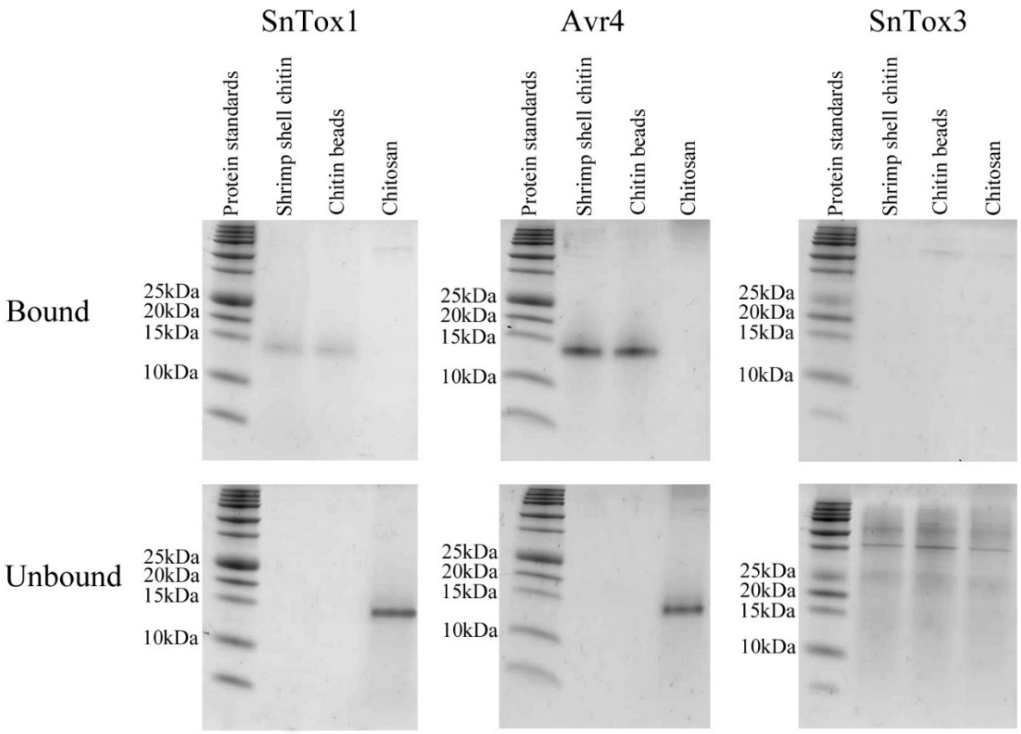

Figure 3.1. Polysaccharide binding assay of SnTox1.

The bound (top) fractions that precipitated with each polysaccharide and the unbound supernatant (bottom) that eluted with the incubation buffer are shown on a 16.5% Tris-Tricine precast gel (Bio-Rad). The size of SnTox3 is indicated by a black arrow. Precision Plus Protein Dual Color Standard (Bio-Rad) was added as a mass standard.

Wheat chitinase expression was up regulated at 8 hours post infiltration of SnTox1

The transcription level of the two wheat chitinase genes *AF112963* and *AF112966* in CS (*Snn1*) and CS1BS18 (*snn1*) leaves was examined using quantitative PCR. The CS and CS1BS18 leaves infiltrated with SnTox1 and the control (the protein peptide from pGAPZα vector) were collected at ten post infiltration time points from 1 h to 72 h. In the control infiltration of CS (*Snn1*) and CS1BS (*Snn1* locus is absent) leaves, in the absence of SnTox1, expression of the chitinase genes was typically at or below that of wheat actin (Figure 3.2. SnTox1-/*Snn1* and SnTox1-/*snn1*). However, in the CS leaves infiltrated with SnTox1, both chitinase genes were significantly up-regulated at 8h post-infiltration (Figure 3.2. SnTox1+/*Snn1*). In the CS1BS18 line infiltrated with SnTox1, the chitinase gene *AF112963* were also up-regulated at the 8 hour time point but with lower levels compared to that of CS (Figure 3.2. SnTox1+/*snn1*), showing that SnTox1 triggers the expression of *AF112963* but that the SnTox1-*Snn1* interaction induces higher expression of the two wheat chitinase genes possibly due to the induction of PCD. Induced by the SnTox1-*Snn1* interaction, expression of *AF112963* increased 5 fold while *AF112966* increased around 2 fold of the actin gene expression at 8h post infiltration, (Figure 3.2).

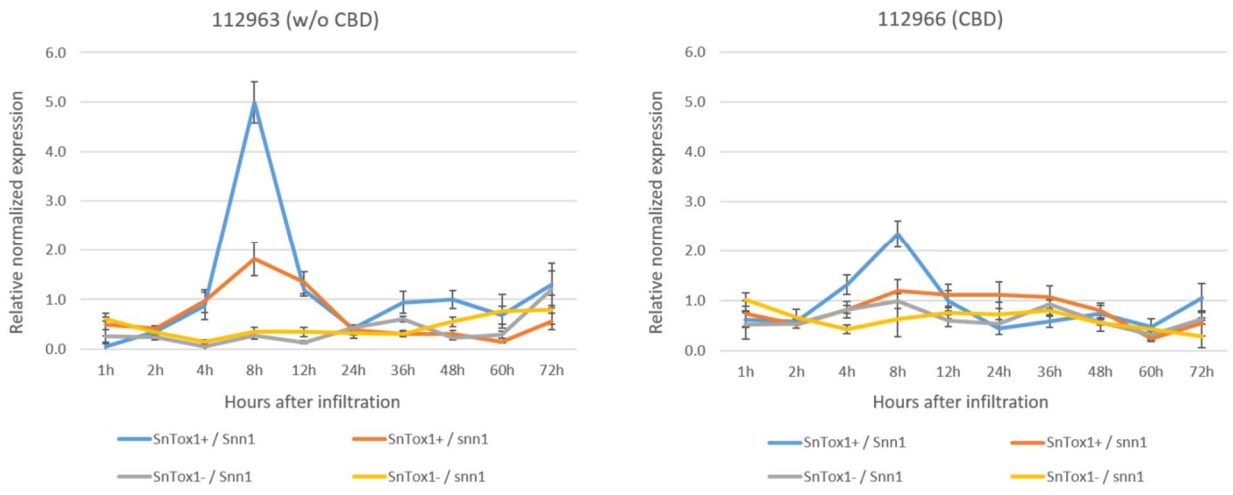

Figure 3.2. SnTox1 induces early upregulation of wheat chitinase genes.

Relative normalized (normalized by the wheat actin gene, NCBI accession number: AB181991) expression of wheat chitinase genes *AF112963* and *AF112966* in the CS (*Snn1*) and CS1BS (*snn1*) leaves infiltrated with SnTox1 (SnTox1+) or the nickel column protein prep from the empty pGAPZα vector (SnTox1-).

SnTox1 has the ability to protect a diversity of fungi from wheat chitinases

Because SnTox1 has chitin binding activity, and chitin is a main component of the fungal cell wall, it was hypothesized that SnTox1 protects the fungal cell wall from plant hydrolytic enzymes, such as chitinases. Wheat chitinase genes *AF112963* and *AF112966* were cloned, expressed, and purified to test the chitinase protection function of SnTox1 for several fungal species, including *P. nodorum*, *N. crassa, P. teres* f. *teres*, and *C. beticola*. In addition, wild type isolates were compared for sensitivity to wheat chitinases to strains of each species that had been transformed with the *SnTox1* gene. SnTox1 transformed strain of *P. nodorum* 79-1087+SnTox1 was reported by Liu et al. (2012). Three SnTox1 transformed strains of *N. crassa* and *P. teres* f. *teres* and two SnTox1 transformed strains of *C. beticola* were obtained and confirmed by PCR (Figure 3.3. A) and culture filtrate infiltration on wheat line CS (Figure 3.3. B).

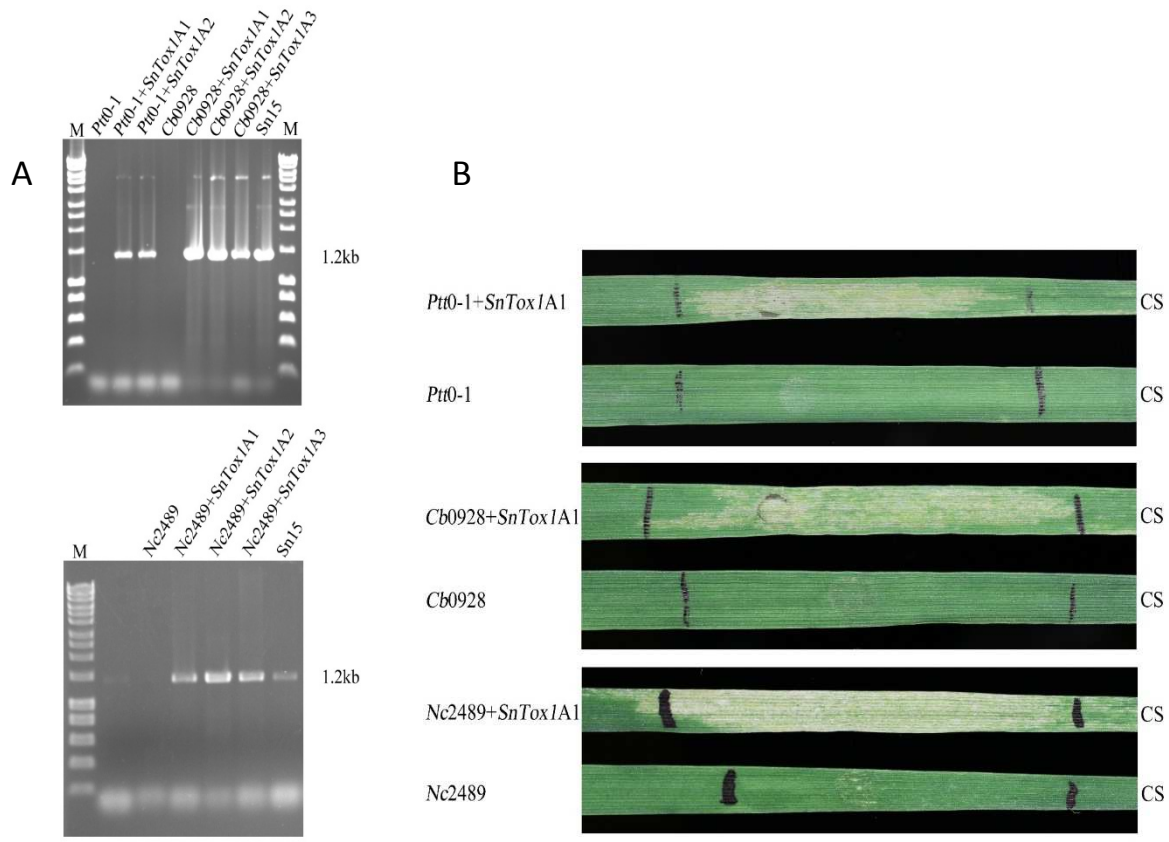

Figure 3.3. Characterization of SnTox1 transformants in *P. teres f. teres* (*Ptt*), *C. beticola* (*Cb*), and *N. crassa* (*Nc*) using PCR testing and culture filtrate infiltrations.

(**A**). PCR testing of *SnTox1* transformant in *P. teres* f. *teres* (top left), *C. beticola* (top right), and *N. crassa* (bottom). The SN15 isolate was used as a positive control and the original isolate was used as a negative control. A DNA ladder (M) was added to confirm the size of PCR amplification. (**B**). Testing of the culture filtrates prepared from the *SnTox1*- transformants in *Ptt* (top), *Cb* (middle), and *Nc* (bottom).

Conidia from all fungal strains including *N. crassa* (*Nc*2489), *C. beticola* (*Cb*0928), *P. teres* f. *teres* (*Ptt*0-1), avirulent *P. nodorum* (*Sn*79-1087), and virulent *P. nodorum* Sn2000 as well as their corresponding *SnTox1* transformed or disrupted strains *Nc*2489+*SnTox1*, *Cb*0928+*SnTox1*, *Ptt*0-1+*SnTox1*, Sn79-1087+*SnTox1*, and Sn2000Δ*SnTox1*, respectively, were able to germinate and grow in the absence of wheat chitinases IV AF112966 (Figure 3.4. E, F), indicating that all fungal spores were viable and conditions were suitable for fungal growth.

When wheat chitinase IV was included in the assay, the germination of the conidia from *P. nodorum* or *N. crassa* were stopped whereas *P. nodorum* Sn2000Δ*SnTox1, C. beticola and P. teres* f. *teres* were able to germinate and grow, but at a significantly reduced rate compared to the untreated control (without chitinases IV) (Figure 3.4. A). This reduced growth rate indicated that the addition of either wheat chitinase partially or completely inhibited the growth of these fungi, most likely due to the enzymatic degradation of the fungal cell wall.

When added to the chitinase IV/spore mixture, purified SnTox1 provided protection from degradation from the wheat chitinases, evidenced by the germination and increased growth of *P. nodorum* Sn79-1087 and *N. crassa Nc*2489 and the visibly increased growth of *P. nodorum* Sn2000ΔSnTox1, *C. beticola Cb*0928 and *P. teres* f. *teres Ptt*0-1 (Figure 3.4. C) after 24 h, similar to what was seen for Avr4 (Figure 3.4. D).

Similarly, the *SnTox1*-transformed *P. nodorum* strain 79-1087+*SnTox1* and *N. crassa Nc*2489+*SnTox1* were capable of germination and hyphal growth. The virulent *P. nodorum* Sn2000 (containing *SnTox1*) and the *SnTox1*-transformed *C. beticola Cb*0928+*SnTox1* and *P. teres* f. *teres Ptt*0-1+*SnTox1* also grew denser fungal mass in the presence of wheat chitinase IV (Figure 3.4. B) compared to the corresponding strains lacking *SnTox1*, demonstrating that SnTox1 has a chitinase protection function that is effective in multiple fungal species. The treatment by wheat chitinase II (AF112963) had similar effects but induced less growth inhibition compare to wheat chitinase IV (Figure 3.5; Figure 3.6). Because the hyphal growth of *P. teres* f. *teres* and *C. beticola* with and without wheat chitinase IV were hard to differentiate under the microscope, another method was used for the chitinase protection assay of SnTox1.

In addition to the visual assessment shown in Figure 3.4 and Figure 3.5, optical density (OD) assay similar to that used for evaluating fungicide resistance (Pryor et al. 2007) was used to

evaluate the effectiveness of SnTox1 in protecting from wheat chitinases over time. Analysis showed that each fungal species transformed with *SnTox1* and *P. nodorum* Sn2000 which had SnTox1 had stronger growth, compared to the corresponding strains that lacked *SnTox1*, evidenced by the increased optical density (Figure 3.6). Addition of purified SnTox1 protein to a final concentration of 25µM also resulted in stronger growth compared to the untreated controls (Figure 3.6). The addition of purified Avr4, also at a final concentration of 25µM, gave results similar to those of SnTox1 (Figure 3.6).

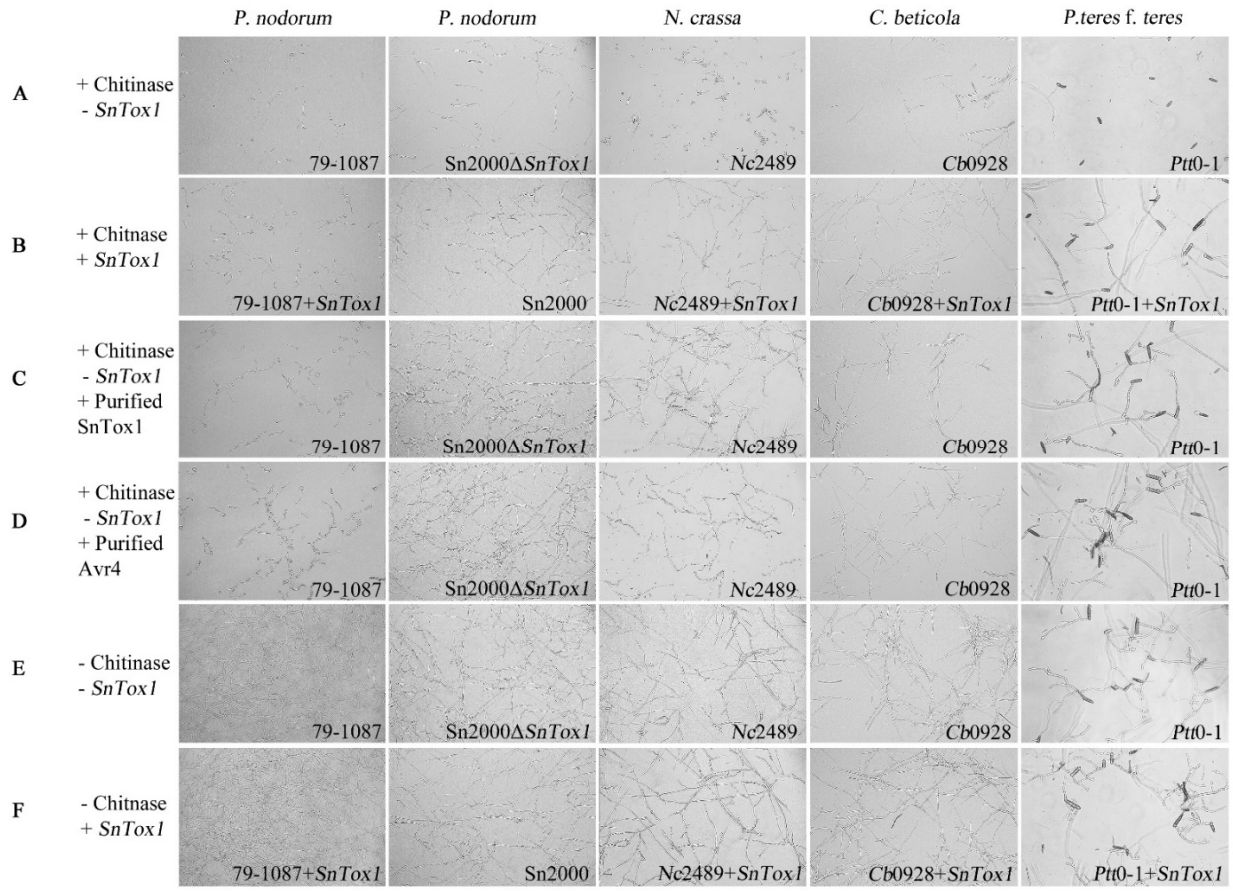

Figure 3.4. SnTox1 is capable of protecting different fungi from the degradation of wheat chitinases IV (AF112966).

P. nodorum, *N. crassa, C. beticola* and *P. teres* f. *teres* were used to evaluate the effectiveness of SnTox1 in protecting from the wheat chitinase AF112966. Conidia of *P. nodorum* Sn79-1087 and Sn2000ΔSnTox1, *N. crassa Nc*2489, *C. beticola Cb*0928 and *P. teres* f. *teres Ptt*0-1 treated with chitinase without the addition of SnTox1 or Avr4 (row **A**) showed limited spore germination or hyphal growth. Conidia of *P. nodorum* strain Sn79-1087+*SnTox1*, *P. nodorum* wild type Sn2000 (has *SnTox1*), *C. beticola* strain *Cb*0928+*SnTox1* and *P. teres* f. *teres* strain *Ptt*0-1+*SnTox1* were treated with chitinase and showed spore germination and more dense hyphal growth than the corresponding strain without the *SnTox1* gene (row **B**). Conidia of strains deficient in SnTox1 including *P. nodorum* Sn79-1087, Sn2000ΔSnTox1, *N. crassa Nc*2489, *C. beticola Cb*0928 and *P. teres* f. *teres Ptt*0-1 were treated with purified SnTox1 protein followed by the addition of purified chitinase protein (row **C**). Each combination with the added SnTox1 protein showed more dense hyphal growth than the corresponding treatment without the addition of SnTox1 (row **A**). Conidia of strains deficient in SnTox1 including *P. nodorum* Sn79-1087, *P. nodorum* Sn2000ΔSnTox1, *C. beticola Cb*0928 and *P. teres* f. *teres Ptt*0-1 treated with Avr4 with the addition of chitinase (row **D**) showed a similar result as the treatment with purified SnTox1and chitinase (row **C**). Strains without *SnTox1* including *P. nodorum* Sn79-1087 and Sn2000ΔSnTox1, *N. crassa Nc*2489, *C. beticola Cb*09-28 and *P. teres* f. *teres Ptt*0-1 without

chitinase, SnTox1 or Avr4 (row E) served as the control and showed dense growth. Strains harboring *SnTox1* including *P. nodorum* Sn79-1087+*SnTox1* and Sn2000, *N. crassa Nc*2489+*SnTox1*, *C. beticola Cb*0928+*SnTox1* and *P. teres* f. *teres Ptt*0-1+*SnTox1* without chitinase, SnTox1 or Avr4 (row **F**) showed dense growth similar to the untreated control (row **E**).

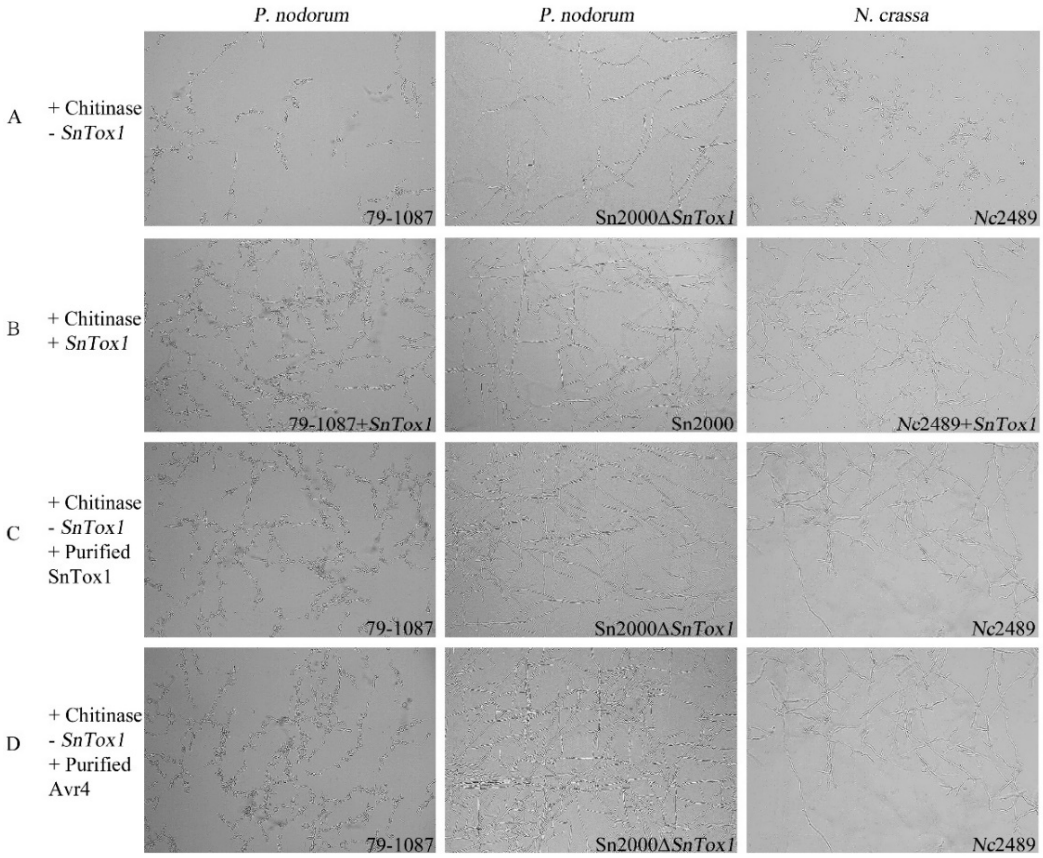

Figure 3.5. SnTox1 is capable of protecting different fungi from the degradation of wheat chitinases II (AF112963).

Protection assay of SnTox1 against wheat chitinase II at 24 h after treatment. Two fungal species were used including *Parastagonospora nodorum*, and *Neurospora crassa.* (**A**). Conidia of *P. nodorum* Sn79-1087 and Sn2000ΔSnTox1, and *N. crassa Nc*2489 treated with AF112963 without the addition of SnTox1 or Avr4 has limited spore germination or hyphal growth. (**B**). Conidia of *P. nodorum* Sn79-1087+*SnTox1* and Sn2000, and *N. crassa Nc*2489+*SnTox1* treated with AF112963 without the addition of SnTox1 or Avr4 showed spore germination and more dense hyphal growth. (**C**). Conidia of strains deficient in SnTox1 including *P. nodorum* Sn79-1087, Sn2000ΔSnTox1, and *N. crassa Nc*2489 treated with AF112963 with the addition of purified SnTox1 protein showed dense hyphal growth. (**D**). Conidia of *P. nodorum* Sn79-1087 and Sn2000ΔSnTox1, and *N. crassa Nc*2489 treated with AF112963 with the addition of Avr4 showed similar result as treatment with AF112963 and purified SnTox1.

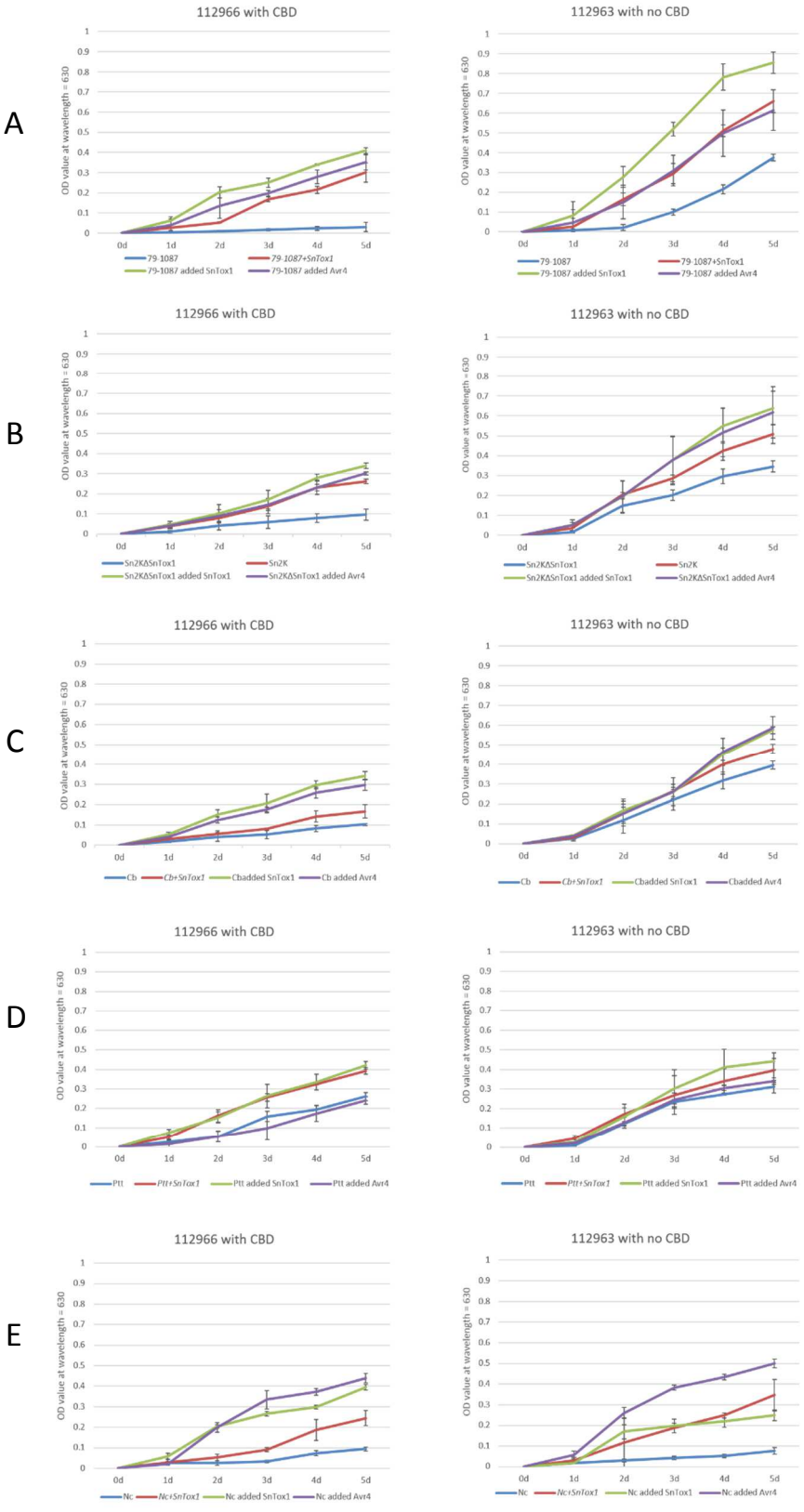

Figure 3.6. Measurement of the density of fungal growth in the presence or absence of SnTox1.

Fungal hyphal growth of *Parastagonospora nodorum* avirulent isolate Sn79-1087 (**A**), *P. nodorum* virulent isolate Sn2000 (**B**), *Cercospora beticola* isolate *Cb*0928 (**C**), *Pyrenophora teres* f. *teres* isolate *Ptt*0-1 (**D**) and *Neurospora crassa isolate Nc2489* (**E**) Each of the five graphs shows a strain that is producing SnTox1 (red), and a strain that is deficient in SnTox1 (blue), as well as a treatment of the SnTox1 deficient strain with purified SnTox1(green) or CfAvr4 (purple). Each of the strain/treatment combinations was treated with either AF12966 (left) or AF112963 (right) and evaluated using optical density (OD). The graphs show that in each case, transformation with SnTox1 (red) or addition of purified SnTox1 (green) increases the ability to grow compared to the SnTox1 deficient control (blue line).

Discussion

In previous work, SnTox1 was shown to induce necrosis in wheat lines harboring *Snn1*, the SnTox1 sensitivity gene. Recognition by the *Snn1* pathway leads to programmed cell death (PCD) as well as several other hallmarks of the defense response, including an increase in reactive oxygen species (ROS), DNA laddering, and up regulation of pathogenesis-related (PR) proteins including chitinases and other antimicrobial proteins (Liu et al., 2012). In this work, the secondary function of SnTox1 was further characterized to show that not only is SnTox1 involved in the induction of PCD, but SnTox1 also provides a level of protection from chitinases that are secreted by the host during an active defense response. To our knowledge, this is the first reported case where an effector protein has been shown to have two functions, both of which facilitate pathogen success, essentially inducing the host defense response to gain nutrient and concurrently providing protection from that host defense response. This interaction is reminiscent of other well studied avirulence effectors, for example, Avr2 and Avr4 from *C. fulvum* (de Wit et al., 2009), that have a virulence function but once recognized by the host, also set off a classical defense response. However, the major difference is that in these cases, the triggering of the defense response via effector recognition results in the hindrance of the pathogen rather than the pathogen gaining the advantage as reported here.

SnTox1 was shown to be present in approximately 84% of a worldwide collection of *P. nodorum*. This was significantly higher than the prevalence of SnToxA and SnTox3 which were present in 40 and 61% (McDonald et al., 2013). It has been speculated that the prevalence of each NE should correspond to the prevalence of the sensitivity gene in the wheat population unless something else is driving the maintenance of this gene. However, based on the limited data on the worldwide collection of hexaploid and tetraploid wheat lines (Faris and Friesen, unpublished data), *SnTox1* would not be expected to be present at higher levels than *SnTox3* and *SnToxA*. The presence of the chitin binding domain and the protection from chitinases that this function provides, supplies a hypothesis as to why SnTox1 is so prevalent in the global population when the corresponding *Snn1* gene is less prevalent.

Wheat chitinases are strongly upregulated at 8h after infiltration with SnTox1 and therefore it is logical that protection from these chitinases would be necessary during the early stages of infection to efficiently colonize the host. Two wheat chitinases, one containing a chitin binding domain (AF112966) and the other without a predicted binding domain (AF112963) were used to evaluate the effectiveness of SnTox1 at protecting the pathogen in vitro. AF112966 was the most effective at limiting the growth of each pathogen used. AF112963 was somewhat less effective, however; the protection assays showed SnTox1 provided protection against both chitinases. The hypothesis was that SnTox1 was competing against host chitinases that require binding in order to effectively hydrolyze chitin. If this hypothesis were completely accurate, SnTox1 would have provided protection against AF112966 but not AF112963. Therefore, it was somewhat surprising when SnTox1 provided a significant level of protection to AF112963 which is not predicted to have a chitin binding domain. Although it is only speculation, it is possible

that SnTox1 is providing a barrier such that all chitinases are reduced in their ability to approach the chitin layer of the fungal cell wall.

Four different fungal species, including *P. nodorum*, *N. crassa*, *P. teres* f. *teres*, and *C. beticola*, were evaluated for their effectiveness in using *SnTox1* in protection from wheat chitinases. Visual estimation at 24 h of growth (Figure 3.5) and optical density analysis (Figure 3.6) showed that all four fungi were more fit in the presence of wheat chitinases when they were expressing SnTox1 or SnTox1 was added to the growth media. Interestingly, *C. beticola* and *P. teres* both showed significantly more growth in the absence of SnTox1 than the avirulent Sn79-1087 and *N. crassa*. This is likely due to these pathogens having evolved their own chitinase protection mechanism. *C. beticola* harbors an *Avr4* homolog and CbAvr4 has been shown to bind chitin, showing a potential role in protection during the necrotrophic phase of pathogenesis (Stergiopoulos et al., 2010). *P. teres* f. *teres* on the other hand does not harbor an Avr4 homolog, however, based on a GO term search of the genome sequence, there are at least four chitin binding proteins that are not predicted to have hydrolase activity. Of these four, two proteins PTT_17444 (NCBI accession number: XP_003304768.1), and PTT_15288 (NCBI accession number: XP_003303172.1) are predicted to be small secreted proteins indicating their potential function in protection from chitinases. The *P. nodorum* virulent strain Sn2000 was also observed to have significantly more growth than Sn79-1087 in the presence of wheat chitinases without SnTox1 (Figure 3.4, 3.5 and 3.6). There is no *Avr4* homolog in the *P. nodorum* reference genome of SN15 (http://genome.jgi-psf.org/Stano2/Stano2.home.html), but a GO term search returned a total of 22 protein hits with a predicted chitin binding domains, and nine proteins, including SnTox1, are predicted to be small secreted proteins without predicted hydrolytic activity (i.e. not chitinases). Additionally, only four of these chitin binding proteins are predicted

to be present in the Sn79-1087 genome sequence (JGI). Based on these predictions it is likely that chitin binding proteins are fairly common in plant pathogens and likely provide redundant or overlapping function.

The chitin binding function of SnTox1 is highly similar to the Avr4 effector, an effector that is produced by *C. fulvum* and also protects from plant chitinases. Theoretically, Avr4 was initially an effector that protected *C. fulvum* from tomato chitinases but was ultimately recognized by the tomato resistance gene *Cf4* resulting in a defense response that leads to an incompatible interaction. SnTox1 has a similar chitinase protection function, however, the recognition of SnTox1 by Snn1 results in a compatible interaction. This is a nice comparison of the independent evolution of two proteins (SnTox1 and Avr4) with similar functions including the induction of the defense response and protection from chitinases. However, *P. nodorum* survives and benefits from recognition of SnTox1 while the recognition of *C. fulvum* Avr4 results in avirulence.

The chitinase protection function of SnTox1 provides added knowledge about the lifestyle of necrotrophs. Necrotrophs are thought to induce cell death through effector recognition but at the same time also produce effectors that modulate the host defense response in a similar way as pathogens classified as biotrophs and hemi-biotrophs. Plant pathologists have tried to classify pathogens into neat groups e.g. biotrophs, hemi-biotrophs, and necrotrophs and further divided these groups into obligate and non-obligate biotrophs, and haustorial and non-haustorial hemi-biotrophs, and necrotrophic specialists and generalists. However, it is important to understand that each host pathogen interaction has evolved independently of the other host-pathogen interactions in its "group". Although the mechanisms of pathogenicity may appear similar, and in many cases could be a result of maintaining an ancestral mechanism of

pathogenicity, evolution (survival) drives each interaction independently toward surviving the defense response long enough to colonize and reproduce. Pathogens classified as biotrophs, hemi-biotrophs, and necrotrophs, all have a similar goal, that is, gain nutrient to reproduce (sporulate). Future discoveries in plant pathogen interactions will likely find more overlap than distinction in "feeding styles" and it may be time to rethink the way we view pathogen groupings.

References

Beintema, J.J. 1994. Structural features of plant chitinases and chitn-binding proteins. Febs Letters 350:159-163.

Cohen-Kupiec, R., and Chet, I. 1998. The molecular biology of chitin digestion. Current Opinion in Biotechnology 9:270-277.

Collinge, D.B., Kragh, K.M., Mikkelsen, J.D., Nielsen, K.K., Rasmussen, U., and Vad, K. 1993. Plant chitinases. Plant Journal 3:31-40.

Datta, S.K., and Muthukrishnan, S. 1999. Pathogenesis-related proteins in plants. CRC press.

de Wit, P.J.G.M., Mehrabi, R., van den Burg, H.A., and Stergiopoulos, I. 2009. Fungal effector proteins: past, present and future. Molecular Plant Pathology 10:735-747.

Friesen, T.L., and Faris, J.D. 2012. Characterization of plant-fungal interactions involving necrotrophic effector-producing plant pathogens. Methods in Molecular Biology. 835:191-207.

Joosten, M., Vogelsang, R., Cozijnsen, T.J., Verberne, M.C., and DeWit, P. 1997. The biotrophic fungus *Cladosporium fulvum* circumvents Cf-4-mediated resistance by producing unstable AVR4 elicitors. Plant Cell 9:367-379.

Jorda, L., and Vera, P. 2000. Local and systemic induction of two defense-related subtilisin-like protease promoters in transgenic Arabidopsis plants. Luciferin induction of PR gene expression. Plant Physiology 124:1049-1057.

Jorda, L., Coego, A., Conejero, V., and Vera, P. 1999. Genomic cluster containing four differentially regulated subtilisin-like processing protease genes is in tomato plants. Journal of Biological Chemistry 274:2360-2365.

Kruger, J., Thomas, C.M., Golstein, C., Dixon, M.S., Smoker, M., Tang, S.K., Mulder, L., and Jones, J.D.G. 2002. A tomato cysteine protease required for Cf-2-dependent disease resistance and suppression of autonecrosis. Science 296:744-747.

Kruger, N.J. 1994. The Bradford method for protein quantitation. Methods in molecular biology. Humana Press. pp. 9-15.

Li, W.L., Faris, J.D., Muthukrishnan, S., Liu, D.J., Chen, P.D., and Gill, B.S. 2001. Isolation and characterization of novel cDNA clones of acidic chitinases and beta-1,3-glucanases from wheat spikes infected by *Fusarium graminearum*. Theoretical and Applied Genetics 102:353-362.

Liu, Z., and Friesen, T.L. 2012. Polyethylene glycol (PEG)-mediated transformation in filamentous fungal pathogens. Plant Fungal Pathogens: Methods and Protocols 835:365-375.

Liu, Z., Faris, J., Meinhardt, S., Ali, S., Rasmussen, J., and Friesen, T. 2004a. Genetic and physical mapping of a gene conditioning sensitivity in wheat to a partially purified host-selective toxin produced by *Stagonospora nodorum*. Phytopathology 94:1056-1060.

Liu, Z., Friesen, T., Rasmussen, J., Ali, S., Meinhardt, S., and Faris, J. 2004b. Quantitative trait loci analysis and mapping of seedling resistance to Stagonospora nodorum leaf blotch in wheat. Phytopathology 94:1061-1067.

Liu, Z., Faris, J.D., Oliver, R.P., Tan, K.C., Solomon, P.S., McDonald, M.C., McDonald, B.A., Nunez, A., Lu, S., and Rasmussen, J.B. 2009. SnTox3 acts in effector triggered susceptibility to induce disease on wheat carrying the *Snn3* gene. PLoS Pathogens 5:e1000581.

Liu, Z., Zhang, Z., Faris, J.D., Oliver, R.P., Syme, R., McDonald, M.C., McDonald, B.A., Solomon, P.S., Lu, S., and Shelver, W.L. 2012. The cysteine rich necrotrophic effector SnTox1 produced by *Stagonospora nodorum* triggers susceptibility of wheat lines harboring *Snn1*. PLoS Pathogens 8:1-24.

McDonald, M.C., Oliver, R.P., Friesen, T.L., Brunner, P.C., and McDonald, B.A. 2013. Global diversity and distribution of three necrotrophic effectors in *Phaeosphaeria nodorum* and related species. New Phytologist 199:241-251.

Stergiopoulos, I., van den Burg, H.A., Okmen, B., Beenen, H.G., van Liere, S., Kema, G.H.J., and de Wit, P.J.G.M. 2010. Tomato Cf resistance proteins mediate recognition of cognate homologous effectors from fungi pathogenic on dicots and monocots. Proceedings of the National Academy of Sciences of the United States of America 107:7610-7615.

Thomas, C.M., Jones, D.A., Parniske, M., Harrison, K., Balint-Kurti, P.J., Hatzixanthis, K., and Jones, J.D.G. 1997. Characterization of the tomato *Cf-4* gene for resistance to

Cladosporium fulvum identifies sequences that determine recognitional specificity in Cf-4 and Cf-9. Plant Cell 9:2209-2224.

van den Burg, H.A., Harrison, S.J., Joosten, M.H.A.J., Vervoort, J., and de Wit, P.J.G.M. 2006. *Cladosporium fulvum* Avr4 protects fungal cell walls against hydrolysis by plant chitinases accumulating during infection. Molecular Plant-Microbe Interactions 19:1420-1430.

CHAPTER 4. GENOME WIDE ASSOCIATION MAPPING OF *PARASTAGONOSPORA NODORUM* IDENTIFIES CANDIDATE NECROTROPHIC EFFECTOR GENES

Abstract

Parastagonospora nodorum produces necrotrophic effectors (NE) that are critical to the virulence of the pathogen. Nine NE-host dominant sensitivity gene interactions have been identified, and three NE genes have been cloned. To identify additional NE gene regions in *P. nodorum*, we developed a genome wide association study (GWAS) using 191 isolates with global diversity. Genotype of the 191 isolates were generated by restriction site associated DNA genotyping-by- sequencing (RAD-GBS). Around 3,000 single nucleotide polymorphism (SNP) markers were identified. Inoculation and infiltration data of the 191 isolates was collected on wheat differential lines including BG223 (SnTox2 sensitive), ITMI37 (SnTox6 sensitive), ITMI44 (SnTox4 sensitive), and LP29 (SnTox5 sensitive). Association analysis were performed by four models including naïve, population structure (Q model), kinship estimated by identity by states (IBS model) and population structure + Kinship (Q+IBS model) models. Many genomic regions associated with NE sensitivity and the underlying candidate NE genes were identified.

Introduction

Genome wide association studies (GWAS) are a powerful way to analyze the DNA sequence variation across a genome to identify genetic variation associated with traits of interest in a natural population (Gibson and Muse, 2009). Numerous quantitative genetic studies have been used to map quantitative trait loci (QTL) in plants (reviewed in Zhao et al., 2014). QTL analysis uses designed, bi-parent populations that segregate for a certain trait or traits. These biparental populations have limited recombination events, and often minor QTL are missed

(Zhao et al., 2011). Because GWAS uses populations that contain natural genetic diversity and high frequency evolutionary and historical recombination, GWAS is often favorable in targeting complex traits because of its relatively high mapping resolution (Doerge, 2002; Holland, 2007). Several negatives exist with GWAS data including most prominent of which is the high chance of the identification of false positives due to population structure from genotypes from common geographic origins, local adaption, and breeding history (Zhu et al., 2008). Therefore, the population structure matrix and the familial relatedness need to be considered in GWAS analysis (Zhu et al., 2008). To date, due to the reduced cost of genomic technology such as high-throughput next generation sequencing, and other genomic technology such as genotyping, gene expression profiling, comparative genomics and bioinformatics that are helpful to identify more markers or functional polymorphisms (Zhu et al., 2008), GWAS is not only widely used to identify gene loci for human diseases (Montgomery, 2011), but has also been used in plants (Zhu et al., 2008). Examples of GWAS application in plants includes maize, Arabidopsis, sorghum, wheat, barley, potato, and rice. Traits identified by GWAS have been used in plants to genetically characterize complex traits such as flowering time, kernel composition, disease resistance, shoot branching, kernel size, and milling quality (Zhu et al., 2008). In fungi, only a few studies using GWAS analysis have been reported. In *Saccharomyces cerevisiae*, a SNP associated with mtDNA copy number was identified by GWAS (Connelly and Akey, 2012). Muller et al. (2011) collected 44 clinical and 44 nonclinical *S. cerevisiae* strains with geographical diversity to identify genetic loci associated with clinical background such as pseudohyphal formation, cell wall maintenance, and cellular detoxification, conferring pathogenesis and virulence-related factors. Dalman et al. (2013) sequenced 23 haploid isolates of *Heterobasidion annosum*, a necrotrophic pathogen of *Picea abies* and *Pinus sylvestris* to identify

33, 018 SNPs. Using GWAS, twelve SNPs were found to be associated with virulence. Genomic regions of the twelve SNPs contained eight candidate virulence genes that showed homology to genes in other fungal pathogens. Palma-Guerrero et al. (2013) took advantage of GWAS to identify a gene homolog encoding a neuronal calcium sensor showing association with germling communication of *Neurospora crassa*. Although GWAS research in fungi is currently relatively less common than in plants and animals, the application of GWAS in fungi has potential because fungi have small genomes, many have a haploid chromosomal stage and a short sexual life cycle resulting in high levels of diversity among natural populations (Dalman et al., 2013). Here we describe the application of GWAS in *Parastagonospora nodorum* to find novel genomic regions containing necrotrophic effector genes conferring virulence on wheat. *P. nodorum* produces necrotrophic effectors (NE) that are critical to the virulence of the pathogen. The NEs produced by *P. nodorum* are recognized directly or indirectly by wheat dominant sensitivity genes that confer susceptibility. Up till now, three NE genes have been cloned including *SnToxA*, *SnTox1* and *SnTox*3. Since sexual populations of *P. nodorum* are difficult to produce under lab conditions, bi-parental populations have not been used to genetically locate genes involved in virulence, namely genes involved in NE production. Therefore, to identify additional NE gene regions, we developed a genome wide association study (GWAS) using 191 isolates with global diversity (13 US states, Australia, Denmark, Finland, Latvia, Lithuania, Norway, Sweden, Brazil, Switzerland, China, South Africa, and Iran). Genomic regions underlying candidate SnTox2, SnTox6 and SnTox5 genes were identified by associating genotypes of the 191 isolates and phenotypes on wheat differential lines including BG223 (SnTox2 sensitive), ITMI37 (SnTox6 sensitive), ITMI44 (SnTox5 sensitive), and LP29 (SnTox5 sensitive).

Materials and methods

Plant and fungal materials

Four differential wheat lines including BG223 (SnTox2 sensitive), ITMI37 (SnTox6 sensitive), ITMI44 (SnTox5 sensitive), and LP29 (SnTox5 sensitive) were used to identify genomic regions of *SnTox2*, *SnTox6* and *SnTox5*. All the wheat lines were inoculated with spores and infiltrated with culture filtrates of 191 *P. nodorum* isolates. The 191 *P. nodorum* isolates with global diversity were collected from 13 US states, Australia, Denmark, Finland, Latvia, Lithuania, Norway, Sweden, Brazil, Switzerland, China, South Africa, and Iran (Table 4.1).

Phenotypic evaluation

Conidia (pycnidiospores) of the 191 *P. nodorum* isolates were collected at a concentration of 1×10^6 spores/ml and sprayed onto seedlings at the two-to-three leaf stage. The inoculated plants were subjected to 100% relative humidity in the light for 24h in a mist chamber and then moved to a growth chamber at 21ºC under a 12h photoperiod for six additional days. The disease on the second leaf of each inoculated plant was scored seven days post-inoculation using a 0-5 rating scale based on lesion type (Liu et al., 2004).

Culture filtrates of the 191 isolates were infiltrated into the second leaf of the wheat lines. The infiltrated plants were grown in a growth chamber at 21 ºC under a 12h photoperiod. The infiltrated leaves were scored three days post-infiltration using a 0-3 scale as described by Friesen and Faris (2012). All inoculation and infiltration experiments consisted of three replicates.

DNA extraction, library preparation, and sequencing

DNA of the 191 *P. nodorum* isolates were extracted using a BioSprint 15 system (QIAGEN). DNA of each isolate was genotyped using a RAD-GBS approach (Elshire et al.,

2011). Briefly, the extracted DNA was digested with *Ape*KI and *Hha*I (NEB), and then ligated with specific barcoded adaptors. The barcoded DNA of 40 isolates were pooled into one tube, so five pooled genomic DNA libraries were made. A 3µl sample from each pooled library was subjected to a 1% agarose gel at 100 volts for 45 min. The DNA fragments between 200 and 250bp were collected and purified using a gel extraction kit (QIAGEN) and then were prepared using the Pippin Prep kit (Life Technologies) for next-generation sequencing using the Ion Torrent™ Personal Genome Machine (PGM) system (Ion Torrent). Library sequencing was performed using five Ion Torrent 318 microprocessor chips (Life Technologies).

Genotypic data analysis

The *P. nodorum* isolate that had the most reads was assembled as the reference sequence using CLC Genomics Workbench. All the sequencing reads were aligned to the reference sequence using the Burrows-Wheeler Aligner 'mem' algorithm. SAM files generated by Burrow-Wheeler Aligner were converted to BAM files to screen SNP markers based on the alignment using SAM tools. SNPs with low quality (<100) were filtered from the database. SNPs having a minor allele frequency less than 5% or missing data greater than 30% were eliminated. Individual genotypes with quality >10 and minimum read depth of 3 were used. For each sequence tag, the single nucleotide polymorphism (SNP) marker with the least missing data was chosen resulting in one SNP marker per tag being used as a genotypic marker. The chosen SNPs were used for population structure analysis, relatedness analysis and association mapping. SNP marker data were imported into Excel and annotated onto sequence of *P. nodorum* SN15 which has been used for whole genome sequencing and de novo assembly (Hane et al., 2007; Syme et al., 2013). SNPs were labeled with the sequence tag ID and the location on the corresponding SN15 assembled scaffold as the annotation file for GWAS analysis.

Population structure analysis

Population structure was analyzed using STRUCTURE 2.3.4 (Pritchard et al., 2000) to estimate the population clusters of the 191 *P. nodorum* isolates. Population structure in STRUCTURE was performed using an admixture model with a burn-in period of 10,000 followed by 50,000 replications of Markov Chain Monte Carlo. Five runs for each cycle were performed with the cluster number between 1 and 10. The optimal value of k (number of clusters) was decided based on the relative rate of change in the likelihood of the value (Δk) between two successive clusters. The value of Δk was calculated as described by Evanno *et al.* (2005) using STRUCTURE Harvester (Earl and vonHoldt, 2012). Further analyses were performed from k=2 to the optimal K plus 3 with a burn-in period of 20,000 followed by 200,000 replications of Markov Chain Monte Carlo with 20 iterations. The membership probability of each isolate at the optimal k was used as the Q matrix for further analysis.

Relatedness analysis

Relative kinship was calculated by estimating the pairwise relatedness of the 191 isolates at each allele of the 2,983 SNP markers using JMP genomics 6.1. The probability of any two individuals sharing the same copy of an allele was computed using Gower's Similarity Metric and a Range Standardization that is referred to as identity by state (IBS) across all markers (Stevens et al., 2011).

Linkage disequilibrium analysis and association mapping

Linkage disequilibrium (LD) between SNP locations were calculated using the squared allele frequency correlation (r^2) which was implemented in JMP genomics 6.1. Decay of LD was calculated by fitting an equation developed by Hill and Robertson (Hill and Robertson, 1968) into a nonlinear regression curve using JMP genomics 6.1. Association analysis was performed

in JMP genomics 6.1. SNPs with the –log10(*p*-value) or adjusted –log10(*p*-value) greater than 3 were considered significant. The naïve model (Pasam et al., 2012), and three mixed models including population structure (Q model), kinship (IBS model) and population structure + kinship (Q+IBS model) (Yu et al., 2006; Listgarten et al., 2012) were used to identify association between SNPs and the phenotypes. False detection rate (pFDR) method was used to reduce false positive (type I error). To test the four models, each model was evaluated by a quantile-quantile plot (testing the fit of the observed *p*-value versus the expected *p*-value of each SNP) and mean square deviation (MSD) in JMP genomics 6.1. A model with the best fit of the observed *p*-value to the expected *p*-value and lowest MSD between observed *p*-value and expected *p*-value was chosen as the best model (Mamidi et al., 2011; Gurung et al., 2014; Kertho et al., 2015; Tamang et al., 2015).

Results

Generation of a genomic data set

Genotyping of the 191 *P. nodorum* isolates was performed using the RAD-GBS technique. Single reads from a 150-base pair (bp) insert library of all the isolates were obtained, and a total of 4,019 Mb with a 148bp mean read length of *P. nodorum* sequence were obtained from the Ion Torrent PGM sequencing platform. The isolate Nor-5 (ID: 143) which had the highest number of reads (343, 439) was chosen as the reference genotype. Sequence tags of Nor-5 were mapped to the reference isolate SN15 (Hane et al., 2007; Syme et al., 2013). By screening out sequence tags with low quality, (less than 5% minor allele frequency, and more than 30% missing data), a total of 2,983 SNPs were identified and used for population structure, kinship estimate, and association analysis, providing an average marker density of one marker every 18kb throughout the 37Mb genome of *P. nodorum*.

Phenotypic analysis of SNB susceptibility and culture filtrate sensitivity of the 191 isolates

Four wheat differential lines including BG223, ITMI37, ITMI44 and LP29 were rated for SNB susceptibility to spore inoculation and sensitivity to culture filtrate infiltration of the 191 *P. nodorum* isolates. Disease reactions were scored using a scale of 0-5 (see chapter 2). Culture filtrate sensitivity was scored using a scale of 0-3 (see chapter 2). Distribution of the average disease reaction types (inoculation) of the 191 isolates varied by the wheat differential lines. For LP 29, the percentage of isolates showed smaller differences in every 0.5 reaction type interval compared to the other differential lines (Figure 4.1).

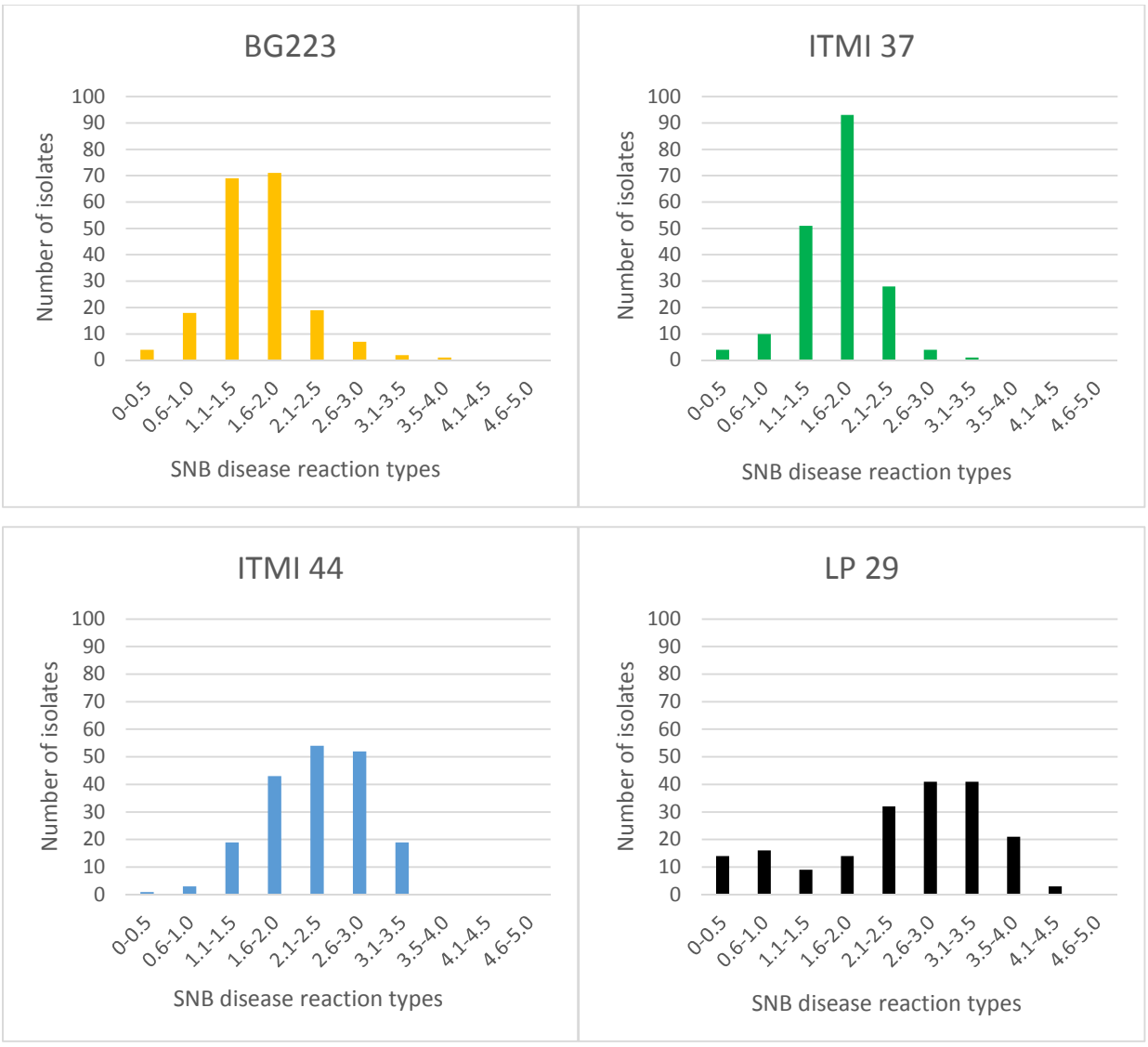

Figure 4.1. Distribution of SNB average disease reaction types of the 191 *P. nodorum* isolates on four wheat genotypes (BG223, ITMI 37, ITMI 44 and LP 29).

Population structure and kinship in the panel of the 191 isolates

Population structure inference for the 191 isolates was conducted using the 2,983 SNP markers with the software STRUCTURE. The structure analyses were performed by setting 20 clusters (*k*) with five replications for each cluster. The mean log likelihood of each *k* displaying an increased pattern from *k*=1 to 5, but decreased after *k*=6 with large error indicating the cluster

value greater than k =6 generating noise and not necessarily useful for analysis. The Δk value showed a large peak at k=3 and dropped dramatically after k=3 (Figure 4.2). Therefore the population structure of the 191 isolates was shown to be made up of three groups (Figure 4.3). Using the cutoff of the membership probability = 0.6, a total of 49 isolates collected from North Dakota, USA, and Iran were clustered in Group 1. Group 2 included 77 isolates with 11 being from the US, one from Lithuania, five from Switzerland, and eight from China. Group three contained 30 isolates from Australia and two from South Africa. The remaining 36 isolates from Denmark, Finland, Norway, Sweden, Brazil, Switzerland, China and South Africa had a lower membership value and were not placed into any of the three groups (Table 4.1). The membership probability of each isolate at k =3 was used as the Q matrix for the following analysis.

The pairwise kinship value was calculated by the similarities between each pair of isolates in JMP genomics 7.0. The average kinship value was 0.852. The minimum kinship value of 0.8102 showed that all 191 isolates had more than 80% similarity (Figure 4.4). Only 25 isolates had 100% identity, and the majority had kinship values in a range between 0.8102-0.9709 (Figure 4.5). This result showed that all 191 isolates had a high level of kinship.

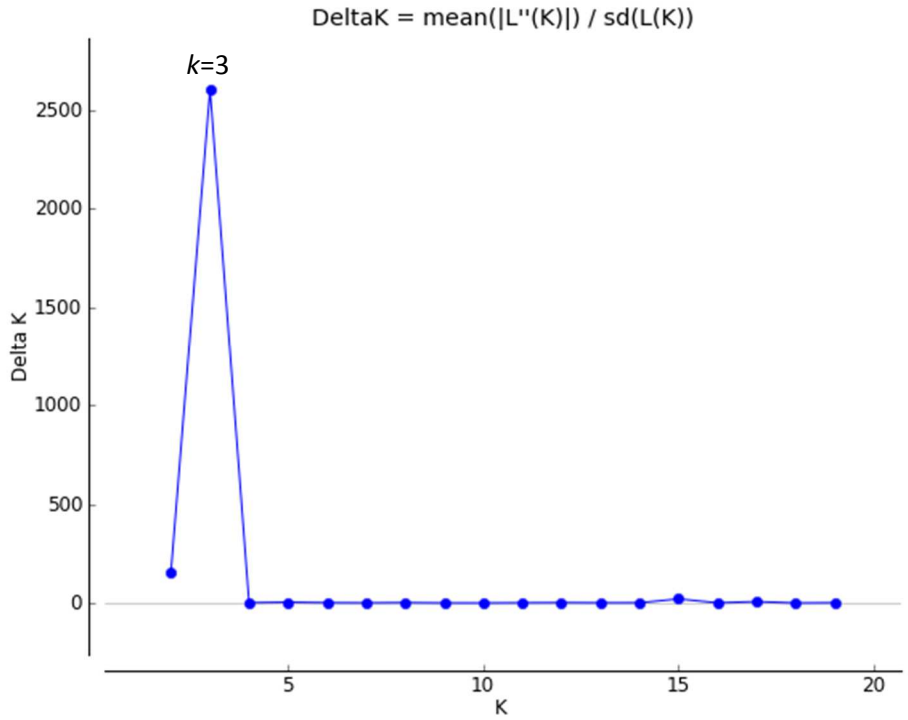

Figure 4.2. Evaluation of *k* using the Evanno method using STRUCTURE. STRUCTURE harvester software was used to visualize the STRUCTURE output.

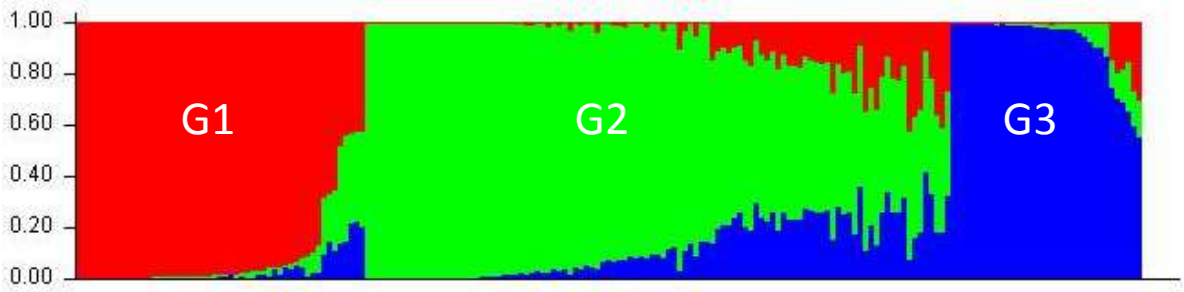

Figure 4.3. Population structure of the 191 *P. nodorum* isolates estimated by the program STRUCTURE for *k*=3.

Membership values (y axis) of every isolate (x axis) belonging to each group are indicated by the distribution of the three colors standing for the three major groups.

Table 4.1. Group structure of the 191 *P. nodorum* isolates

Group ID	Isolate ID	Number of isolates	Location
G1	1-19	19	North Dakota, US
	23-34	12	Minnesota, US
	187-199	13	Iran
G2	36-41	6	Oregon, US
	42-45	4	Arkansas, US
	46-49	4	Georgia, US
	50, 51	2	Maryland, US
	52-59	8	North Carolina, US
	61-62	3	South Carolina, US
	63-66	4	Tennessee, US
	67-69	3	Virginia, US
	70, 72-85	15	Ohio, US
	86-90	5	Texas, US
	92-100	9	New York, US
	138	1	Lithuania
	153, 158, 160-162	5	Switzerland
	163, 164, 173, 175-179	8	China
G3	101-130	30	Australia
	181, 184	2	South Africa
Unknown	131, 132	2	Denmark
	133-135	3	Finland
	139-146	8	Norway
	147-149	3	Sweden
	150-152	3	Brazil
	154-157, 159	5	Switzerland
	165-172, 174, 180	10	China
	182, 183	2	South Africa

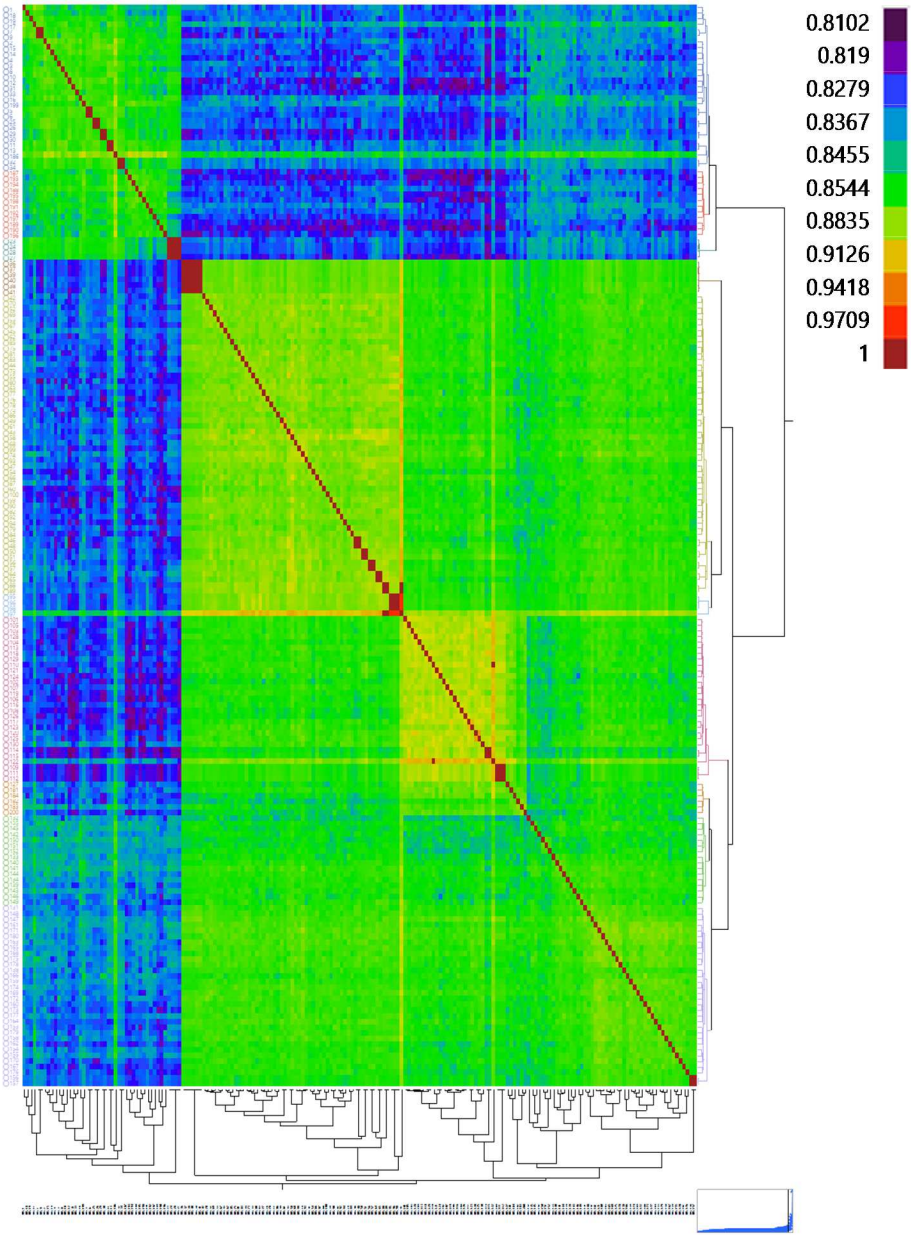

Figure 4.4. Relationship matrix of the 191 *P. nodorum* isolates. Isolates from different areas were labeled by numeric ID on the left with different colors.

From top to bottom, Blue = North Dakota, Minnesota, US, and two Iran isolates; Red = Iran; Light blue = some Minnesota, US isolates not shown in the blue cluster; Brown = Oregon, US; Yellow green = other isolates from South East US states in this study except Oregon; Blue green = some New York isolates not shown in the yellow green cluster, US; Pink = Australia; Light Brown = South Africa; Green = European countries including Finland and Norway, and Brazil; Purple = European countries including Denmark, Sweden and Switzerland, and China. Hierarchical clustering is based on the Fast Ward method. Similarity shared by pairs of the 191 *P. nodorum* isolates were indicated by colors from dark red to dark purple and kinship values from 0.8102 to 1 at right side.

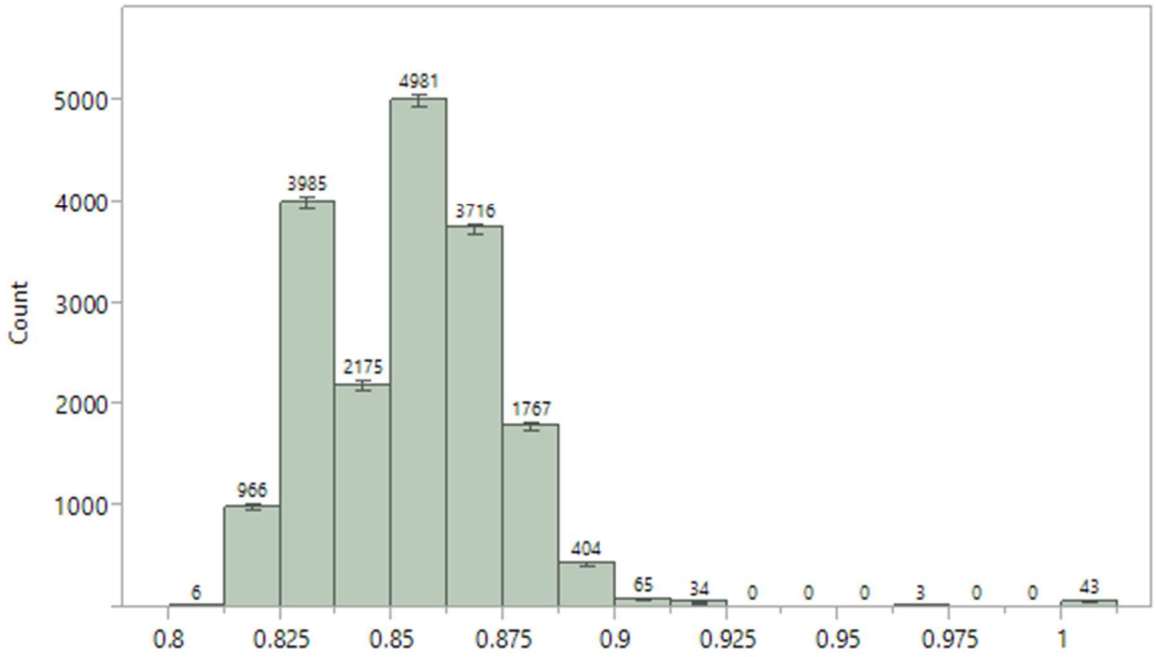

Figure 4.5. Distribution of pairwise relative kinship estimated by IBS in the population of 191 *P. nodorum* isolates.

The number of isolate pairs within every 0.125 kinship value between 0.8 and 1.0 are indicated on the top of each column. Error bars were calculated by standard deviation.

Linkage disequilibrium and LD decay

Pairwise linkage disequilibrium was calculated using all 2,983 SNP markers across all 191 isolates. The average r^2 of all the SNP pairs was 0.0432 showing a low LD level amongst the 191 isolates. LD decay was estimated by regressing the r^2 value of all 191 isolate pairs on the physical distance using the non-linear regression model. The genome-wide LD decay was between 10 and 20 Kb at r^2<0.1, showing the average density of SNPs obtained (one SNP every 18 Kb) meets the minimum requirement for MTA identification (one SNP every 10-20 Kb) (Figure 4.6).

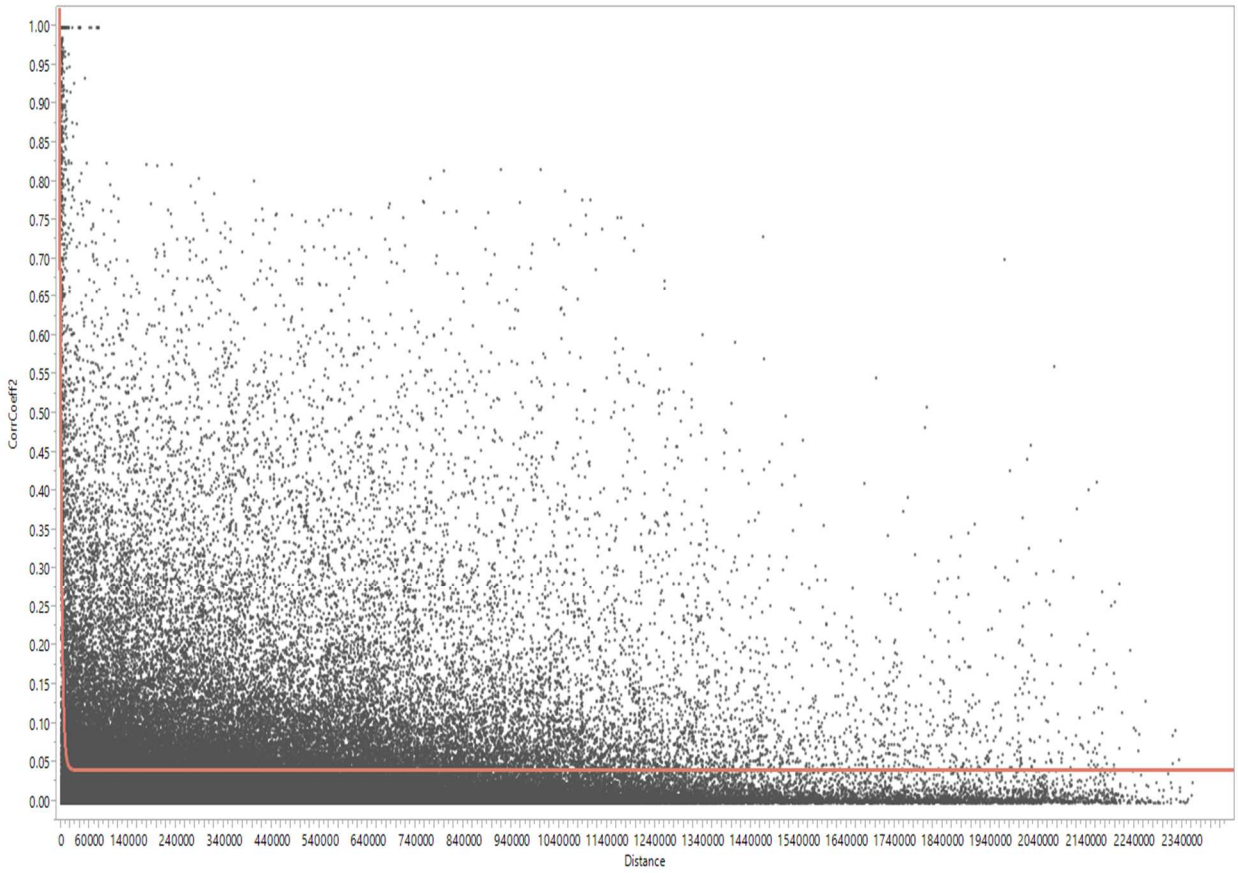

Figure 4.6. Genome-wide linkage disequilibrium (LD) decay plot.

The LD value was calculated by the square of correlation coefficient (r^2) between pairs of SNPs. The LD value of each SNP (*y*-axis) was plotted against the physical distance (*x*-axis) of the assembled *P. nodorum* SN15 genome scaffolds.

GWAS model evaluation and identification of marker trait associations

To identify specific NEs that induce sensitivity on host lines harboring a corresponding sensitivity gene (analyzed by culture filtrate infiltration) and then result in SNB disease (analyzed by spore inoculation), four models including population structure (Q), kinship (IBS), Q+IBS, and a Naïve model were used for four genotypes including BG 223 (has the SnTox2 sensitivity gene *Snn2*), ITMI 37 (has the SnTox6 sensitivity gene *Snn6*), ITMI 44 and LP 29 (both have the SnTox5 sensitivity gene *Snn5*). To test the four models, each was evaluated by

quantile-quantile plot (Figure 4.7) and mean square deviation (MSD) estimation (Table 4.2). Theoretically, a model with the best fit of the observed *p*-value to the expected *p*-value and lowest MSD should be the best model. To identify the SNPs associated with SnTox2, SnTox6 and SnTox5 sensitivity and SNB disease, the Q model was chosen for genotype BG 223. For genotypes ITMI 37, ITMI 44 and LP 29, both the Q and Naïve models were taken into account because these two models showed a better fit for the observed *p*-value to the expected *p*-value of the SNP markers (Figure 4.7. A) and because the MSD values of the two models were close and lower than the other models (Table 4.2). However, in the Q model, significant SNPs were not detected for genotype ITMI 37, ITMI 44 or LP 29. Therefore, the Naïve model was chosen as the best model for the three genotypes. Similarly, to identify the MTA with host sensitivity conferred by SnTox2, SnTox6 and SnTox5, by comparing the four models for the four genotype datasets, Q and Q+IBS models were first selected for genotype BG 223, IBS and Q+IBS models were chosen for ITMI 44; Q, IBS, and Q+IBS models were chosen for ITMI 37, and the Q and the Naïve models were chosen for LP 29 (Figure 4.7. B, Table 4.2). Because the IBS and Q+IBS models added stringency to the *p*-value for genotypes BG 223 and ITMI 37, the Q model was selected for BG 223 and ITMI 37. The IBS model generated increased noise for ITMI 44, so the Q+IBS model was selected for ITMI 44. The Naïve and Q model showed similar result for genotype LP 29, and the Q model added more stringency, therefore, the Q model was selected for LP 29.

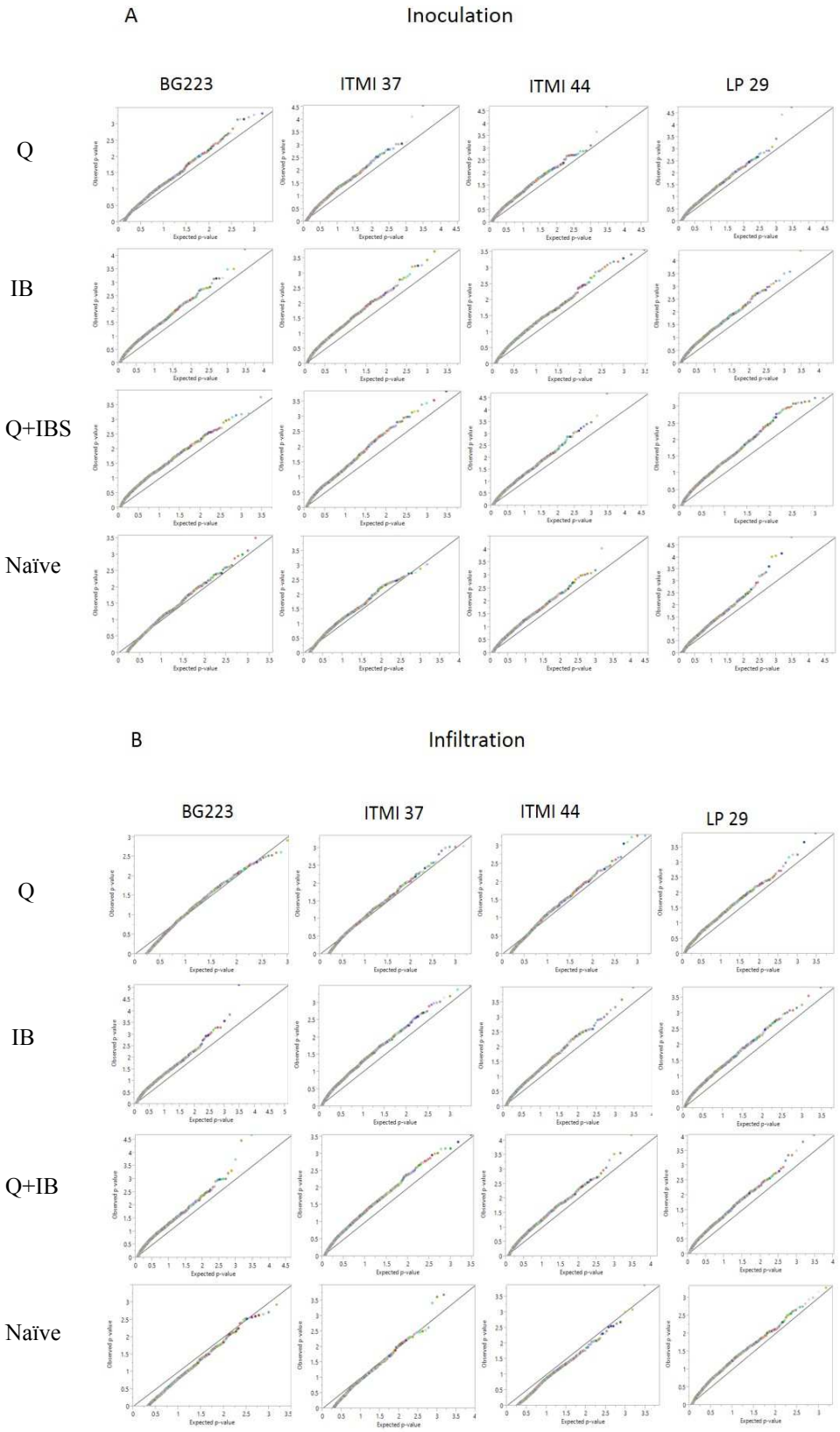

Figure 4.7. Evaluation of models used in marker trait association.

Model comparison for inoculation (A) and infiltration (B) data of the 191 isolates on the four wheat genotypes (BG 223, ITMI 37, ITMI 44, LP 29) by quantile-quantile plots. The observed – log(*p*-value) (*y*-axis) versus the expected -log(*p*-value) (*x*-axis) are shown for the Q, IBS, Q+IBS, and the Naïve models. The perfect fit curve between observed and expected *p*-value is shown by the gray diagonal line.

Table 4.2. Mean square deviation (MSD) of the four GWAS models analyzing the inoculation and infiltration data of the four wheat genotypes

Genotype		Model MSD				Best model
		Q	IBS	Q+IBS	Naive	
Inoculation	BG 223	0.0053	0.0108	0.0106	0.0100	Q
	ITMI 37	0.0077	0.0108	0.0100	0.0069	Naïve
	ITMI 44	0.0065	0.0074	0.0081	0.0062	Naïve
	LP 29	0.0064	0.0112	0.0110	0.0069	Naïve
Infiltration	BG223	0.0092	0.0166	0.0094	0.0441	Q
	ITMI 37	0.0094	0.0081	0.0083	0.0269	Q
	ITMI 44	0.0106	0.0076	0.0076	0.0324	Q+IBS
	LP 29	0.0064	0.0098	0.0106	0.0052	Q

Marker trait association (MTA) analysis was conducted using the best model for the four wheat genotypes. One marker SNP4 with a –log10(*p*-value) = 3.4 (above the threshold) was identified by spore inoculation on ITMI 44 (*Snn5*) (Figure 4.7. A, Table 4.3). Using inoculation data from LP29 (*Snn5*), SNP4 had a –log10(p-value) = 1.8, lower than the calculated significance threshold, but higher than most of the other SNPs used (Figure 4.7. A). Two common SNPs, SNP1 and SNP2 with significant –log10(p-value) (Table 4.3) were identified by spore inoculation on BG 223 (*Snn2*) and ITMI37 (*Snn6*) (Figure 4.7. A). Unpublished

observations from our lab have shown that SnTox2 and SnTox6 are difficult to separate and therefore could be one in the same but may interact with two different host sensitivity genes. The two common SNPs, SNP1 and SNP2 and one additional SNP, SNP3 with MTAs with spore inoculations on BG 223 (Figure 4.7. A, Table 4.3) were also identified by culture filtrate infiltration on BG 223 and ITMI 37 (Figure 4.7. B, Table 4.3). By investigating the genomic regions within the flanking markers of SNP1, SNP2 and SNP3 (associated with SNB susceptibility conferred by the SnTox2-*Snn2* interaction), 15 genes were detected based on the gene annotation of *P. nodorum* isolate SN15. Among the 15 genes, one gene, gene-3 encodes a small secreted protein and is the strongest candidate gene in this region for SnTox2/ SnTox6 (Figure 4.8. A). Similarly, 14 genes were detected in the genomic region of SNP4 (associated with SNB susceptibility conferred by the SnTox5-*Snn5* interaction), and three small secreted protein genes were prioritized as candidate genes for SnTox5 (Figure 4.8. B).

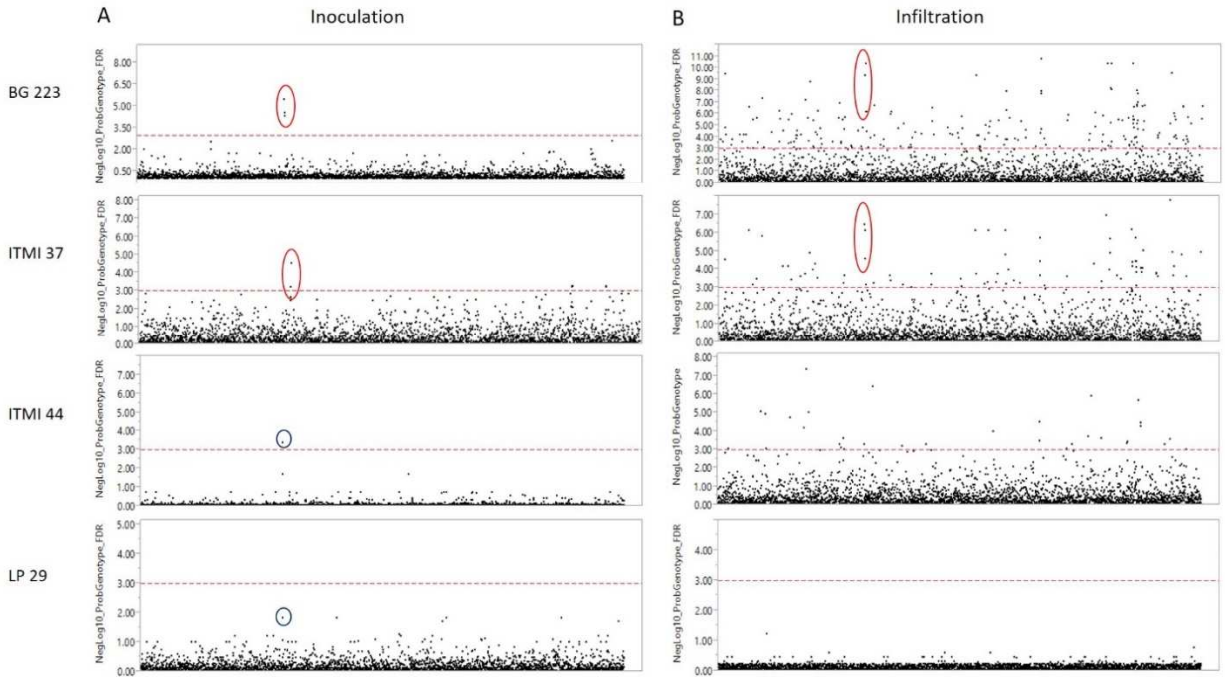

Figure 4.8. Manhattan plots of marker trait association analysis.

SNPs associated with SNB disease was analyzed by spore inoculation (A) and NE sensitivity analyzed by culture filtrate infiltration (B) caused by a specific NE on the four genotypes. –log10(p-value) or –log10(p-value) corrected by FDR for each SNP is indicated by the y-axis and physical distances of the SNPs are mapped on the x-axis (scaffold numbers are not shown). SNPs with P values below –log10(p-value) are not shown. Threshold of significance at P<0.001 appears as the red dashed line. Common SNPs are labeled by circles with the same color.

Table 4.3 Significant SNPs (-log10(*p*-value) > 3) identified by GWAS analysis

Trait	SNP ID	Wheat genotype	Treatment	-log10(*p*-value)
SnTox2 / SnTox6	SNP1	BG 223	Inoculation	5.5
			Infiltration	9.3
		ITMI 37	Inoculation	4.6
			Infiltration	6.4
	SNP2	BG 223	Inoculation	4.5
			Infiltration	6.2
		ITMI 37	Inoculation	3.1
			Infiltration	4.6
	SNP3	BG 223	Inoculation	4.3
			Infiltration	10.4
		ITMI 37	Inoculation	6.1
SnTox5	SNP4	ITMI 44	Infiltration	3.4

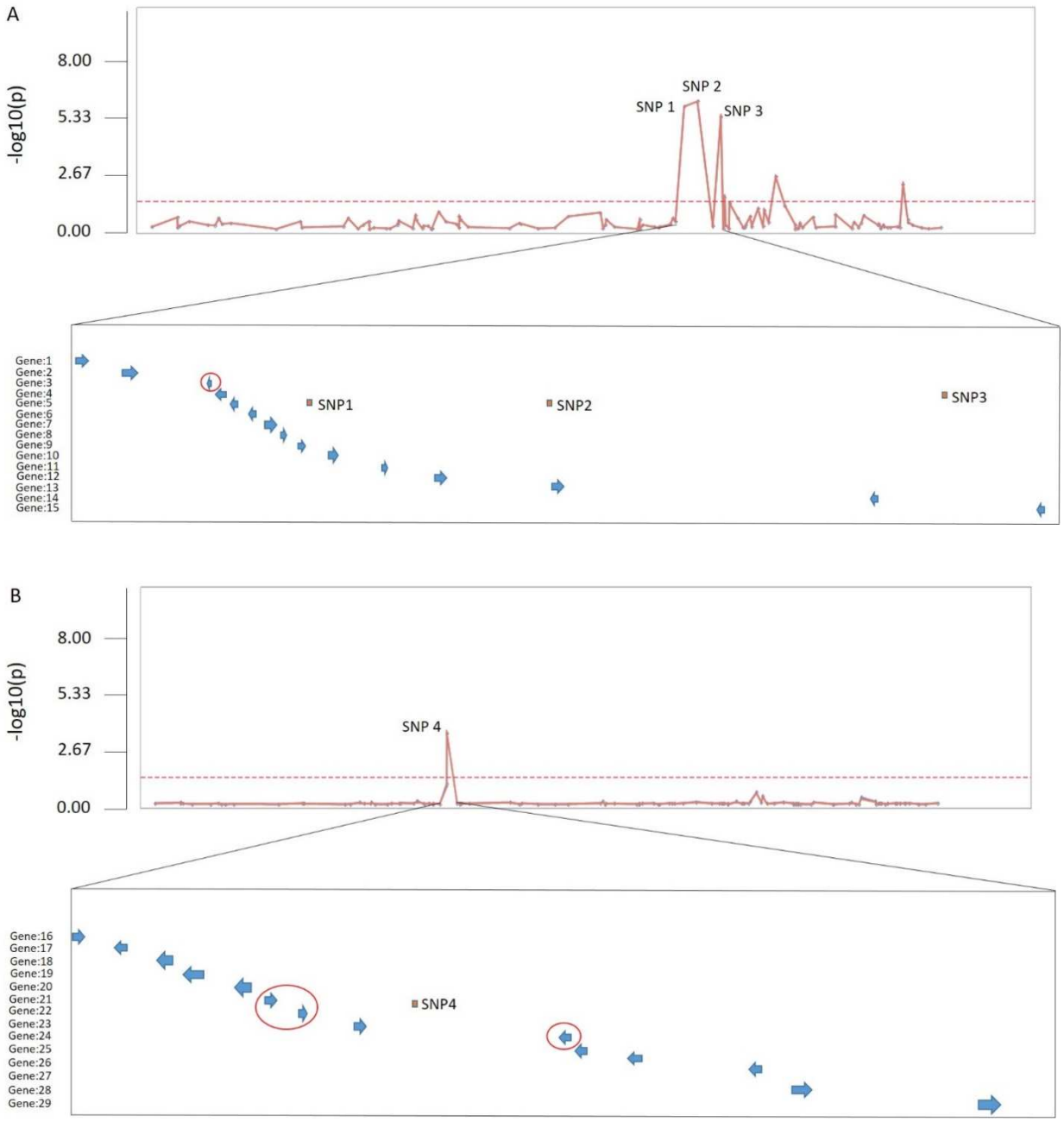

Figure 4.9. Genomic regions of SNPs associated with susceptibility conferred by the SnTox2-*Snn2* interaction (A), and the SnTox5-*Snn5* interaction (B).

All genes in the genomic regions of the significant SNPs are listed by the blue arrows. Candidate NE genes for SnTox5, SnTox2 and/or SnTox6 are circled in red.

Discussion

Parastagonospora nodorum, causal agent of Septoria nodorum blotch of wheat produces multiple necrotrophic effectors (NE) that are critical for SNB disease development. To identify the novel NE genes *SnTox2*, *SnTox6* and *SnTox5*, 191 *P. nodorum* isolates with global distribution were phenotyped on four wheat lines. A RAD-GBS approach to SNP discovery resulted in the identification of 2,983 SNP markers with a minor allele frequency >5% that could be used in GWAS. To test the independency of the SNP markers, linkage disequilibrium (LD) was computed for every pair of the 2,983 SNPs. The average r^2 of LD was 0.0432 showing low linkage disequilibrium within the 191 *P. nodorum* isolate population, indicating that the isolates used in this panel were diverse enough and provided adequate power for the GWAS analysis. The average distance of SNP pairs at LD r^2 value >0.8 (a threshold showing a pair of SNPs are tightly dependent in a distance at this r^2 value) (Bastien et al., 2014) is 25,234bp, indicating that on average, one SNP every 25kb is adequate to detect marker trait associations (MTA). In this study, the average coverage of SNPs over the whole *P. nodorum* genome is approximately one SNP every 18kb, showing the SNPs used in this study have adequate average coverage, however the SNP density on each scaffold does vary. For example, in scaffold 1, the average coverage of SNPs is one marker every 8 kb, but the markers in scaffold 49 distribute at an average rate of one marker every 32 kb, showing the uneven distribution of SNPs across the whole *P. nodorum* genome. Unequal distribution may be due to the numerous repetitive regions, leading to difficulties in identifying polymorphic markers across isolates. Fortunately, all the large scaffolds from scaffold 1 to 45 (98% of the whole genome) have coverage averaging at least one tag every 17kb, satisfying the estimated average coverage that is required (one marker every 25kb) for investigating MTAs.

One of the major problems in GWAS analysis is the occurrence of false positive MTAs (type I error) generated by the simplest linear model (Naïve model). To address this problem, two solutions were used in this study. First was the use of mixed models that considered population structure, relatedness kinship, or both. The mixed models found significant MTAs and were useful in reducing false positives compared to the Naïve model. The second approach to reduce type I error was to correct the *p*-value of each MTA using a positive false detection rate (pFDR) method. Theoretically, the chance of identifying false positive MTAs would be reduced if both population structure and kinship were used along with pFDR correction in GWAS, however, the more factors (population structure, kinship, and *p*-value adjustment) that are added to the models, the higher the chance of not identifying real MTAs (false negatives). Therefore, we used a quantile-quantile plot and calculated the mean square deviation (MSD) to evaluate all the models including the Naïve, IBS (kinship), Q (population structure) and Q+IBS models. In this study, the Q model was selected to identify SNPs associated with SNB disease susceptibility on BG 223, and SNPs associated with NE sensitivity on BG 223 and ITMI 37. The Naïve model was selected to identify SNPs associated with SNB disease susceptibility on ITMI 37, ITMI 44 and LP 29, and SNPs associated with NE sensitivity on LP 29 (Table 4. 2). The Q and Naïve model for all the analysis generated background noise; therefore, to reduce the false positives, pFDR was used to adjust the *p*-value for all the SNPs. To identify the NE sensitivity on ITMI 44, Q+IBS was selected as the optimal model. Because both population structure and relatedness kinship were accounted for, reducing the possibility of type I error, pFDR was not conducted. The IBS model was not used for the MTA analysis in this study, and the kinship value was only used to investigate NE sensitivity in ITMI 44 due to the quantile-quantile plot and MSD test for adding IBS into the analysis was not optimal. An additional reason for not including these

models is that, based on the kinship evaluation of the 191 *P. nodorum* isolate panel, all the isolates showed high relatedness, indicating kinship may have affected the GWAS analysis slightly. In contrast, the Q matrix was more important than the kinship matrix, because most isolates (128 isolates out of the 191 isolates) had a high likelihood (membership value) to be classified into a specific group (Figure 4.3), showing that the panel of 191 isolates had significant population structure, making it necessary to add the Q matrix to the GWAS study. The Q model, however, did not detect any MTAs associated with SNB susceptibility on ITMI 37, ITMI 44, or LP 29. It is possible that the markers associated with the trait may also contribute to the population structure, resulting in the reduction of significance of the SNPs. In this case, the Naïve model with *p*-value adjustment may be optimal for GWAS analysis of this data set.

As mentioned in the previous chapters, *P. nodorum* produces multiple NEs that interact with corresponding sensitivity genes in wheat to induce programmed cell death. *P. nodorum* is a necrotrophic fungal pathogen and has the ability to take advantage of cell death to benefit itself. Finally, the PCD response results in SNB disease susceptibility in wheat cultivars harboring the corresponding host sensitivity gene. Based on this hypothesis, two phenotypic data sets were used including spore inoculation of the 191 *P. nodorum* isolates onto susceptible wheat lines and culture filtrate infiltration of the same 191 *P. nodorum* isolates on the same wheat set to investigate the NE-host sensitivity. To make the connection of a specific NE-host sensitivity interaction, such as the SnTox2-*Snn2*, SnTox6-*Snn6*, and SnTox5-*Snn5* interactions, with the SNB disease occurrence, a MTA identified in spore inoculation data would also be expected to be identified using the culture filtrate data set. On BG 223 (*Snn2*), three MTAs, SNP1, SNP2 and SNP3, significant for spore inoculation (Figure 4.7. A, Table 4.3) were also significant for

culture filtrate infiltration data (Figure 4.7. B, Table 4.3). Interestingly, the three SNPs also showed significant MTAs using culture filtrate infiltration on ITMI 37 (*Snn6*) (Figure 4.7 B, Table 4.3) and two of the three, SNP1 and SNP2 were also significant when using the ITMI 37 spore inoculation data set (Figure 4.7. A, Table 4.3). BG 223 and ITMI 37 contain *Snn2* and *Snn6* which confer sensitivity to SnTox2 and SnTox6, respectively. Previous studies in our lab have shown that the SnTox2 and SnTox6 proteins were difficult to separate by chromatography, indicating that *SnTox2* and *SnTox6* could be the same gene and this NE corresponds with two different host sensitivity genes. These results provide evidence that the genomic region of *SnTox2* and *SnTox6* may be the same and this gene product may interact with both *Snn2* and *Snn6*, resulting in sensitivity and susceptibility on BG 223 and ITMI 37, respectively. One marker, SNP4, was associated with SNB susceptibility on ITMI 44 (*Snn5*). When analyzing spore inoculation data on LP 29 (*Snn5*), SNP4 had a –log10(*p*-value) = 1.8, higher than most of the other SNPs, even though the –log10(*p*-value) was below the significance threshold (Figure 4.7. A). A possible reason for the reduced significance of SNP4 associated with LP 29 spore inoculation may have been due to the relatively similar percentage of isolates in each reaction type category on LP 29 (Figure 4.1). Another possible reason is that the SNP4 is not close enough to the real SnTox5 gene, thereby, to show significance, more SNP markers are needed in the future work. Unlike SNP1-3, SNP4 was not identified using culture filtrate infiltration data of LP 29. This may be explained by the secretion of SnTox5 in planta, but lack of production in culture filtrates.

The flanking markers of the significant SNPs possibly associated with SnTox2/SnTox6 span a genomic region of more than 25kb, the estimated minimum physical distance needed to detect MTAs. In other words, more markers may be needed to strongly detect the candidate

genes for this or other novel NE or NEs. Since the *P. nodorum* SN15 whole genome sequence is assembled and annotated (Hane et al., 2007; Syme et al., 2013) gene annotation information can be used to predict candidate genes for SnTox2, SnTox6 or SnTox5. Three high priority genes have been identified for *SnTox5* and one gene has been identified for *SnTox2*. Downstream characterization and validation such as heterologous expression, gene transformation, and site directed gene knock-outs are required to confirm the function of these candidate genes and this work is in progress.

References

Bastien, M., Sonah, H., and Belzile, F. 2014. Genome wide association mapping of *Sclerotinia sclerotiorum* resistance in soybean with a genotyping-by-sequencing approach. The Plant Genome 7. doi:10.3835/plantgenome2013.10.0030.

Connelly, C.F., and Akey, J.M. 2012. On the Prospects of Whole-genome association mapping in *Saccharomyces cerevisiae*. Genetics 191:1345-U1414.

Dalman, K., Himmelstrand, K., Olson, A., Lind, M., Brandstrom-Durling, M., and Stenlid, J. 2013. A genome-wide association study identifies genomic regions for virulence in the non-model organism *Heterobasidion annosum* s.s. Plos One 8:e53525

Doerge, R.W. 2002. Mapping and analysis of quantitative trait loci in experimental populations. Nature Reviews Genetics 3:43-52.

Earl, D.A., and vonHoldt, B.M. 2012. STRUCTURE HARVESTER: a website and program for visualizing STRUCTURE output and implementing the Evanno method. Conservation Genetics Resources 4:359-361.

Elshire, R.J., Glaubitz, J.C., Sun, Q., Poland, J.A., Kawamoto, K., Buckler, E.S., and Mitchell, S.E. 2011. A robust, simple genotyping-by-sequencing (GBS) approach for high diversity species. Plos One 6:e19379.

Evanno, G., Regnaut, S., and Goudet, J. 2005. Detecting the number of clusters of individuals using the software STRUCTURE: a simulation study. Molecular Ecology 14:2611-2620.

Friesen, T.L., and Faris, J.D. 2012. Characterization of plant-fungal interactions involving necrotrophic effector-producing plant pathogens. Methods in Molecular Biology. 835:191-207.

Gibson, G., and Muse, S.V. 2009. A primer of genome science. A primer of genome science:i-xiii, 1-347.

Gurung, S., Mamidi, S., Bonman, J.M., Xiong, M., Brown-Guedira, G., and Adhikari, T.B. 2014. Genome-wide association study reveals novel quantitative trait loci associated with resistance to multiple leaf spot diseases of spring wheat. Plos One 9:e108179.

Hane, J.K., Lowe, R.G.T., Solomon, P.S., Tan, K.C., Schoch, C.L., Spatafora, J.W., Crous, P.W., Kodira, C., Birren, B.W., Galagan, J.E., Torriani, S.F.F., McDonald, B.A., and Oliver, R.P. 2007. Dothideomycete-plant interactions illuminated by genome sequencing and EST analysis of the wheat pathogen *Stagonospora nodorum*. Plant Cell 19:3347-3368.

Hill, W.G., and Robertson, A. 1968. Linkage disequilibrium in finite populations. Theoretical and Applied Genetics 38:226-231.

Holland, J.B. 2007. Genetic architecture of complex traits in plants. Current Opinion in Plant Biology 10:156-161.

Kertho, A., Mamidi, S., Bonman, J.M., McClean, P.E., and Acevedo, M. 2015. Genome-wide association mapping for resistance to leaf and stripe rust in winter-habit hexaploid wheat landraces. Plos One 10:e0129580.

Listgarten, J., Lippert, C., Kadie, C.M., Davidson, R.I., Eskin, E., and Heckerman, D. 2012. Improved linear mixed models for genome-wide association studies. Nature Methods 9:525-526.

Liu, Z., Friesen, T., Rasmussen, J., Ali, S., Meinhardt, S., and Faris, J. 2004. Quantitative trait loci analysis and mapping of seedling resistance to *Stagonospora nodorum* leaf blotch in wheat. Phytopathology 94:1061-1067.

Mamidi, S., Chikara, S., Goos, R.J., Hyten, D.L., Annam, D., Moghaddam, S.M., Lee, R.K., Cregan, P.B., and McClean, P.E. 2011. Genome-wide association analysis identifies candidate genes associated with iron deficiency chlorosis in soybean. Plant Genome 4:154-164.

Montgomery, G.W. 2011. Genome-wide association studies and genetic architecture of common human diseases. BioMed Central proceedings 5 Suppl 4:S16-S16.

Muller, L.A.H., Lucas, J.E., Georgianna, D.R., and McCusker, J.H. 2011. Genome-wide association analysis of clinical vs. nonclinical origin provides insights into *Saccharomyces cerevisiae* pathogenesis. Molecular Ecology 20:4085-4097.

Palma-Guerrero, J., Hall, C.R., Kowbel, D., Welch, J., Taylor, J.W., Brem, R.B., and Glass, N.L. 2013. Genome wide association identifies novel loci involved in fungal communication. Plos Genetics 9: e1003669.

Pasam, R.K., Sharma, R., Malosetti, M., van Eeuwijk, F.A., Haseneyer, G., Kilian, B., and Graner, A. 2012. Genome-wide association studies for agronomical traits in a world wide spring barley collection. BioMed Central Plant Biology 12.

Pritchard, J.K., Stephens, M., and Donnelly, P. 2000. Inference of population structure using multilocus genotype data. Genetics 155:945-959.

Stevens, E.L., Heckenberg, G., Roberson, E.D.O., Baugher, J.D., Downey, T.J., and Pevsner, J. 2011. Inference of Relationships in population data using identity-by-descent and identity-by-state. Plos Genetics 7: e1002287.

Syme, R.A., Hane, J.K., Friesen, T.L., and Oliver, R.P. 2013. Resequencing and Comparative Genomics of *Stagonospora nodorum*: sectional gene absence and effector discovery. G3-Genes Genomes Genetics 3:959-969.

Tamang, P., Neupane, A., Mamidi, S., Friesen, T., and Brueggeman, R. 2015. Association mapping of seedling resistance to spot form net blotch in a worldwide collection of barley. Phytopathology 105:500-508.

Yu, J.M., Pressoir, G., Briggs, W.H., Bi, I.V., Yamasaki, M., Doebley, J.F., McMullen, M.D., Gaut, B.S., Nielsen, D.M., Holland, J.B., Kresovich, S., and Buckler, E.S. 2006. A unified mixed-model method for association mapping that accounts for multiple levels of relatedness. Nature Genetics 38:203-208.

Zhao, K., Tung, C.-W., Eizenga, G.C., Wright, M.H., Ali, M.L., Price, A.H., Norton, G.J., Islam, M.R., Reynolds, A., Mezey, J., McClung, A.M., Bustamante, C.D., and McCouch, S.R. 2011. Genome-wide association mapping reveals a rich genetic architecture of complex traits in Oryza sativa. Nature Communications 2:467.

Zhao, Y., Wang, H., Chen, W., and Li, Y. 2014. Genetic structure, linkage disequilibrium and association mapping of verticillium wilt resistance in elite cotton (*Gossypium hirsutum* L.) germplasm population. Plos One 9: e86308.

Zhu, C., Gore, M., Buckler, E.S., and Yu, J. 2008. Status and Prospects of Association Mapping in Plants. Plant Genome 1:5-20.